REPORT DOCUMENTATION PAGE

Form Approved
OMB No. 0704-0188

AD-A249 984

2. REPORT DATE	3. REPORT TYPE AND DATES COVERED
June 1991	THESIS/DISSERTATION

4. TITLE AND SUBTITLE
Sun-View-Target Geometry Effects on Spectrally-Derived Vegtative Index Estimates of Absorbed Radiation and Leaf Area

5. FUNDING NUMBERS

6. AUTHOR(S)
Daniel Cornell, Capt

7. PERFORMING ORGANIZATION NAME(S) AND ADDRESS(ES)
AFIT Student Attending: University of Nebraska

8. PERFORMING ORGANIZATION REPORT NUMBER
AFIT/CI/CIA- 91-114

9. SPONSORING/MONITORING AGENCY NAME(S) AND ADDRESS(ES)
AFIT/CI
Wright-Patterson AFB OH 45433-6583

10. SPONSORING/MONITORING AGENCY REPORT NUMBER

11. SUPPLEMENTARY NOTES

12a. DISTRIBUTION/AVAILABILITY STATEMENT
Approved for Public Release IAW 190-1
Distributed Unlimited
ERNEST A. HAYGOOD, Captain, USAF
Executive Officer

12b. DISTRIBUTION CODE

13. ABSTRACT *(Maximum 200 words)*

14. SUBJECT TERMS	15. NUMBER OF PAGES 132
	16. PRICE CODE

17. SECURITY CLASSIFICATION OF REPORT	18. SECURITY CLASSIFICATION OF THIS PAGE	19. SECURITY CLASSIFICATION OF ABSTRACT	20. LIMITATION OF ABSTRACT

SUN-VIEW-TARGET GEOMETRY EFFECTS ON SPECTRALLY-DERIVED VEGETATIVE INDEX ESTIMATES OF ABSORBED RADIATION AND LEAF AREA

Daniel Cornell, M.S.

University of Nebraska, 1991

Advisor: Dr. Elizabeth A. Walter-Shea

Estimating the quantity and quality of vegetation is a primary goal of remote sensing. The impact of changing sun-view-target geometry on spectral measures of vegetative amount (vegetative indices, VIs) has been a major source of concern with this pursuit. A field experiment was conducted to test the statistical significance of solar and view zenith angle effects on the regression coefficients of relationships established between the simple ratio and normalized difference vegetation indices and the biophysical parameters fraction of absorbed photosynthetically active radiation (APAR) and leaf area index (LAI). Measurements of spectral bidirectional reflectance and biophysical parameters were made in an alfalfa (*Medicago Sativa*, L.) field located near Mead, NE throughout the 1990 growing season. View and solar zenith angle effects on VIs were found to statistically affect (at $\alpha = 0.05$) the regression coefficients for relationships established between VIs and APAR, LAI. While APAR was best estimated with nadir or near nadir-derived VIs for all solar zenith angles, no one view zenith angle at all solar zenith angles best estimated LAI from the two VIs. Despite the statistical significance of view and solar zenith angle effects on regression parameters, estimation of APAR and LAI with VIs derived from off-nadir spectral data used in nadir derived regression relationships resulted in D-indices of agreement greater than 0.94 with measured values of APAR and LAI. Predicting above

ground dry weight by accumulating VIs or measuring LAI (with LAI-2000) resulted in a lower mean relative error than using measured or estimated values of accumulated APAR. The variation in regression coefficients for the relationships between VIs and APAR and LAI as a result of differences in view and solar zenith angle though statistically significant may be of less concern than previously thought.

SUN-VIEW-TARGET GEOMETRY EFFECTS ON SPECTRALLY-DERIVED VEGETATIVE INDEX ESTIMATES OF ABSORBED RADIATION AND LEAF AREA

by

Daniel Cornell

A THESIS

Presented to the Faculty of

The Graduate College of the University of Nebraska

In Partial Fulfillment of Requirements

For the Degree of Master of Science

Major: Agronomy (Agricultural Meteorology)

Under the Supervision of Professor Elizabeth A. Walter-Shea

Lincoln, Nebraska

June, 1991

SUN-VIEW-TARGET GEOMETRY EFFECTS ON SPECTRALLY-DERIVED VEGETATIVE INDEX ESTIMATES OF ABSORBED RADIATION AND LEAF AREA

Daniel Cornell, M.S.

University of Nebraska, 1991

Advisor: Dr. Elizabeth A. Walter-Shea

Estimating the quantity and quality of vegetation is a primary goal of remote sensing. The impact of changing sun-view-target geometry on spectral measures of vegetative amount (vegetative indices, VIs) has been a major source of concern with this pursuit. A field experiment was conducted to test the statistical significance of solar and view zenith angle effects on the regression coefficients of relationships established between the simple ratio and normalized difference vegetation indices and the biophysical parameters fraction of absorbed photosynthetically active radiation (APAR) and leaf area index (LAI). Measurements of spectral bidirectional reflectance and biophysical parameters were made in an alfalfa (*Medicago Sativa*, L.) field located near Mead, NE throughout the 1990 growing season. View and solar zenith angle effects on VIs were found to statistically affect (at $\alpha = 0.05$) the regression coefficients for relationships established between VIs and APAR, LAI. While APAR was best estimated with nadir or near nadir-derived VIs for all solar zenith angles, no one view zenith angle at all solar zenith angles best estimated LAI from the two VIs. Despite the statistical significance of view and solar zenith angle effects on regression parameters, estimation of APAR and LAI with VIs derived from off-nadir spectral data used in nadir derived regression relationships resulted in D-indices of agreement

greater than 0.94 with measured values of APAR and LAI. Predicting above ground dry weight by accumulating VIs or measuring LAI (with LAI-2000) resulted in a lower mean relative error than using measured or estimated values of accumulated APAR. The variation in regression coefficients for the relationships between VIs and APAR and LAI as a result of differences in view and solar zenith angle though statistically significant may be of less concern than previously thought.

ACKNOWLEDGEMENTS

I gratefully acknowledge the guidance and assistance provided to me by my advisor Dr. Betty Walter-Shea and her two professional and selfless research assistants Mark Mesarch and Cindy Hays. Credit is also extended to Dr. Kent Eskridge for his assistance in the statistical design and analysis.

I would be amiss if I did not recognize the staff of the Department of Agricultural Meteorology, the other graduate students in the Department, and my family for their support and encouragement. Thank you.

Table of Contents

List of Figures

List of Tables

INTRODUCTION

Remote sensing is most commonly thought of as the acquisition of reflected or emitted electromagnetic energy from surfaces. The usefulness of these data is dependent upon our knowledge of the radiative transfer processes involved and the understanding of observed relationships between the detected radiation and biophysical processes. Perhaps the most promising application of remote sensing is the large scale monitoring of agriculture. The ability to reliably identify crops and estimate agronomic variables related to yield from multispectral data derived from sensors aboard satellites would offer the opportunity to implement growth and yield models over large areas.

With this in mind, much research has been focused on understanding radiative transfer in the atmosphere as well as in agricultural and natural vegetative canopies. This research has led to the development of vegetative indices (VIs) (combinations of spectral bands) which correlate well with many biophysical parameters. The most relevant of these parameters in terms of yield forecasting is the fraction of absorbed photosynthetically active radiation (APAR). Another important biophysical parameter is leaf area index (LAI) which is used in energy balance determinations and the partitioning of evapotranspiration into evaporation from the soil and transpiration through the plant.

Most of the established relationships between VIs and biophysical parameters have been established with nadir or near-nadir viewing sensors. However, the temporal resolution of near-nadir looking satellites, such as

LANDSAT, is too low to effectively monitor dynamically growing vegetation. Subsequently, data from the AVHRR (Advanced Very High Resolution Radiometer) sensor flown on the NOAA meteorological satellites, whose ± 56° scanning capabilities allows for daily coverage, has been used increasingly in recent years to analyze regional and global vegetation.

Many factors such as the optical properties of the vegetative elements, percent ground cover, canopy geometry, atmospheric optical depth, and sun-view-target geometry interact to give the recorded spectral reflectance. Subsequently, many of the established relationships between VIs and biophysical parameters are site and time specific. Therefore, the need arises to characterize the significance of these external factors on the relationships between VIs and biophysical parameters. If the effect of external factors such as changing sun-view-target geometry can be quantified, the possibility exists that remotely sensed data can be processed so that relationships can be defined that will hold over a broad range of viewing conditions.

The objective of this research is to gain an understanding of the relationship between two commonly used vegetative indices (the simple ratio, SRVI and the normalized difference, NDVI) and LAI and APAR of a developing alfalfa canopy under a variety of solar and view zenith angle conditions.

LITERATURE REVIEW

Since vegetation is a natural resource on which all animal life depends, it is one of the most fundamentally important targets for remote sensing by aircraft and satellite-borne sensors (Smith, 1981). The basis of our ability to distinguish vegetation by remote sensing techniques stems from the unique way in which electromagnetic radiation (EMR) interacts with green vegetation. Reflected solar radiation is most commonly used in remote sensing of vegetation, although radiation in the thermal infrared and microwave regions of the electromagnetic spectrum (EMS) are also employed. Unfortunately, measured reflectance or radiance from a vegetative area depends not only on the optical properties of the canopy components (leaves, stems, and reproductive organs) and the underlying soil background but is a complex function of solar zenith angle, atmospheric condition, sensor view angle, and canopy geometry. Because the interaction of radiant energy with a canopy is a function of all these factors, the results of experiments designed to highlight certain effects are necessarily difficult to interpret. But this has not reduced the research effort; the literature with respect to these phenomena is quite extensive. The following is a summary of research on the nature and significance of parameters determining canopy reflectance as well as on the use of canopy reflectance to predict biophysical properties.

Vegetation

Reflection of incident solar radiation from the outer surface of a leaf (specular reflection) is small (2-3%) and relatively wavelength independent (Knipling, 1970). Radiation entering the leaf undergoes refractive-reflective scattering within the leaf, mostly at interfaces between the cell walls and intercellular air spaces. This scattering is significant because it: 1) increases the optical path length within the leaf, facilitating the absorption of visible light by chlorophyll and other pigments; and 2) randomizes the direction of light so that the probabilities of light escaping back through the top portion of the leaf (reflected) or passing through the bottom of the leaf (transmitted) become fairly equal (Smith, 1981). This second result accounts for the close correlation between the reflectance and transmittance spectra of a leaf and the increase in near-infrared (NIR) canopy reflectance with increasing LAI. The increase in NIR canopy reflectance occurs because a good percentage of the transmitted NIR radiation is reflected from lower layers of vegetation and subsequently retransmitted through the upper layers. Canopy reflectance differs from leaf reflectance due to variations in the effective illumination angle as a result of the canopy architecture (leaf orientation and distribution) and the presence of other canopy components and the soil background (Knipling, 1970). Some researchers have alluded to the significance of non-Lambertian leaf properties with respect to canopy reflectance (Breece and Holmes, 1971; Walter-Shea 1987) but these properties may have little impact when integrated over the large ground

resolution elements associated with remote sensing from satellites (Pinker and Stowe, 1990).

Soil

Soil spectra display a gradual increase in reflectance from the visible (10-12%) to the NIR (17-22%) in contrast to vegetation spectra with low visible reflectance (<5%) and high reflectance in the NIR (30-40%) (Ranson et al., 1985a). Spectral reflectance from bare soil is characterized by strong backscattering and is affected by soil mineralogy, fraction of organic matter, moisture content, texture, and surface roughness characteristics (Irons et al., 1989).

Soil reflectance influence on the observed composite canopy reflectance is a function of the quantity and quality of transmitted radiation through the overlying canopy and the soil brightness (Heilman and Kress, 1987). The sensitivity of the composite canopy reflectance to differences in soil background are greatest for canopies of intermediate levels of vegetation (40-60% ground cover) overlying bright soils since canopy scattered, soil reflected radiation is enriched in the NIR and therefore strongly resembles the vegetative spectral response (Huete et al., 1985). Thus, soil and plant spectra interactively mix in a non-additive, partly correlated manner to produce the composite canopy spectra.

Atmosphere

Radiative transfer processes through the atmosphere influence the interpretation of remotely sensed data by altering: 1) the proportion of direct and diffuse irradiance components on a remotely sensed target; and 2) the amount of reflected radiation reaching the sensor. This latter influence plays only a minor role in ground-based measurements but becomes significant for measurements made at aircraft altitudes (Royer et al., 1985).

Under clear sky conditions, the irradiance on a horizontal surface can be characterized by the solar zenith angle and optical depth of the atmosphere (Kriebel, 1976). The optical depth of the atmosphere ultimately determines the percentage of diffuse radiation and therefore the significance of shadows. In general, all atmospheric effects are wavelength dependent. The impact of the atmosphere decreases with increasing wavelength.

Ground-based reflectance measurements have shown that atmospheric effects may differ with variations in canopy cover and architecture. Deering and Eck (1987) found that reflectance factors (RFs), the ratio of reflectance to irradiance, from a full cover canopy decreased with increasing atmospheric optical depth but RF values from an incomplete canopy increased with increasing atmospheric optical depth. NIR RF changes were less than those in the visible. Under higher optical thickness conditions, a greater percentage of the incoming radiation is diffuse. Deering and Eck reasoned that the full canopy RFs decreased as optical thickness increased due to less specular reflection and greater

penetration of diffuse radiation into the canopy while the increase in canopy RFs under the higher optical depth conditions for the incomplete canopy was the result of a lessening of shadows. An increase in atmospheric optical thickness decreases the soil induced variations in canopy reflectance (Huete and Jackson, 1988).

Solar Zenith Angle

There seems to be no clear increasing or decreasing trend of canopy reflectance as a function of solar zenith angle with variations resulting from differences in LAI, percent cover, canopy geometry and planting configuration (Kimes et al., 1980b). However, both simulated and field data have shown that nadir-viewed canopy reflectances decrease with increasing solar zenith angle for incomplete canopies as a result of an increase in shadows. Changes in the amount of shadow have a greater affect in the visible than in the NIR due to the lower leaf transmittance in the visible compared to the NIR. Therefore, solar zenith angle effects on canopy reflectance are greater for visible than NIR radiation. Changes in canopy reflectance as a result of changes in solar zenith angle decrease as the canopy cover increases and/or the canopy geometry becomes more planophile (horizontal) (Ranson et al., 1985a; Kirchner et al., 1982).

Canopy Geometry

For a given amount of vegetation (equal leaf area/phytomass), a change in the distribution and orientation of the canopy elements can bring about large differences in the observed reflectance. These differences are due to changes in the probability of gap, i.e. the probability of a light ray penetrating a canopy without contacting any vegetative elements. The impact of changes in canopy geometry on canopy reflectance will depend on the solar angle and the amount of sky (diffuse) irradiance.

Pinter et al. (1985) observed major differences in reflection among six full cover spring wheat cultivar canopies despite similarities in green leaf area, biomass, and measured leaf optical properties. Differences in reflectance were attributed to differences in canopy geometry. The most planophile canopy exhibited the highest reflectance and the smallest diurnal variation for all measured spectral bands, while the most erectophile canopy had the lowest reflectance and the largest diurnal variation. Differences in reflectance between the different cultivars varied with both solar zenith angle and wavelength of sensed radiation. Maximum differences among cultivars occurred near solar noon in the NIR while, in the visible waveband, cultivar differences in reflectance were minimal at solar noon. Different results could be expected for incomplete canopies as the soil reflectance contribution becomes more significant, especially in the visible wavelengths.

Because a planophile canopy maintains a relatively constant probability of gap with changing solar zenith angle, the reflectance from

a planophile canopy is expected to be more affected by any canopy geometry change as a result of wind, environmental stress or heliotropism than reflectance from an erectophile canopy (Kimes, 1984). However, in a study on the effect of wind on barley (an erectophile) and alfalfa (a planophile) canopy reflectances, Lord and Desjardins (1985) found that a planophile canopy will, in general, be less affected by wind. Within windy and calm periods, extreme values of barley canopy reflectance differed by 60% and 12% respectively in the red portion of the EMS, and by 40% and 8% in the NIR. Reflectance differences from the alfalfa canopy, which is more compact and dense then barley, reached a maximum of only 10% for both periods and spectral regions. Lord and Desjardins concluded that stem bending movement in the barley introduced larger fluctuations in canopy geometry and thus reflectance than the leaf fluttering observed in the alfalfa. Analysis of the data also showed that deviations in visible and NIR reflectance were mostly positive during windy periods for both crops. Wright (1986) observed that wind had no significant effect on barley canopy reflectance until the plants achieved inflorescence (flowering). Moran et al. (1989), monitoring the diurnal changes in canopy geometry and reflectance in alfalfa, a diaheliotropic plant, observed a significant decrease in canopy reflectance during periods of water stress. The decrease in canopy reflectance was attributed to the canopy elements being more vertical during periods of water stress as a result of leaflet cupping along with a diminished capacity for the leaves to track the sun due to decreased plant water potential.

Off-Nadir Viewing

Because all natural surfaces have anisotropic reflectance properties, the use of off-nadir view angles further complicates the analysis of remote sensing data. However, unlike some of the previously mentioned causes of variation in reflectance, off-nadir viewing provides some beneficial inputs to the remote sensing process. First, off-nadir viewing increases the temporal resolution of polar orbiting satellites and secondly, it provides additional information for target identification (classification) purposes (Tucker, 1980; Gerstl and Simmer, 1986). Reported influences of off-nadir viewing on changes in reflectance are not consistent. The inconsistency can be attributed to differences in the parameters previously discussed (ground cover, soil type, atmospheric turbidity, solar angle, and canopy geometry) as well as experimental procedure (sensor field of view, ground resolution element, spectral resolution, target homogeneity, and simulation model used).

In general, for complete homogeneous canopies, the major trend at all solar zenith angles and wavelengths is a minimum reflectance near nadir with increasing reflectances as off-nadir view zenith angle increases. This is the result of the sensor viewing a higher proportion of the brighter upper canopy at oblique view angles than is viewed at nadir and slightly off-nadir angles. For incomplete canopies, off-nadir viewed visible and NIR reflectances differ because of the contrast in reflectance of soils and vegetation with respect to these wavelength regions. Soils have a relatively high visible reflectance as compared to vegetation and a strong backscattering characteristic while in the NIR soils generally

have a lower reflectance than vegetation and the backscattering component is not as strong as in the visible. Therefore, for an incomplete canopy, the visible reflectance shows a strong asymmetry about nadir with minimum reflectances occurring at extreme off-nadir view angles and local maximums occurring either side of nadir. For the NIR wavelengths, the response for full and incomplete canopies is similar with a minimum at nadir and increasing reflectance with increasing view zenith angle (Kimes, 1983).

Kirchner et al. (1981), using simulated data, found the effects of off-nadir viewing more pronounced in the red than the NIR. Similar results have been observed for an alfalfa canopy (Kimes, 1983). In contrast, Barnsley (1984) using a narrow band airborne multispectral scanner (MSS) found the greatest response to off-nadir viewing to be in the NIR rather than in the red. He suggested that the differences were possibly due to the fact that Kimes (1983) used an instrument replicating the relatively wide bands of the AVHRR (Advanced Very High Resolution Radiometer) aboard NOAA meteorological satellites. Kirchner et al. (1982) observed that as the leaf area increases, the variation in reflectance with changing view zenith angle decreases for visible wavelengths but increases in the NIR. As the canopy geometry becomes more horizontal the effects of off-nadir viewing decrease for all wavelengths (Kirchner et al, 1981; Kimes, 1983).

Off-nadir viewing effects are enhanced at large solar zenith angles (Kriebel, 1978; Kirchner et al., 1981) and are maximized when the scanning direction is parallel to the incoming direct solar radiation, i.e. viewing in the solar principal plane (Royer et al., 1985). Kimes (1984) and Slater and Jackson (1982) used ground-based reflectance measurements and

an atmospheric radiative transfer model to simulate satellite measured radiances for different atmospheric optical depths. Both found that the atmosphere caused an increase in off-nadir response, with the variation in response increasing with increasing atmospheric turbidity. Holben et al. (1986), also simulating atmospheric effects, found that the atmosphere changed the magnitude of response relative to the surface but did not alter the off-nadir trend (i.e. the shape of the off-nadir response curve). Results from MSS data taken from an aircraft show that scan angle contrast (relative increase between minimum and maximum radiance) increases with increasing atmospheric turbidity (Royer et al., 1985).

Vegetative indices

Combinations of spectral bands (vegetative indices) have been designed to exploit the differences between the reflectance of green vegetation and its soil background. An ideal vegetation index (VI) would also retain maximum sensitivity to crop characteristics while being relatively unaffected by solar angle, atmospheric turbidity, topography, and viewing direction (Pinter et al., 1987b). Unfortunately, an ideal VI does not exist. However, some of the changes in individual wave band reflectances, due to the external factors mentioned above, can be compensated for by ratioing individual wave bands or using linear combinations of wave bands. The most commonly used ratio indices are the simple ratio vegetation index (SRVI) which is the ratio of reflectance/radiance in the near-infrared (NIR) to the reflectance/radiance in the red (R) portion of the EMS (i.e. NIR/R) and the normalized difference vegetation index, NDVI = (NIR-

R)/(NIR+R). Linear combinations are usually orthogonal transformations such as the 2-dimensional perpendicular vegetation index (PVI) (Richardson and Wiegand, 1977) and the 4-dimensional tasselled cap transformation (Kauth and Thomas, 1976). These indices assume that soil, vegetation, and other spectral features are non-interacting and therefore can be added linearly to come up with the composite reflectance. However, this is not the case.

Though variations in reflectance data due to changes in the soil background are reduced by transforming data into VIs (Kollenkark et al., 1982; Walburg et al., 1982), the soil background condition still exerts a considerable influence on the calculated VI for incomplete canopies. For a given amount of vegetation, darker soils result in higher values for both the SRVI and NDVI as compared to lighter soils. The opposite occurs with the PVI, with brighter soils resulting in higher index values for a given quantity of incomplete vegetative cover than darker soils (Huete, 1988). Recently, some VIs have been developed that are intended to remove the effects of varying soil moisture on canopy reflectance with a specific soil background (Huete, 1988; Clevers, 1988), but the application of these indices to a large area where a mixture of soil types exist is impractical.

In most instances, atmospheric effects reduce the value of the VI (Holben and Fraser, 1984). However, interactions with the effects of soil and canopy geometry causes deviations from this trend. Huete and Jackson (1988), using a radiative transfer model to simulate the atmospheric effect on reflected radiation, observed that atmospheric induced reductions in the SRVI and NDVI were greatest over canopies with darker

soils and were not detectable over canopies with light colored soils. Degradation of the PVI was consistent for all soil backgrounds. Deering and Eck (1987) reported an increase in atmospheric turbidity decreased NDVI for two partial cover orchard grass canopies but increased NDVI for a full cover soybean canopy. Results from Jackson et al. (1980) and Pinter et al. (1987a) show how the SRVI was able to normalize atmospheric variations due to variable cloudiness.

Kirchner et al. (1981), using simulated data, reported an increase in NDVI with increasing solar zenith angle. Kanemasu (1974) found that the ratio of green reflectance to NIR reflectance was apparently not influenced by changes in solar zenith angle.

In a laboratory experiment, Wardley (1984) indicated that ratio VIs are less affected by viewing geometry then non-ratioed indices. In contrast, ground-based reflectance measurements from a wheat canopy at full cover indicated that greenness (a non-ratio VI) displayed less variability with viewing geometry than the SRVI (Pinter et al., 1987b). Vygodshaya et al. (1989) used a theoretical argument to conclude that the SRVI and NDVI would be invariant to changes in canopy geometry, whereas, the PVI would be highly sensitive to changing canopy geometry. Spectral reflectance and canopy geometry data from an experiment with alfalfa support this conclusion (Moran et al., 1989).

Many of the various VIs are highly correlated to each other and none can be ranked as superior (Ahlichs and Bauer, 1983). Perry and Lautenschlager (1984) showed that several widely used VIs are functionally equivalent. NDVI is the most widely used vegetation index because of its ability to partially compensate for changing illumination conditions,

surface slope, and viewing aspect (although, the evidence is certainly not clear that it does all these things better than any other VI).

Relationship between VIs and biophysical parameters

Strong correlations between various VIs and biophysical parameters such as fraction of ground cover, wet and dry biomass, leaf area index (LAI), and plant water content have been found (see for e.g. Tucker 1980; Holben et al., 1980). Because certain biophysical variables are highly correlated to each other, some of the relationships between biophysical variables and VIs can be considered redundant (Kimes et al., 1981). Basic questions still remain concerning the linearity of these relationships and the extent of their applicability.

Most commonly, the relationships between VIs and biophysical parameters are reported as linear or quadratic even though there may be no physical or biological reasoning behind these types of relationships. In many cases, a limited growth or exponential model makes more physical sense. NDVI has a nonlinear asymptotic relationship with LAI while the SRVI has a more linear relationship with LAI, at least at high LAIs (Holben et al., 1980). Best and Harlan (1985) found exponential models of spectral data in the form of various VIs accounted for more of the variance in LAI than a linear regression model derived from stepwise multiple regression techniques. Tucker (1979) concluded that the accumulation of standing dead vegetation had a linearization effect upon the relationship between quanity of vegetation and the various VIs.

Weiser et al. (1986) reported that the direct relationship between VIs and gross biophysical parameters such as LAI were site dependent and time specific. On a single site study, Aase and Siddoway (1980) found separate relationships between NDVI and LAI for different planting densities of winter wheat. Dave (1980) simulating different atmospheric conditions found that the regression parameters for the relationship between the SRVI and leaf water content were dependent on the atmospheric aerosol content.

Even though it is generally agreed that VIs account for more of the variation in biophysical parameters than single band reflectances, certainly no one VI can be considered as best. Gardner et al. (1985) found that the best prediction equations for several different agronomic parameters always contained at least two ratios. Dusek et al. (1985) found ratio VIs to have higher coefficients of determination with five plant parameters than orthogonal transformations. The commonly used SRVI produced considerably lower coefficients of determination than many other ratio VIs. Because the NDVI becomes less sensitive to vegetation at high LAIs and the SRVI is not as sensitive to vegetation as NDVI at low LAIs, Jackson et al. (1983) concluded that no one VI can optimally assess vegetation over an entire growing season and that using several indices may help determine whether VI values changed from one data acquisition period to the next because of changes in vegetation, soil background, or atmospheric conditions.

The penetration of light into a vegetative canopy is basic to the understanding of the photosynthetic productivity of a crop (Sinclair and Lemon, 1974). In a healthy crop, adequately supplied with water, the production of dry matter (DM) is proportional to the amount of

photosynthetically active radiation (PAR) absorbed by the canopy. More specifically, (from Daughtry et al., 1983)

$$DM = \Sigma\ APAR * I_{par} * Ec\ \Delta t$$

where,

APAR = Daily fraction of absorbed photosynthetically active radiation.

I_{par} = Quantity of incoming PAR radiation, $MJm^{-2}day^{-1}$.

Ec = Efficiency of conversion of radiant energy to dry matter, gMJ^{-1} (a function of the availability of water and nitrogen).

t = time period, day.

The daily fraction of APAR is a difficult parameter to quantify. APAR changes throughout the day as the solar zenith angle and canopy geometry interact to determine the probability of gap. Subsequently, a single measurement of APAR is not likely to be representative for the whole day. Most researchers have taken APAR measurements at solar noon, when APAR is at its minimum value, to represent the daily estimate of APAR. Using solar noon measurements to estimate daily APAR for an erectophile canopy may underestimate daily APAR by as much as 50% (Richardson and Weigand, 1989).

Several theoretical models have been developed to predict APAR for a vegetative canopy (e.g. Anderson, 1966; Cowan, 1968). These models generally take a form of the Bouger-Lambert law where the extinction of direct radiation is an exponential function of leaf area and an extinction coefficient (K), i.e. APAR = (1 - exp(-K * LAI)). The extinction coefficient, K, is a function of solar zenith angle and canopy geometry (Sinclair and Lemon, 1974). These same parameters also directly affect canopy reflectance. Therefore, spectral reflectance in the form of a VI

may be a good estimator of APAR. Tucker and Sellers (1986) used a theoretical argument to conclude that canopy reflectance is a more reliable indicator of APAR then of a purely structural parameter such as LAI. Wiegand et al. (1986) added that VIs may provide a more accurate monitor of crop photosynthetic capacity than LAI since spectral indices can respond to non-leaf photosynthetically active organs. In fact, Daughtry et al. (1983) showed that the VI greenness was a better predictor of APAR than LAI.

The capacity to estimate APAR from VIs is significant since the canopy reflectance will often reflect differences in agronomic management techniques (Crist, 1984), lessening the need for detailed knowledge of management practices and increasing the feasibility of applying the relationship between APAR and VIs to large areas (Wiegand and Richardson, 1984). Results from Hatfield et al. (1984) showed that the relationship between APAR and NDVI for wheat was the same from year to year and independent of planting date. Wieser et al. (1986) found that LAI and phytomass could be more consistently estimated indirectly from APAR estimates based on VIs from year to year and site to site than directly from VIs.

As with the relationship between VIs and other agronomic parameters, there is no consensus on the linearity of the relationship between VIs and APAR. Kumar and Monteith (1981) made a theoretical argument for the SRVI being linearly related to APAR while, Asrar et al. (1984) and Sellers (1985) showed APAR to be linearly related to NDVI and nonlinearly related to the SRVI. An exponential relationship has been observed between the SRVI and APAR for sugar beets (Steven et al., 1983) while quadratic

equations have been fit for the relationships between various VIs and APAR data from corn (Gallo et al., 1985). Choudhury (1987) found the relationship between VI and APAR to be curvilinear with curvilinearity decreasing as the magnitude of the soil reflectance increased. He also observed that while the curvilinearity between NDVI and APAR increased with increasing solar zenith angle, the curvilinearity between the SRVI and APAR decreased with increasing solar zenith angle. Recently, Bartlett et al. (1990) observed a linear relationship between APAR and NDVI and suggested that the relationship would hold over a range of solar zenith angles because APAR and NDVI change with solar zenith angle in a similar manner.

EXPERIMENTAL METHODS

Field work for this research project was conducted at the University of Nebraska Agriculture Research and Development Center near Mead, NE (41° 09'N, 96° 30'W, 354m AMSL) in an irrigated alfalfa (Medicago sativa L.) field during the 1990 growing season from May through September. Bidirectional multispectral reflectance factors, APAR, and various canopy and soil parameters were measured. Alfalfa management practices allow a repeated opportunity to observe a range of leaf area indices (LAIs) during one growing season.

Experimental plots

Experimental plots were set up in a 2.8 ha stand of 'Perry' alfalfa planted (drilled, rolled) on 21 Apr 1988; the field was well established with the original N-S row structure not readily evident by the time of this experiment. The soil was a Sharpsburg Silty Clay loam which is very dark grayish brown (2.5Y 3/0) in color when wet and grayish brown (2.5Y 5/2) when dry. Eight plots were defined based on visually determined canopy uniformity. Adjacent plots formed a block with odd number plots measured prior to solar noon (AM) and even number plots measured at solar noon and after (PM) (Fig. 1). Agronomic data requiring destructive collection methods were collected to the north and south of areas in which spectral data were collected.

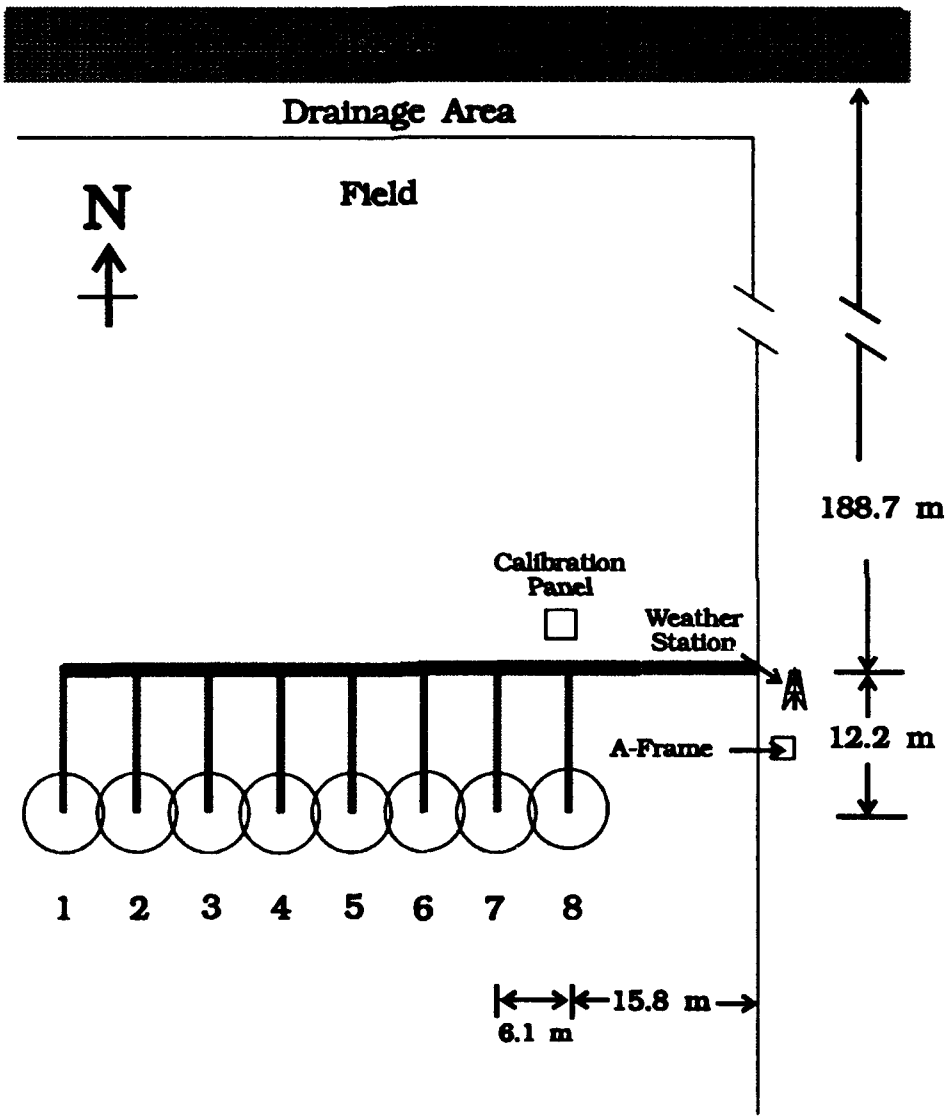

Fig. 1. Layout of research plots and supporting instrumentation. Agronomic measurements were taken to the north and south of depicted circles which indicate areas of spectral measurements.

Agronomic measurements.

Agronomic measurements included, leaf area index (LAI), mean tilt angle (MTA), canopy height, above ground dry phytomass weight, and soil moisture. LAI and MTA were estimated from measures of radiation less than 0.490 μm incident above and transmitted through the alfalfa using a LI-COR LAI 2000 Plant Canopy Analyzer (LI-COR, Lincoln NE). LAI estimates were made one or two times a day (early AM and/or mid PM) with a 90° view restrictor placed on the lens of the LAI-2000. The portion of the alfalfa plot used for LAI estimates was shaded with a 0.9m by 0.6m piece of plywood to meet the diffuse lighting requirement for proper use of the LAI-2000. MTA was estimated after every run using the LAI-2000 with the same procedure as for LAI with the exception that the canopy was not shaded. Direct sunlight does not affect the MTA estimation (LAI 2000 instruction manual). Dry above ground phytomass weight for each plot was determined by oven drying a 0.1m^2 harvested area to the south of the spectral measurement area. Canopy height was inferred from the average of three height measurements from each plot area taken with a meter stick. Gravimetric means were used to determine the average percent soil moisture by mass of three 0.15m soil cores centered at 0.15, 0.45, and 0.76m depths at each plot, north of spectral measurement area. Additionally, the Munsell color code (Munsell Soil Color Chart, Macbeth Division of Kollmorgen Inst. Corp., Baltimore MD) was used to characterize the soil surface color in each plot area at mid-morning and mid-afternoon.

Leaf optical measurements

Leaf transmittances and reflectances were calculated from transmitted and reflected PAR measurements using a LI-COR LI-1800-12 Integrating Sphere equipped with a LI-190SA quantum sensor. Voltage outputs were recorded on an Omnidata Polycorder. Measurements were made throughout the study period on adaxial and abaxial alfalfa terminal leaflet surfaces from upper and lower canopy portions.

An SE-590 spectrometer (Spectron Engineering, Denver, CO) was used with the Integrating Sphere to measure the spectral response of abaxial and adaxial leaflet surfaces from forty leaves on Day of Year (DOY) 268. The narrow band responses as measured with the SE-590 were then integrated over the bandwidths sensed by the multiband radiometer used in the experiment.

Reflectance factor measurements

Canopy bidirectional reflectance factors (BRFs) were derived from measurements taken over canopy and reference panel targets with a Barnes 12-1000 Modular Multiband Radiometer (MMR) and recorded on a series 700 polycorder (Omnidata Intl. Inc., Logan, UT). The MMR produces a voltage proportional to scene radiance in seven reflective wavelength bands from visible to middle infrared and one in the thermal infrared region which was not used in this study. These spectral bands are the same as aboard the LANDSAT Thematic Mapper (TM), except the MMR has an additional near-infrared wavelength band (Table 1). The radiometer was attached to a

pivoting extension atop a three meter aluminum mast (Fig. 2). The MMR was set with a 15° instantaneous field of view (FOV). The pivoting extension allowed orientation of the MMR at view zenith angles (VZAs) ranging from 50° (forward-scatter direction) to -50° (backscatter direction). The footprint at ground level varied from 0.49m^2 at a nadir view to 1.9m^2 for a VZA equal to ± 50° (Fig. 3). Additionally, a 35mm camera was attached to the same bracket as the MMR and color photographs were taken at -50, 50, and 0° VZAs to provide a permanent record of the targeted scene. Occasionally, photographs were taken at all measured VZAs.

TABLE 1

Nominal wavelength intervals of the Barnes MMR and equivalent Thematic Mapper (TM) spectral bands.

MMR Band	Wavelength (μm)	TM Band
1	0.45 - 0.52	1
2	0.52 - 0.60	2
3	0.63 - 0.69	3
4	0.76 - 0.90	4
5	1.15 - 1.30	-
6	1.55 - 1.75	5
7	2.08 - 2.35	7
8	10.4 - 12.5	6

The MMR was always orientated to view in the solar principal plane. Prior to DOY 171, VZAs were measured with an inclinometer held against the lever arm attached to the MMR bracket. Estimated VZA measurement error was ± 2° with this technique. Subsequently, VZAs were measured using an electronic level (Smartlevel, Wedge Innovations, Sunnyvale, CA) attached to the MMR

(a) (b)

Fig. 2. a) MMR, 35mm camera, and electronic level mounted on bracket. Lever arm positioned for 50° view zenith angle. b) MMR mast positioned over Halon panel.

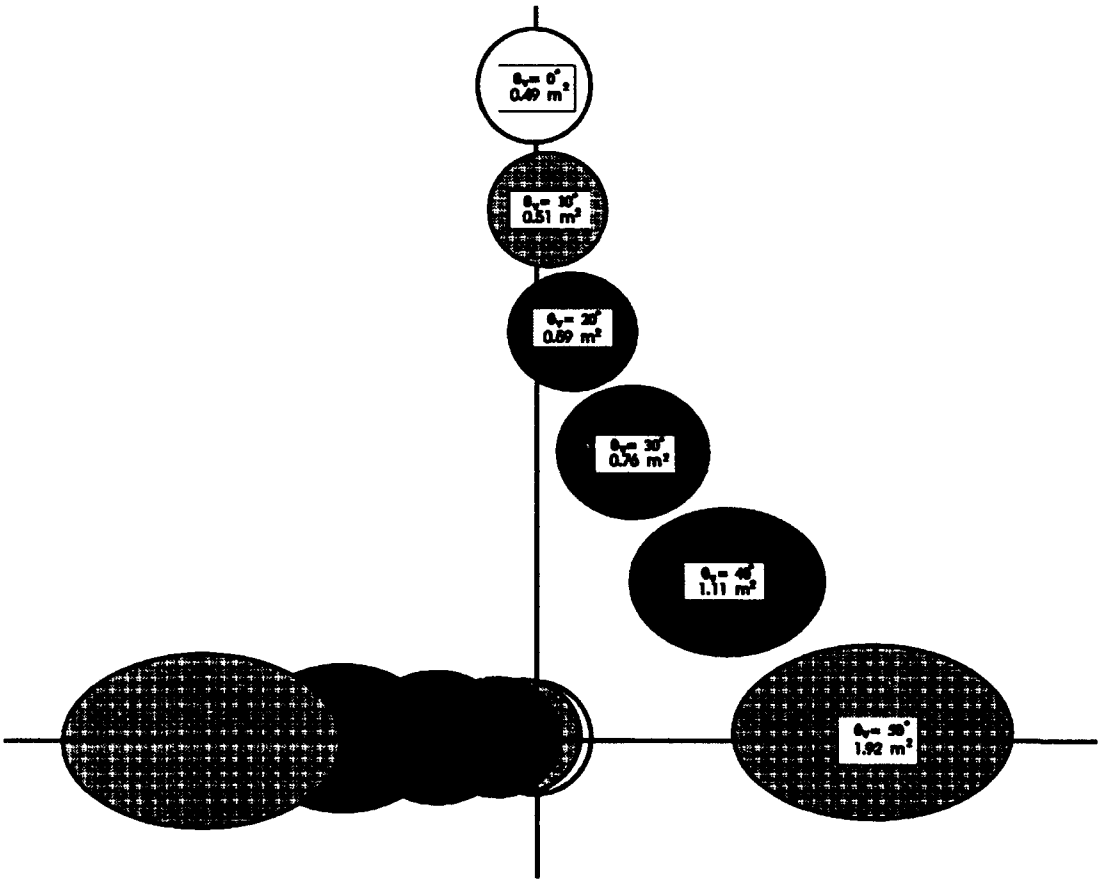

Fig. 3. Ground level footprint as a function of view zenith angle (θ_v) for 15° FOV and sensor height of 3m.

bracket improving VZA measurements to ± 1°. During very windy conditions VZA measurement errors increased slightly.

Data collection was bracketed around solar zenith angles (SZAs) of 55° through solar noon at 10° increments. The number of SZAs represented on a given day was a function of sky condition as well as the time of year. At most nine SZAs (55, 45, 35 and 25 before and after solar noon as well a solar noon of 18°) were represented on DOY 176. In contrast, only five SZAs (55 and 45 before and after solar noon as well as a solar noon of 43°) are represented on DOY 267, the last day of field measurements. Every effort was made to take measurements only when the direct solar path was free of clouds. Each data set required between 15 and 20 minutes to complete. Canopy spectral measurements were expressed as bidirectional reflectance factors (BRFs) which correct for irradiance differences and facilitate comparison within and among dates (Bauer et al., 1981). The reflectance factor was calculated as the ratio of the output voltage proportional to the spectral response measured over the canopy to the output voltage proportional to the irradiance. Irradiance was inferred from nadir-viewed MMR measurements over a calibrated 1.2m x 1.2m molded Halon panel (Labspere Inc., North Sutton, NH) horizontally leveled within the field. The Halon panel reflected data were obtained at the start and finish of each measurement sequence (run). A time based linear interpolation was used to estimate irradiance from these data at the time when individual targets were measured (Robinson and Biehl, 1979). Correction factors were applied to the Halon data to compensate for the non-Lambertian behavior of the panel, a function of the changing SZA

(Kimes and Kirchner, 1982). Correction factors for the Halon panel were derived from the technique of Jackson et al. (1987).

APAR measurements.

APAR values were calculated based on the measurements made with a LI-191SA line quantum sensor (LI-COR, Lincoln, NE) which produces a output voltage which is converted to radiance and recorded on a series 516 Polycorder. Measurements were made in each plot immediately after the MMR measurements. The line quantum sensor was orientated perpendicular to the solar principal plane so that APAR measurements were made in the same plane as MMR measurements. The following sequence of measurements with the line quantum sensor was repeated three times for each plot:

1) Upright about 0.5m above the canopy for measure of PAR irradiance (PAR);
2) Inverted over the canopy at the same height as the incident PAR measurement for measurement of canopy reflected PAR ($RPAR_c$);
3) Inserted in the canopy in an upright position at the soil surface for measurement of transmitted PAR (TPAR); and
4) Inserted in the canopy but inverted approximately 5cm above the soil surface for reflected PAR from the soil surface ($RPAR_s$).

APAR was calculated as, $APAR = 1 + (RPAR_s - TPAR - RPAR_c)/PAR$.

Meteorological measurements

Micrometeorological data useful for describing the conditions under which measurements were made were collected on days when spectral data were acquired. Temperature, relative humidity (RH), wind speed and direction were collected using a Campbell 207 Temperature/RH sensor (Campbell Scientific, Logan, UT), and a Met One Wind sensor (Met One Inc., Grant Pass, OR) mounted on a Campbell Scientific meteorological station 3m tripod at standard instrument heights. Total and diffuse incoming Solar and PAR radiation were measured using two LI-200SA Pyranometer sensors and two LI-190SA Quantum sensors (LI-COR Inc, Lincoln, NE). Diffuse components were measured by mounting one of each sensor under shadow bands built to LI-COR specifications. A correction factor was applied to the data to account for that part of the total diffuse radiation obstructed by the shadow band (LI-COR 2010S Miniature shadow band Instruction manual). All four sensors were mounted at a height of 1.5m on an A-Frame located approximately 4m south of the meteorological station (Fig. 1). All micrometeorological data were recorded on a Campbell Scientific CR21-X data recording micrologger. Prior to DOY 241, all data were recorded in five minute averages. Subsequently, data were recorded in one minute averages to provide a better indication of short term variability of sensed parameters. Additionally, hemispherical sky photographs were taken before and after each data run to provide a permanent record of sky condition.

Statistical analysis

The experimental design was a split-split plot with a whole plot treatment factor of time of day (AM vs PM). The first split plot treatment was solar zenith angle (SZA) with four levels (25, 35, 45, 55) and the second split plot treatment was view zenith angle (VZA) with eleven levels (± 50, ± 40, ± 30, ± 20, ± 10, 0). Adjacent AM and PM plots formed a block (Fig. 1). The ground resolution element or footprint was the experimental unit (Fig. 3). Mean values for the BRFs, VIs, APAR, LAI, and MTA along with the regression parameters for the relationships of interest (APAR,LAI vs VIs) were computed for each plot for each SZA and VZA combination for a total of 352 mean values or pairs of regression coefficients. Linear regression using the least squares method of estimation was used in all cases with appropriate transformations made for exponential or logarithmic curves. Analysis of variance (ANOVA) was performed on the resulting means and regression coefficients and appropriate tests were made for significant differences of relationships between VIs, LAI and APAR at different SZAs and VZAs at $\alpha = 0.05$. Table 2 shows a skeleton ANOVA with sources of variation, degrees of freedom, and appropriate F ratio.

TABLE 2
Skeleton analysis of variance table with sources of variation, degrees of freedom, and appropriate ratio of mean square values (F ratio) to test for significance of differences due to the main effects of AM versus PM (AMPM), solar zenith angle (SZA), and view zenith angle (VZA) and their interactions.

Source of Variation	Degrees of Freedom	Test F Ratio
BLOCK	3	
AMPM	1	AMPM/BLOCK*AMPM
BLOCK * AMPM	3	
SZA	3	SZA/SZA*BLOCK(AMPM)
SZA * AMPM	3	SZA/SZA*BLOCK(AMPM)
SZA * BLOCK(AMPM)	18	
VZA	10	VZA/ERROR
VZA * AMPM	10	VZA*AMPM/ERROR
VZA * SZA	30	VZA*SZA/ERROR
VZA * SZA * AMPM	30	VZA*SZA*AMPM/ERROR
ERROR	240	
TOTAL	351	

RESULTS AND DISCUSSION

Spectral and agronomic measurements were taken on 24 days with a total of 107 data runs. Sky condition was subjectively classified for each run as either steady (S) or variable (V) based on a review of recorded direct and diffuse irradiance data. Table 3 provides a summary of the acquisition dates; an "S" or "V" sky condition designator is placed at each solar zenith angle (SZA) at which spectral data were taken.

Data were taken at all four SZAs before and after solar noon on only two occasions (DOY 176, 218). To use all data less that taken at solar noon in an analysis of variance (ANOVA) would violate the assumption of homogeneity of error variance since the SZAs are not equally represented (i.e. treatments have different sample sizes). The F test for treatment differences is fairly robust to this violation (K.M. Eskridge, Biometry Dept., Univ. of Nebraska-Lincoln, personal communication), however, two subsets of data were created to duplicate some of the statistical test. One data set, which will be referred to as SYM (symmetrical with respect to solar noon), consists of data runs where both AM and PM measurements were made for a particular SZA during the same day. These data were tested using both split-split plot and split-plot (data grouped by SZA) designs. The second data set, which will be referred to as AMBAL (the SZAs are equally represented, i.e. balanced), consist of the six days (DOY 137, 173, 176, 212, 218) where all four levels of SZA were measured prior to solar noon. Additionally, a data set was formed by first averaging the data across the plots for a run. This data set is not appropriate for statistical tests since it smooths out the plot to plot variability but by

TABLE 3.
Summary of data acquisition periods by day of year (DOY) and solar zenith angle (SZA). S (steady) and V (variable) refer to sky condition during data run. Leaf area index (LAI) is the mean for day.

	Solar Zenith Angle										
	AM					PM					
DOY	55	45	35	25	SN	25	35	45	55	LAI	Comments
130					V	V				3.72	
137	S	S	S	S	S	S	S	S		4.02	
148		S	V	V						4.57	
149		S								4.68	
155	S	S	S		V					4.07	Canopy lodged
171		S	S	V	V	V	V	S	S	0.80	Soil 2.5Y 3/2 (moist)
173	S	S	S	S	V					0.89	Soil 2.5Y 5/2 (dry)
176	S	S	S	S	S	V	V	S	V	1.39	Insect damage noted
179	S	S	S	S	S					2.29	Windy
198				V						0.41	
204			S							0.41	
212	S	S	V	V	V	V				1.43	Heavy AM dew
218	S	S	S	V		V	V	V	V	1.82	Light AM dew
220						S	S	S	S	1.67	
221	S	S	V			V	V			2.00	
229	S	S								2.79	
241							V	V	V	0.29	
242							S	S	S	0.33	
243	S	S	S		S					0.47	
247	S	S	S				S	S	S	0.70	
249		S			S			S	S	0.97	
255	S	S			V			S	S	1.39	

doing so it better simulates air or satellite-borne sensor data and is useful in identifying general trends. This data set will be referred to as AVG (it represents average values for a data run). Statistical tests from SYM and AMBAL will be compared to tests made of the data set for all data less that taken at solar noon, hereafter referred to as the LSN (less solar noon) data set. Regression parameters tested with the SYM and AMBAL data sets are based on only five to eight points while from eight to eighteen points are used to estimate the regression parameters with the LSN data set.

A more detailed description of the environmental conditions for each data run as well as the coefficient of variation (CV) across the eleven VZAs for band 3 (red) and band 4 (NIR) BRFs, NDVI, and SRVI can be found in Appendix A. Table 4 provides the Pearson correlation coefficients, r, between selected environmental and canopy parameters and these coefficients of variation. The Pearson correlation coefficient provides a measure of the strength of the linear relationship between two variables. By far, the largest influences with respect to a linear relationship on the variations in BRFs and VIs across the measured VZAs are the SZA and the LAI. Though a low r value does not necessarily indicate that two variables are not correlated (i.e. they may be correlated in a non-linear manner), for this analysis, it is assumed that changes in environmental conditions other than SZA (i.e. the fraction of diffuse PAR radiation (%QDIF), sky condition (steady or variable), relative humidity (RH), and wind (speed and direction)) did not have a significant impact on band 3 and band 4 BRFs and subsequently calculated VIs.

TABLE 4.
Matrix of Pearson correlation coefficients between coefficients of variation (CV) across all view zenith angles for red (B3) and near infrared (NIR) (B4) bidirectional reflectance factors, normalized difference (ND) and simple ratio (SR) vegetative indices and means for selected environmental and agronomic parameters.

	B3CV	B4CV	NDCV	SRCV	%QDIF	SZA	LAI	SKY	WS	WD
B3CV	1									
B4CV	0.660	1								
NDCV	0.177	0.526	1							
SRCV	0.636	0.427	0.507	1						
%QDIF	0.091	-0.010	-0.229	-0.180	1					
SZA	0.678	0.730	-0.037	0.048	0.220	1				
LAI	-0.050	-0.610	-0.785	-0.200	0.102	-0.100	1			
SKY	0.208	-0.320	0.116	0.004	0.312	-0.440	-0.030	1		
WS	-0.320	-0.070	-0.290	-0.340	-0.185	0.010	0.201	-0.277	1	
WD	-0.160	0.053	0.149	0.022	-0.440	-0.030	-0.030	-0.155	0.380	1

Table 5 lists the daily means and standard deviations for the agronomic parameters measured. The alfalfa was harvested on three dates (DOY 155, 192, 234) and was irrigated only after the first cutting. Little change was noted in the soil color over the experimental period as observed using the Munsell color code, therefore, changes in reflectance as a result of soil moisture differences were considered to be minimal.

The minimum, maximum and mean coefficients of variation for red and NIR BRFs and NDVI, SRVI across all VZAs and APAR and LAI by data run are listed in Table 6. These data indicate that variability of measurements of LAI and APAR are similar to that exhibited by the VIs as a result of view zenith angle changes.

General trends in spectral measurements

Review of the sun-sensor-target geometry is appropriate to understanding trends in spectral data. Alfalfa is a diaheliotropic plant, following the sun as it progresses across the sky. However, most of this movement with the sun is azimuthal with very little change occurring in leaf orientation with respect to the horizontal (Travis and Reed, 1983). The solar tracking is most pronounced at large SZAs (Moran et al., 1989). In this experiment, tracking was visually obvious for SZAs greater than 35° as almost all the leaves were azimuthally aligned perpendicular to the solar principal plane. The mean tilt angle (MTA) of the alfalfa progressed from near vertical after cutting to around 50° from the horizontal when mature (Fig. 4). The average MTA was 53° and the average LAI was 1.86. Fig. 5 schematically shows the geometry between the average MTA and solar and view angles significant to the interpretation of

TABLE 5
Daily means and standard deviations (SD) for measured agronomic parameters of Leaf Area Index (LAI), Canopy height (Canopy Hgt), Above Ground Dry Weight (ABGDWT), and percent soil moisture mass.

	LAI		Canopy Hgt (cm)		ABGDWT (gm^{-1})		Percent Soil Moisture Mass	
DOY	Mean	SD	Mean	SD	Mean	SD	Mean	SD
130	3.72	0.65	36	2	389	81	24.85	1.52
137	4.02	0.43	48	3	433	59	25.55	1.11
148	4.57	0.55	69	3	534	118	25.83	2.02
149	4.68	0.35	-	-	-	-	-	-
155	4.07	0.55	65	10	822	103	22.83	1.74
171	0.80	0.20	16	5	137	28	25.56	2.87
173	0.89	0.41	27	5	134	48	26.89	2.29
176	1.39	0.30	37	5	123	37	25.48	2.77
179	2.29	0.25	43	5	238	66	23.70	2.41
198	0.20	0.09	9	1	-	-	-	-
204	0.41	0.08	12	2	148	36	-	-
212	1.43	0.31	22	3	183	45	23.71	1.97
218	1.82	0.39	32	5	191	44	23.71	2.32
220	1.67	0.50	36	3	192	44	-	-
221	2.00	0.54	38	2	249	70	23.98	2.49
229	2.79	0.59	50	3	396	62	23.54	2.65
241	0.29	0.05	12	2	66	23	21.17	1.60
242	0.33	0.05	11	1	82	21	20.53	1.76
243	0.47	0.18	12	1	113	22	20.80	2.59
247	0.72	0.20	23	2	138	29	-	-
249	0.97	0.25	25	2	164	33	-	-
255	1.46	0.37	33	5	238	43	21.40	2.27
257	1.62	0.47	34	4	240	45	-	-
267	2.27	0.39	39	4	293	52	19.62	2.12

TABLE 6
Minimum, maximum and mean coefficient of variation by run for red and NIR bidirectional reflectance factors (BRFs), NDVI, SRVI, APAR, and LAI. Coefficient of variation for BRFs, NDVI, and SRVI for all view zenith angles.

	Coefficient of Variation (%)					
	Red	NIR	NDVI	SRVI	APAR	LAI
Minimum	16	6	1	7	1	8
Maximum	42	27	21	43	71	45
Mean	29	18	9	25	22	23

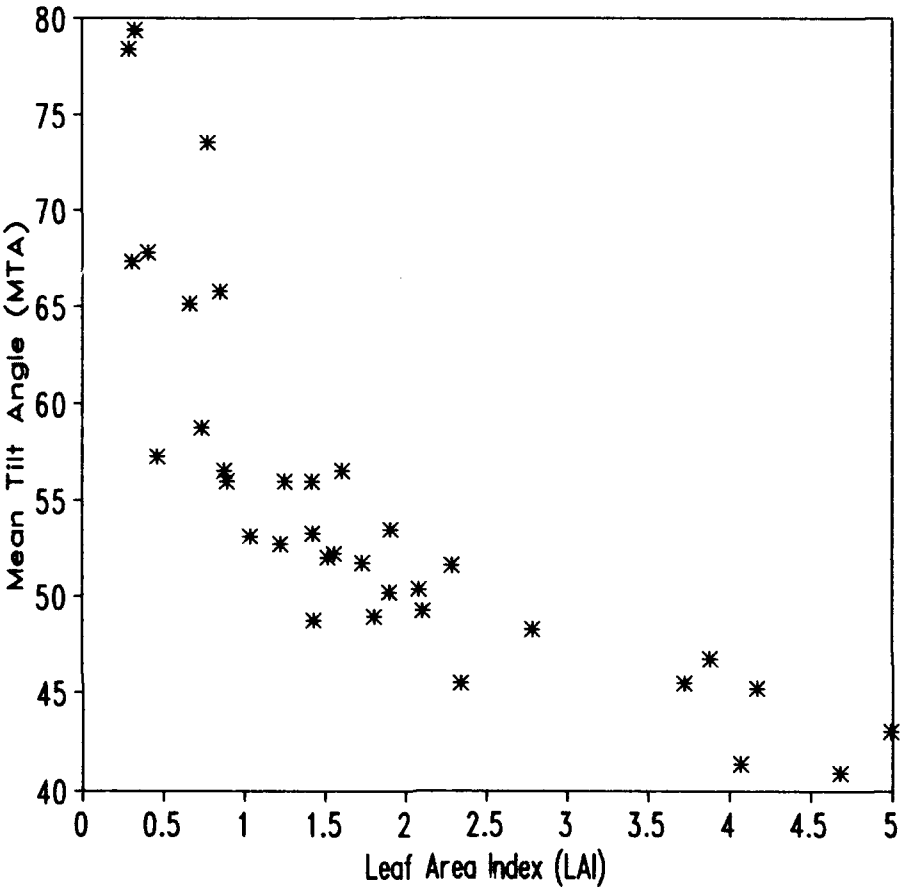

Fig. 4. Mean leaf tilt angle as a function of leaf area index.

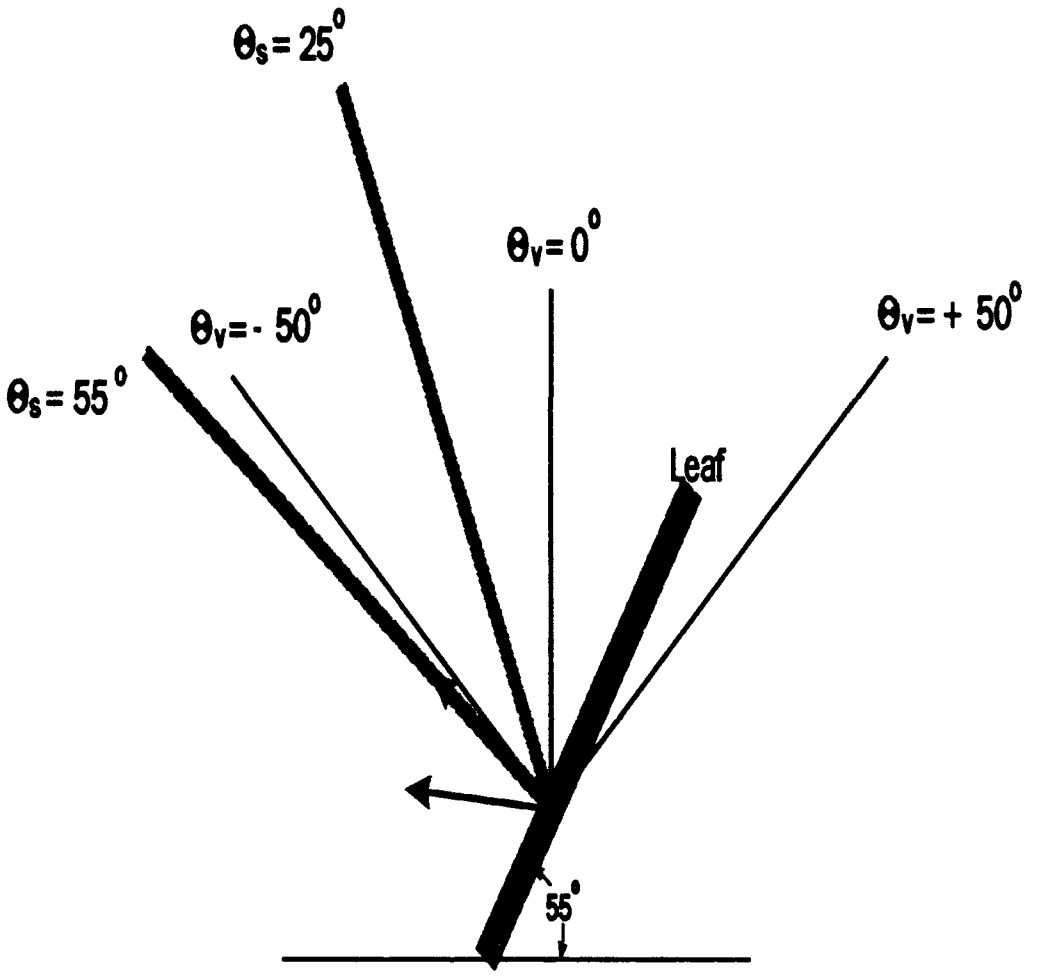

Fig. 5. Sun-view-target geometry for leaf angled 55° from horizontal where θ_s and θ_v are the solar and view zenith angles, respectively.

reflectance trends. As the SZA (θ_s) increases from 25° to 55° a leaf inclined at 55° will exhibit a more Lambertian reflectance pattern (Walter-Shea et al., 1989). At θ_s of 25° much of the reflectance from a leaf will be directed downwards toward the soil (strong forward scattering) while at θ_s of 55° (normal incidence) the reflectance distribution is near-Lambertian, changing little with view angle. Also, a sensor viewing in the backscatter direction will see mostly sunlit adaxial (top) leaf surfaces while a sensor viewing toward the sun (forward scatter direction) will see mostly shaded abaxial (bottom) leaf surfaces. Thus, the quantity of sensed radiation will be dependent on both solar and view zenith angles.

Results of leaf optical measurements showed hemispherical PAR RFs to be statistically different between adaxial and abaxial leaflet surfaces. PAR reflectances ranged from 8-10% for adaxial surfaces and 12-16% for abaxial surfaces indicating a higher concentration of chlorophyll and other light absorbing pigments along the top surface of the leaf. Transmittances of PAR through both leaf surfaces were similar (3-7%). PAR reflectance and transmittance for both sides of the leaflet gradually decreased as LAI increased. NIR reflectance and transmittance were similar both in magnitude (46-48%) and with respect to the adaxial versus abaxial surfaces.

Statistical test results on time averaged (average for all LAIs) red and NIR canopy BRFs and VIs from the LSN data set are given in Table 7. Data appear symmetrical about solar noon (insignificant AMPM main effect), however, the significance of the VZA * AMPM interaction term complicates the interpretation of the AMPM main effect. The significance of the VZA

TABLE 7.
Probability of a larger F value for ratio of appropriate mean square errors to test significance of source of variation. Probability < 0.05 indicates differences in red and NIR bidirectional reflectance factors and normalized difference and simple ratio vegetative indices (NDVI, SRVI) (from LSN data set) as a result of source of variation are significant.

	Probabilty > F			
Source of Variation	Red	NIR	NDVI	SRVI
AMPM	0.63	0.43	0.53	0.62
SZA	0.00	0.00	0.00	0.00
SZA * AMPM	0.10	0.19	0.22	0.16
VZA	0.00	0.00	0.00	0.00
VZA * AMPM	0.04	0.00	0.00	0.01
VZA * SZA	0.00	0.00	0.57	0.01
VZA * AMPM * SZA	0.87	0.10	0.73	0.46

* AMPM term implies that the AMPM differences in BRFs and VIs are dependent on VZA. The statistical test run on the SYM data set grouped by SZA (split-plot design) indicate that VZA * AMPM interaction is not significant for band 4 (NIR) or the VIs at SZAs of 45 and 55° but is for SZAs of 25 and 35° (Table 8). VZA * AMPM interaction was not significant for band 3 (red) at any of the SZAs. The significance of VZA * AMPM interaction for the NIR BRFs and VIs at small SZAs is most likely the result of a change in canopy geometry as alfalfa leaflet solar tracking decreases and the leaflet azimuthal distribution becomes more uniformly distributed at small solar zenith angles (Travis and Reed, 1983). VZA and SZA effects are also significant as is the VZA * SZA interaction term (except for NDVI). Thus, as indicated by previous research (eg. Kirchner et al., 1982; Wardley, 1984), red and NIR BRFs, NDVI, and SRVI change as view geometry changes and the amount of these changes is a function of the SZA. Differences in BRFs and VIs with different view and solar zenith angles can be attributed to changes in the amount of shadow and brightness of the canopy components (vegetative and non-vegetative), and with the case of alfalfa, changes in canopy geometry.

The SYM data set was used to show time averaged trends for the red and NIR BRFs and VIs in the solar principal plane as a function of VZA for the four SZAs (Figs. 6-9). AM and PM SZA data have been combined. The mean LAIs associated with the data range from a low of 1.61 for SZA of 55° to 1.91 for SZA of 25°. In the forward scatter direction, band 3 (red) BRFs decrease as VZA increases, as the sensor sees more shaded vegetation and less soil. At large VZAs in the forward scatter direction the decrease in red BRF levels off. At small SZAs with less shadows overall, the

TABLE 8.
Probability of a larger F value for ratio of appropriate mean square errors to test for significance of source of variation for specified solar zenith angle (SZA). Probability < 0.05 indicates differences in red and NIR bidirectional reflectance factors and normalized difference and simple ratio vegetative indices (NDVI, SRVI) (from SYM data set) as a result of source of variation are significant.

		Probability of > F			
Source of Variation	SZA	Red	NIR	NDVI	SRVI
AMPM	25	0.83	0.21	0.48	0.53
	35	0.96	0.72	0.93	0.47
	45	0.45	0.50	0.44	0.51
	55	0.47	0.26	0.41	0.47
VZA	25	0.00	0.00	0.00	0.00
	35	0.00	0.00	0.00	0.00
	45	0.00	0.00	0.01	0.00
	55	0.00	0.00	0.02	0.00
VZA * AMPM	25	0.10	0.00	0.04	0.01
	35	0.51	0.00	0.06	0.03
	45	0.79	0.07	0.58	0.67
	55	0.84	0.32	0.78	0.55

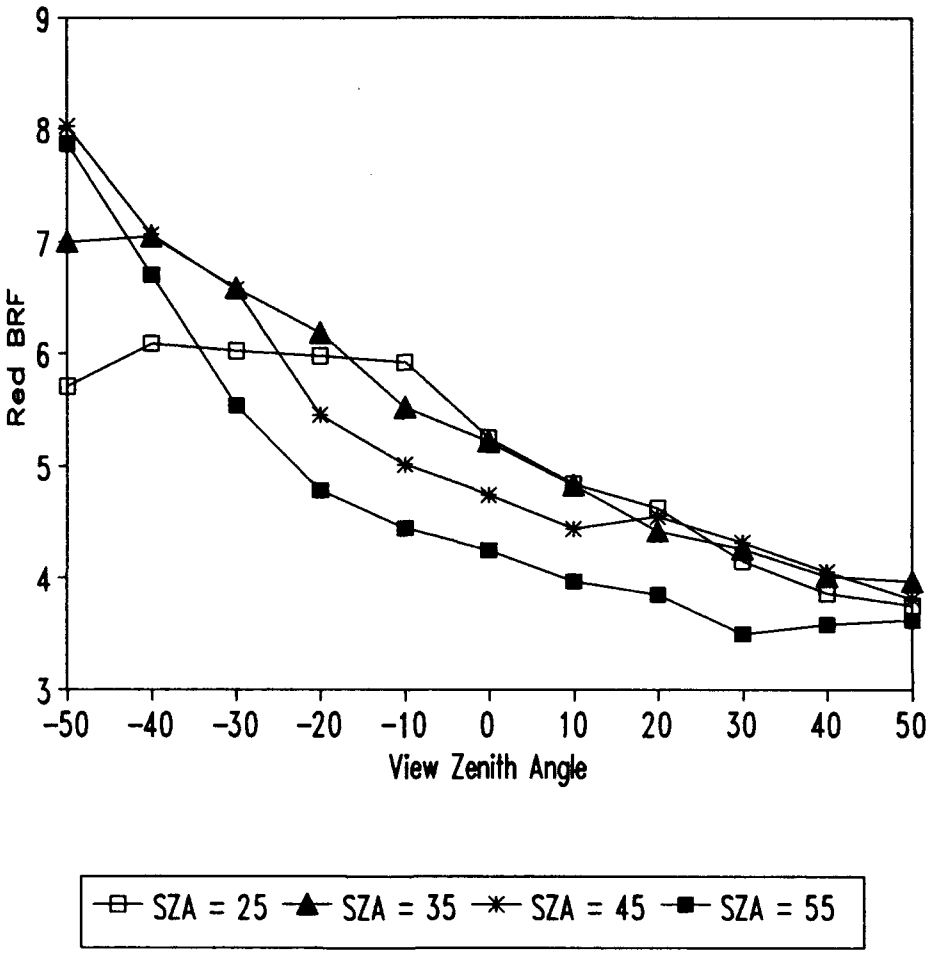

Fig. 6. Red bidirectional reflectance factor (BRF) as a function of view zenith angle at four different solar zenith angles (SZA). Negative view zenith angle indicates backscattering.

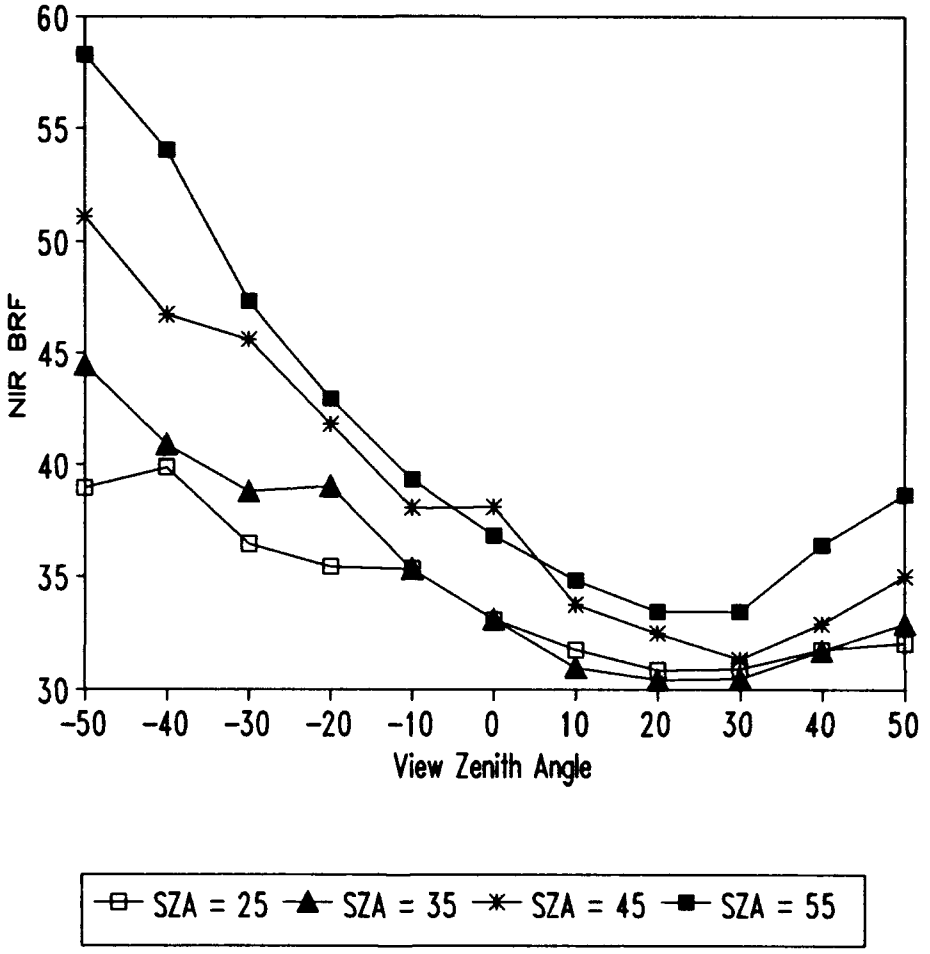

Fig. 7. Near-infrared (NIR) bidirectional reflectance factor (BRF) as a function of view zenith angle at four different solar zenith angles (SZA). Negative view zenith angle indicates backscattering.

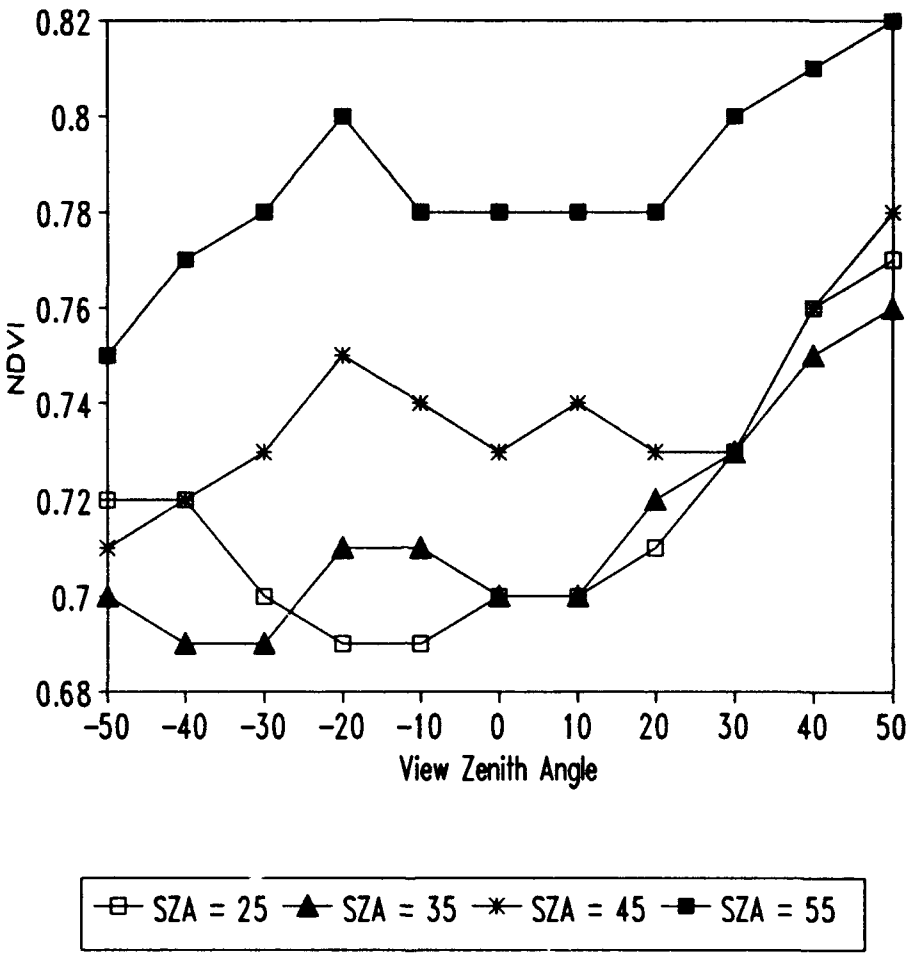

Fig. 8. NDVI as a function of view zenith angle at four different solar zenith angles (SZA). Negative view zenith angle indicates backscattering.

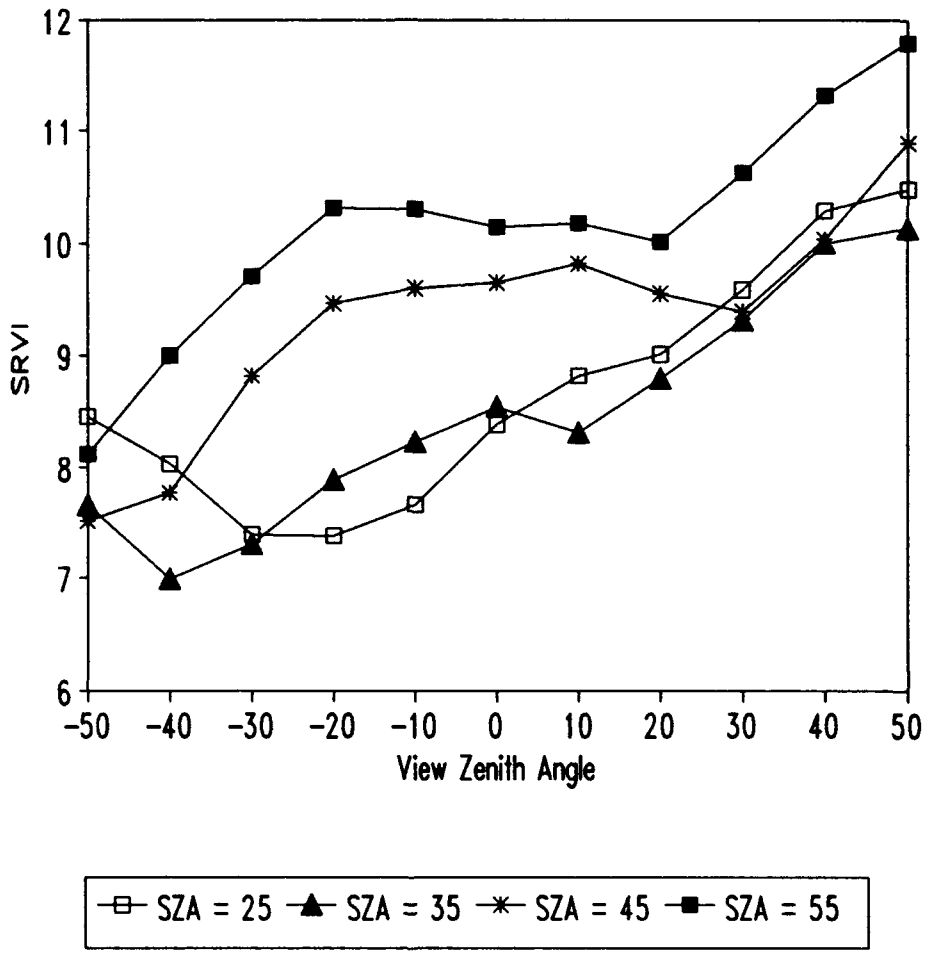

Fig. 9. SRVI as a function of view zenith angle at four different solar zenith angles (SZA). Negative view zenith angle indicates backscattering.

reflectance levels out at about a VZA of 40°, while at higher SZAs with more shadows the minimum reflectance is reached at about a VZA of 30°. In the backscatter direction, reflectance increases due to the strong backscattering characteristics of soil and the sensor viewing a greater amount of sunlit vegetation than is viewed in the forward scatter direction. A "hot spot" in the backscatter direction, as has been observed by Deering and Middleton (1990), is not detected because of the shadow cast by the MMR. The rapid leveling off of red BRF at SZA of 25° could be the result of a combination of the shadow effect of the MMR and the fact that at this incidence angle most of the radiation penetrates into the canopy. For most VZAs the red BRF decreases with increasing SZA because of an increase in canopy shadows. Trends in Band 4 (NIR) BRF are similar to those in the red, however, there are some differences. In the forward scattering direction, after an initial decrease in reflectance with increasing VZA, the NIR BRF increases gradually as VZA increases beyond 30° due to the sensor viewing more vegetation and less soil. Because transmittance through vegetation is high in the NIR as compared to the red, the shadow effect in the NIR is not as strong as in the visible. In the backscatter direction, the leveling off of NIR BRF at small SZA is not as abrupt as for the red BRF because of the decreased influence of shadows on the NIR BRF as compared to the red. In addition, the NIR BRF increases with increasing SZA whereas the red BRF decreases. This can be attributed to the fact that less light penetrates into the canopy as SZA increases, reducing the influence of soil reflectance on the composite canopy reflectance. The net effect is a decrease in red BRF and an increase in NIR BRF with increasing SZA. These trends in red and NIR BRF

are similar to those reported by Kirchner et al. (1982) for an incomplete alfalfa canopy.

Generally, both NDVI and SRVI show an increasing trend in magnitude from far backscattering to far forward scattering. The major exception to this generalization is at small SZAs where both VIs increase as VZA increases beyond 20° in the backscatter direction. This is a result of the red BRF leveling off while the NIR BRF continued to increase as VZA increased (became more negative) in the backscatter direction.

Red BRF decreases while NIR BRF increases with increasing LAI (Figs. 10-13). The general trends in BRFs with respect to view and solar zenith angles at different LAIs are similar to those just described for the average LAI. While both NDVI and SRVI increase with increasing LAI, their trends with respect to view and solar zenith angle as LAI increases are quite different. Whereas, the NDVI response with respect to solar and view zenith angles becomes smoother with increasing LAI, the opposite occurs for SRVI. This is a consequence of Band 3 losing its sensitivity to changes in LAI as LAI increases and the different formulations for the VIs.

Estimation of LAI.

Scatter plots of LAI versus the VIs (Figs. 14-15) showed SRVI to have a linear trend with LAI while NDVI showed an exponential relationship. Overall regressions were performed to determine if adjusting the LAI for the SZA would improve the goodness of fit (Wiegand and Richardson, 1990).

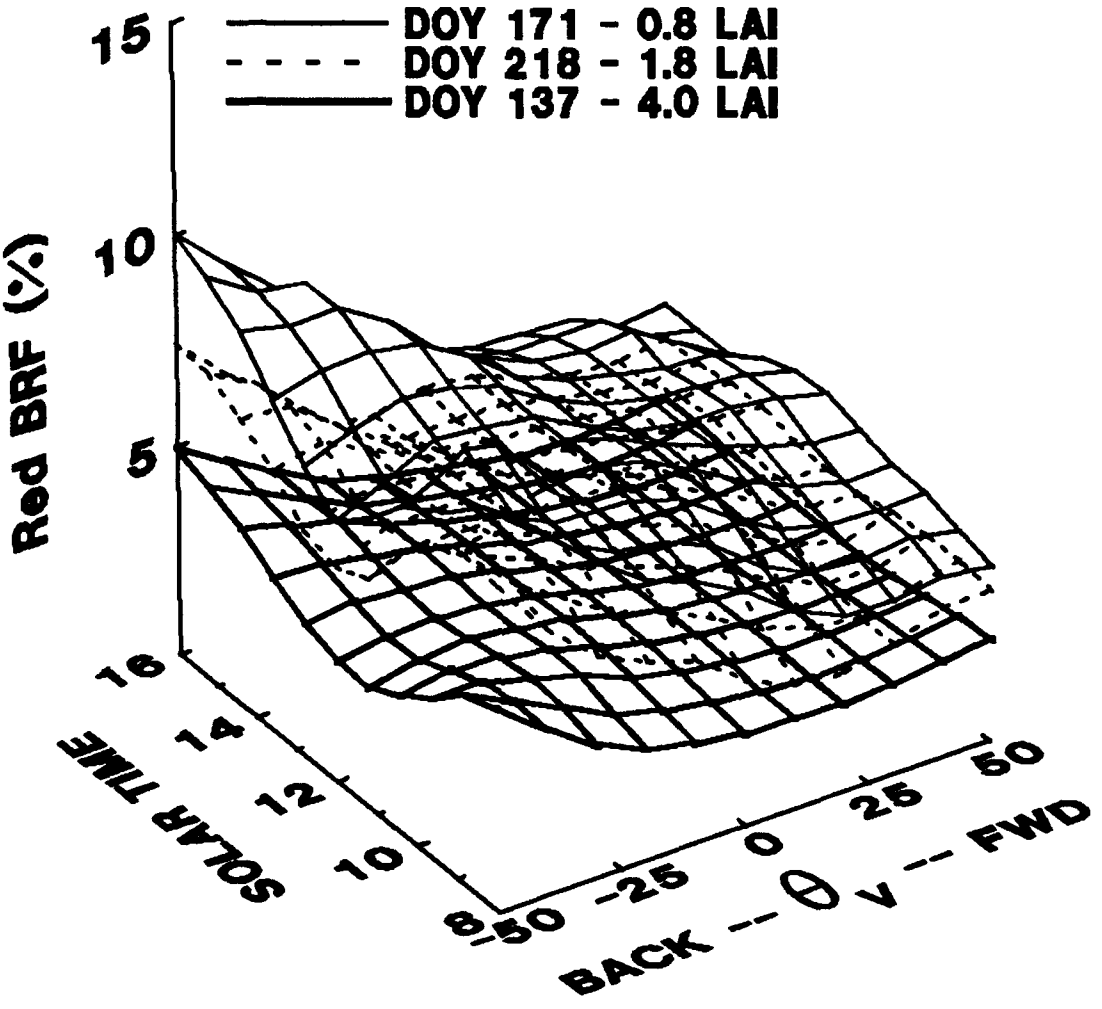

Fig. 10. Red bidirectional reflectance factor (BRF) as a function of view (θ_v) and solar zenith (represented as solar time) angles for different alfalfa canopy LAIs.

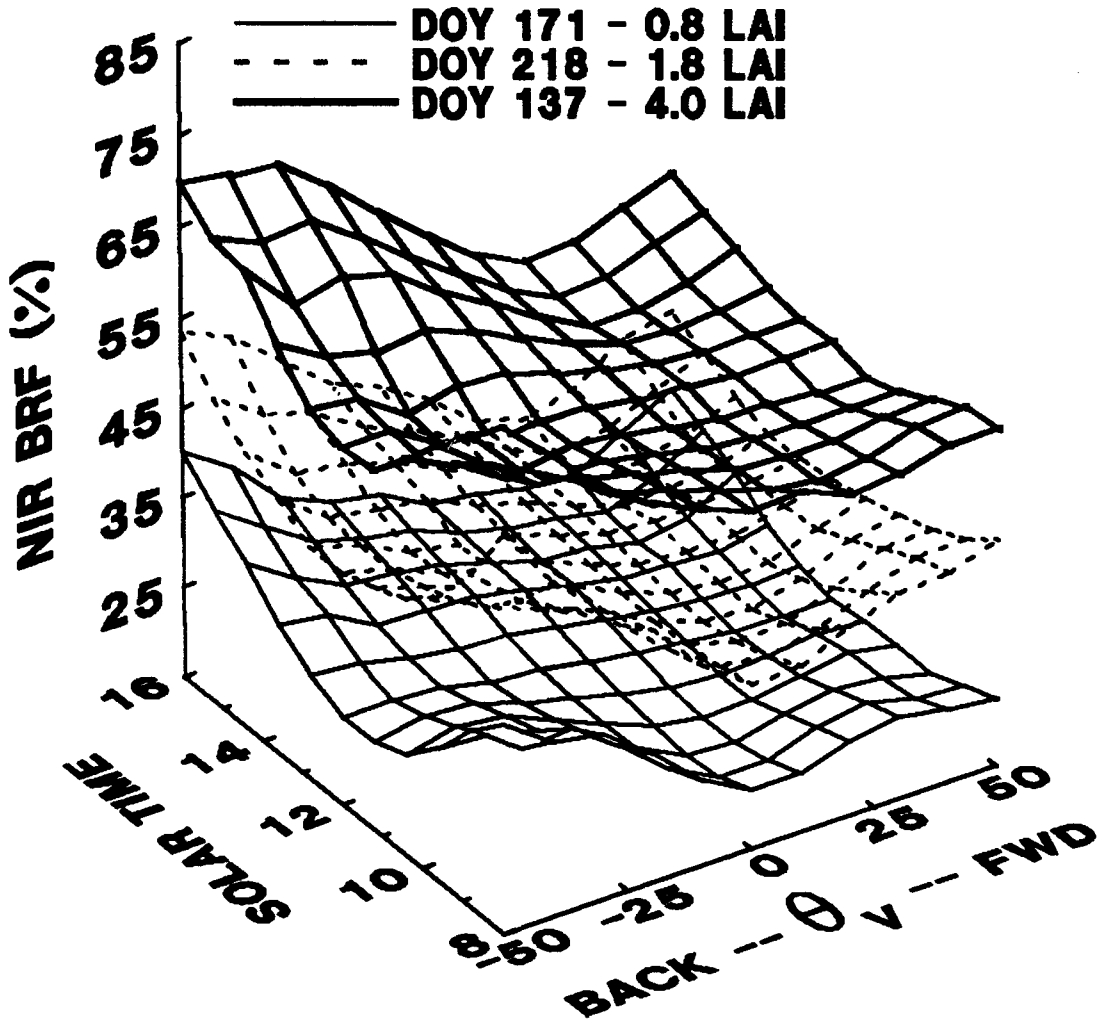

Fig. 11. Near-infrared (NIR) bidirectional reflectance factor (BRF) as a function of view (θ_v) and solar zenith (represented as solar time) angles for different alfalfa canopy LAIs.

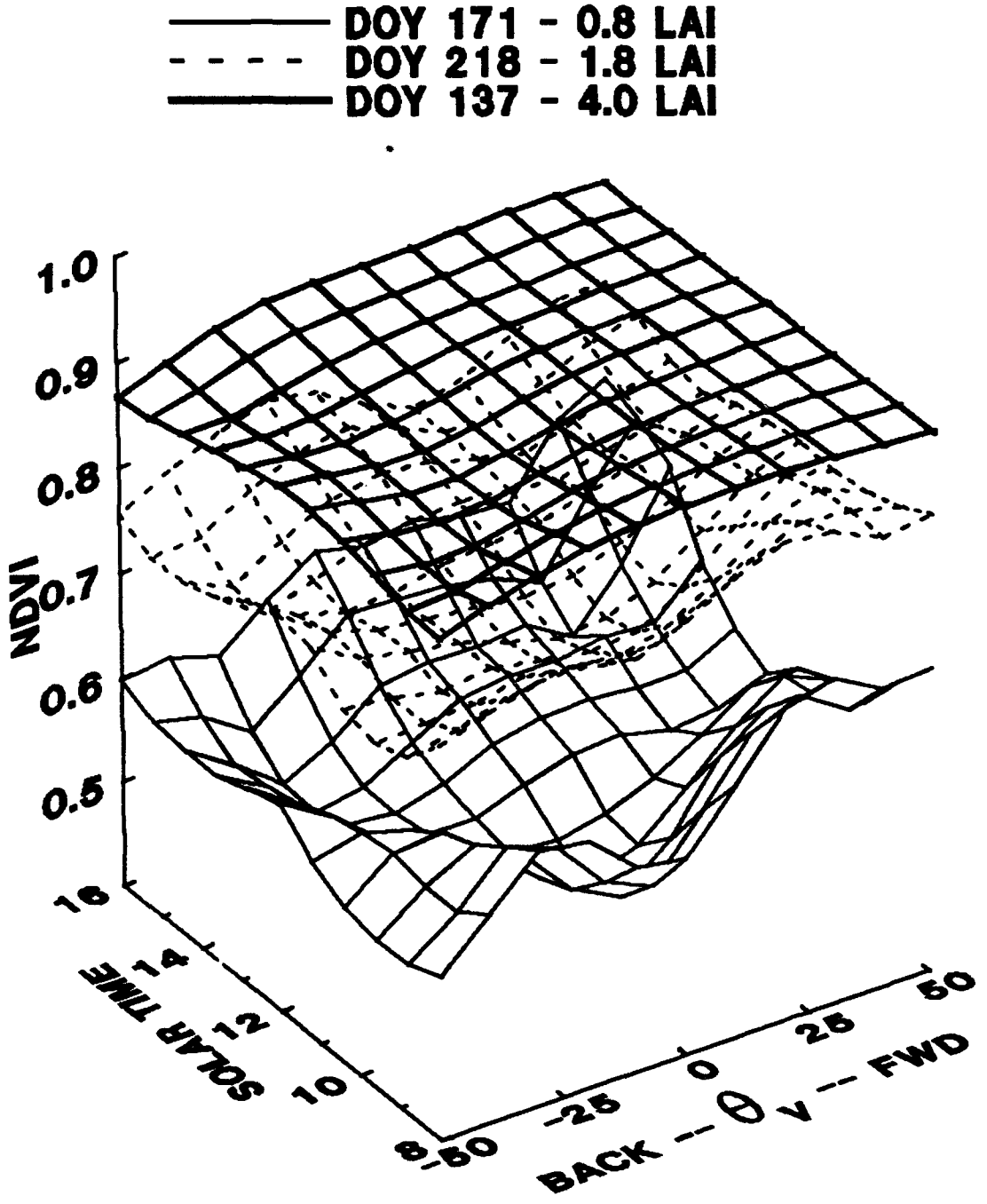

Fig. 12. NDVI as a function of view (θ_v) and solar zenith (represented as solar time) angles for different alfalfa canopy LAIs.

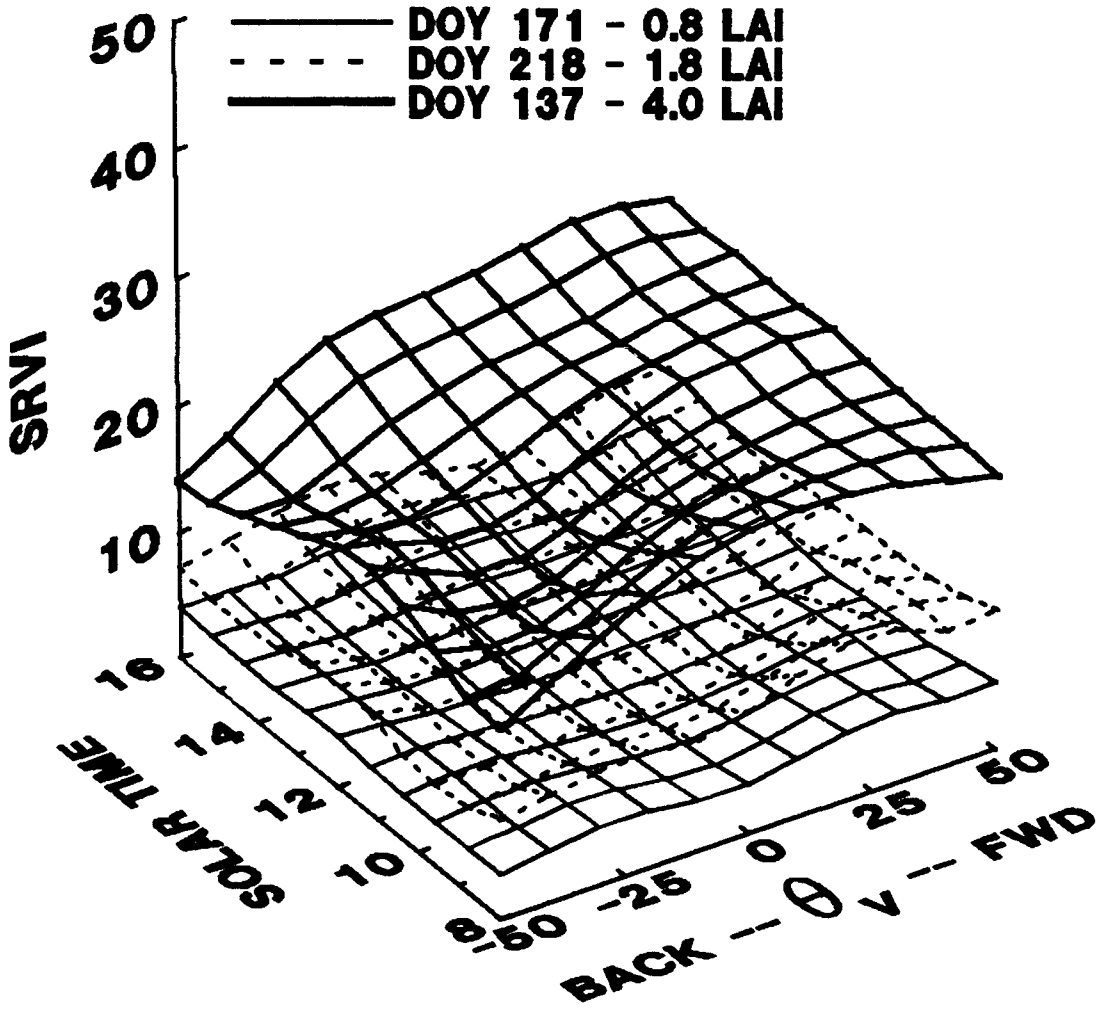

Fig. 13. SRVI as a function of view (θ_v) and solar zenith (represented as solar time) angles for different alfalfa canopy LAIs.

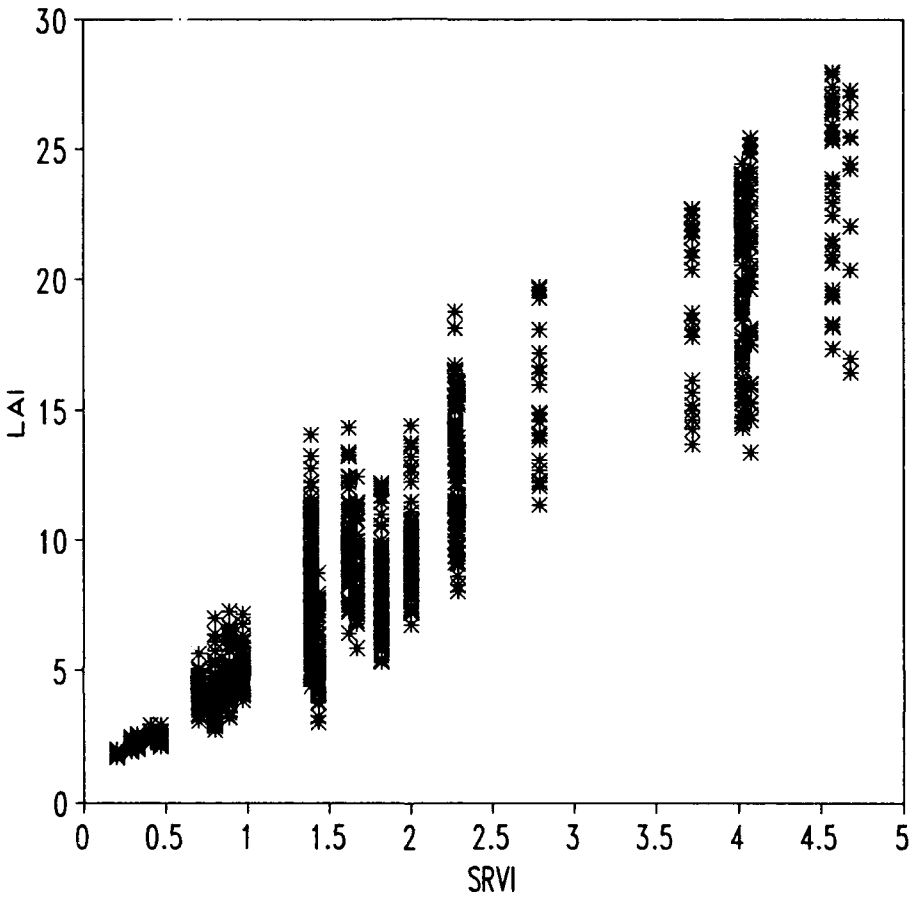

Fig. 14. Scatter plot of simple ratio vegetative index (SRVI) versus leaf area index (LAI). Data averaged by run (AVG data set).

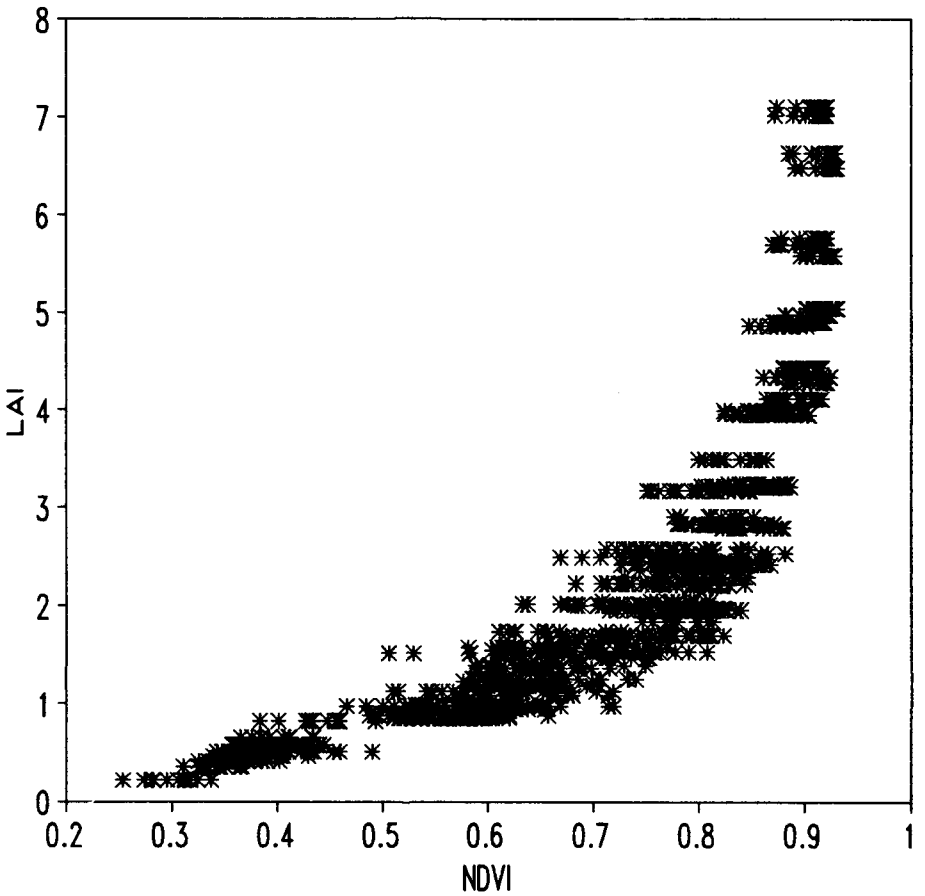

Fig. 15. Scatter plot of normalized difference vegetative index (NDVI) versus leaf area index (LAI) divided by cosine of solar zenith angle. Data averaged by run (AVG data set).

Subsequently, the regression models for the estimation of LAI took the following forms:

$$LAI = \beta_0 + \beta_1 * SRVI$$

$$\ln(LAI/\cos(SZA)) = \beta_0 + \beta_1 * NDVI$$

LAI was not adjusted for SZA when being estimated by the SRVI because doing so increased the root mean square error (RMSE).

The Pearson correlation coefficient, r, provides a simple measure of the goodness of fit for a linear relationship between two variables. The Pearson correlation coefficients between the variables of the above linear relationships are high for all view and solar zenith angles (Figs. 16-17). For both relationships, the Pearson correlation coefficients increase as SZA decreases during the morning hours but no consistent trend is seen with regard to SZA in the PM. This difference in the trend in Pearson correlation coefficients with SZA between AM and PM is reflected in the ANOVA for the regression slope coefficients as a significant AMPM * SZA interaction (Table 9). The ANOVA generated using the SYM data set on a by SZA basis shows that while AMPM was not significant for SZAs of 45 or 55°, it was for SZAs of 25 and 35° (Table 10). As previously discussed, a decrease or lag in leaflet solar tracking at small SZAs is the probable cause for the differences in canopy reflectance which in turn are affecting the relationships between VIs and LAI. The VZA main effect on the regression parameters is significant for both relationships.

VZA main effects on the NDVI vs LAI regression parameters are most evident in the far forward scattering direction where the slope coefficient increases while the regression intercept decreases as VZA increase beyond 20° (Fig. 18). Orthogonal contrast for linear and

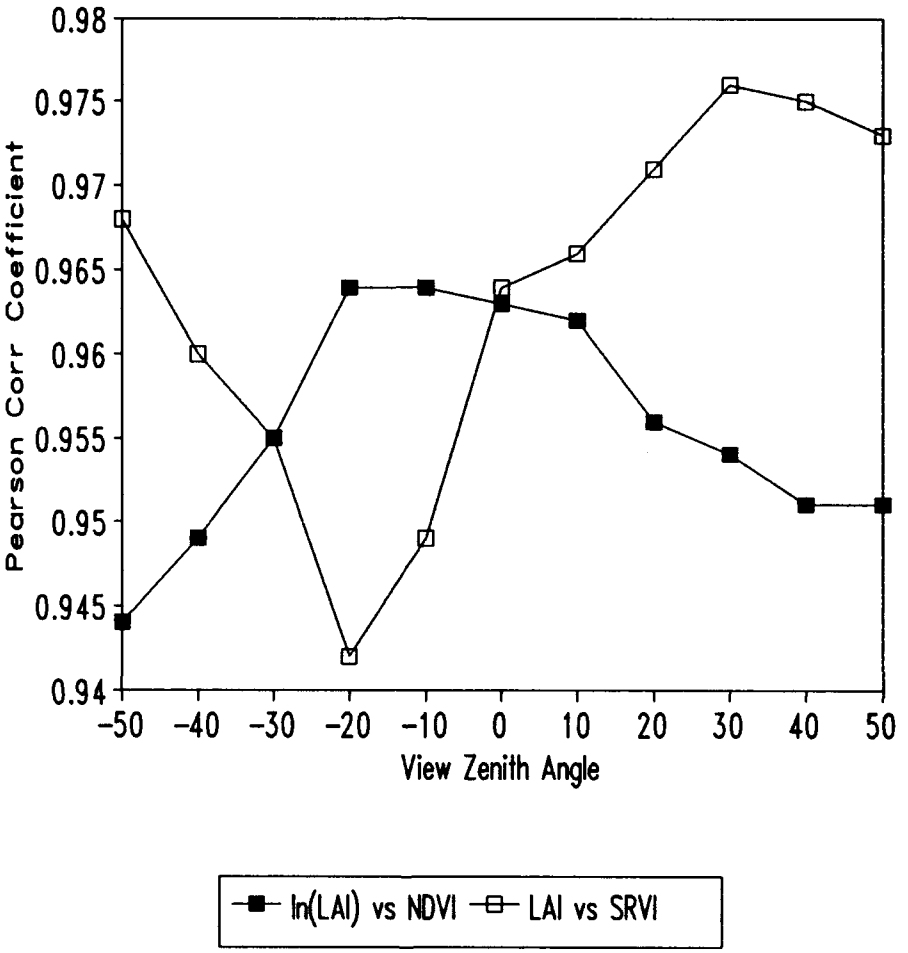

Fig. 16. Person correlation coefficient as a function of view zenith angle for $\ln(LAI/\cos(\theta_s))$ vs NDVI (where LAI is adjusted for solar zenith angle (θ_s)) and LAI vs SRVI. Negative view zenith angle indicates backscattering.

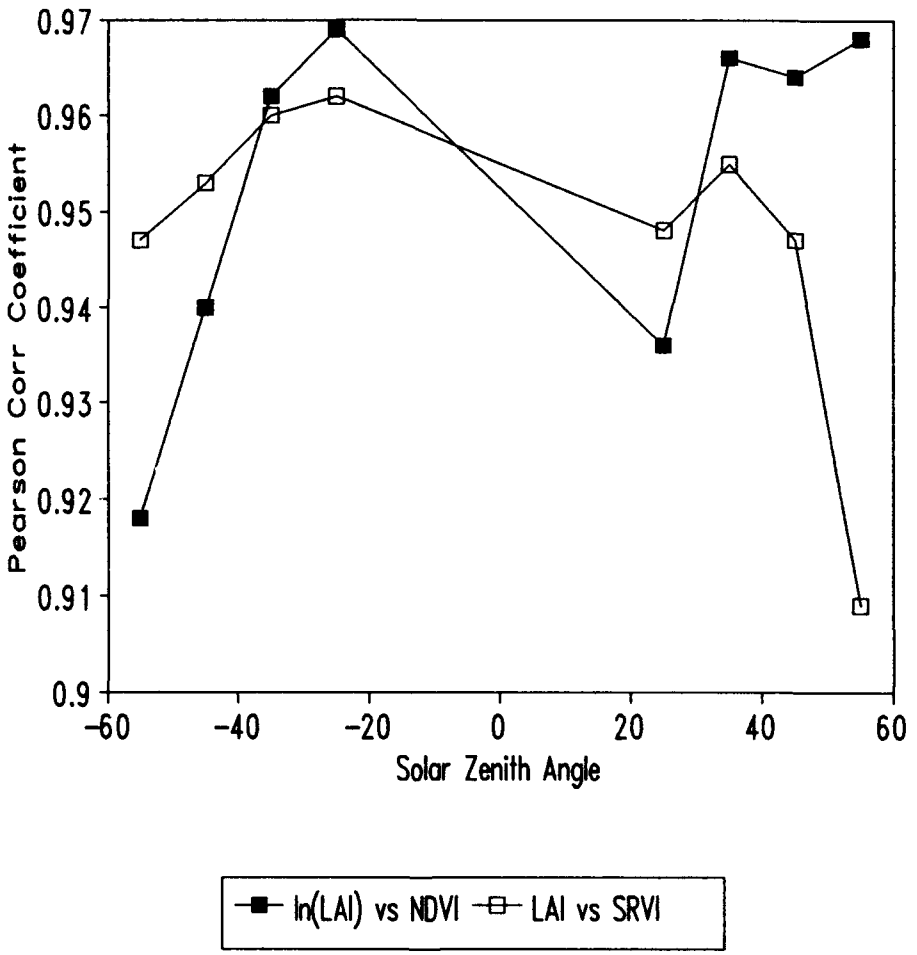

Fig. 17. Pearson correlation coefficient as a function of solar zenith angle (θ_s) for ln(LAI/Cos(θ_s)) vs NDVI and LAI vs SRVI. Solar zenith angles prior to solar noon are negative.

TABLE 9.
Probability of a larger F value for ratio of appropriate mean square error to test significance of source of variation. Probability < 0.05 indicates differences in regression slope coefficients for stated relationship (from LSN data set) as a result of source of variation are significant.

	Probabilty > F	
Source of variation	LAI vs NDVI	LAI vs SRVI
AMPM	0.12	0.00
SZA	0.17	0.00
AMPM * SZA	0.01	0.00
VZA	0.00	0.00
VZA * SZA	0.98	0.00
VZA * AMPM	0.90	0.29
VZA * AMPM * SZA	0.97	0.51

TABLE 10.
Probability of a larger F value for ratio of appropriate mean square errors to test for significance of source of variation for specified solar zenith angle (SZA). Probability < 0.05 indicates differences in regression coefficients for stated relationship (from SYM data set) as a result of source of variation are significant.

		Probability > F	
Source of variation	SZA	LAI vs NDVI	LAI vs SRVI
AMPM	25	0.00	0.00
	35	0.04	0.01
	45	0.10	0.08
	55	0.66	0.20
VZA	25	0.21	0.00
	35	0.12	0.00
	45	0.03	0.00
	55	0.34	0.00
VZA * AMPM	25	0.37	0.07
	35	0.70	0.93
	45	0.63	0.70
	55	0.58	0.84

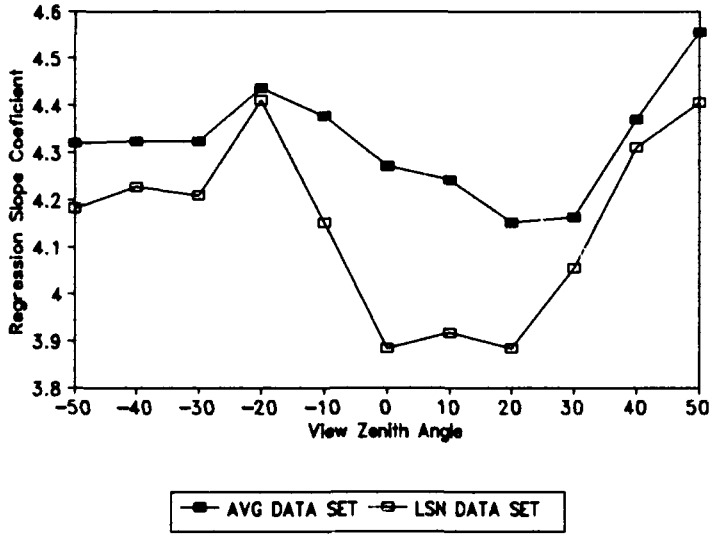

(a)

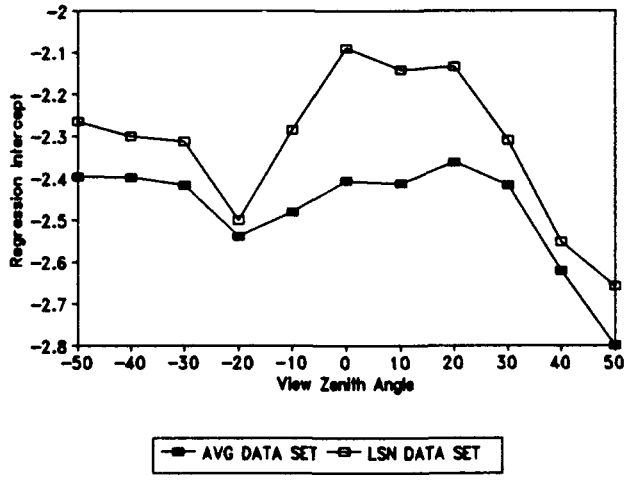

(b)

Fig. 18. Regression coefficients as a function of view zenith angle for NDVI vs LAI relationship. Negative view zenith angle indicates backscattering. a) Regression slope coefficient. b) Regression intercept.

quadratic response of the regression parameters as a function of VZA were both significant. No consistent trend with SZA is exhibited by the regression parameters for the NDVI vs LAI relationship (Fig. 19) and none of the orthogonal contrast (linear, quadratic, or cubic) were significant. For the relationship between LAI and SRVI the regression parameters show a strong functional relationship with VZA (Fig. 20). The slope coefficient for the SRVI vs LAI relationship responds to changes in VZA in a manner similar to the NIR response to VZA. The regression parameters for the SRVI vs LAI relationship reflect the AMPM * SZA interaction with different trends as a function of SZA between morning and afternoon (Fig. 21).

Appendix B provides a complete listing of the regression parameters for the VIs vs LAI relationship, the coefficients of determination (r^2), and the RMSEs for each combination of SZA and VZA for both the LSN and AVG data sets. These data do not indicate that any combination of view and solar zenith angles would consistently provide the best estimation of LAI. It appears that a separate regression equation would be required to best describe the relationship between LAI and VIs for different view and solar zenith angle combinations and that these different regression parameters are in some cases functionally related to the changes in view and solar zenith angle. However, Figs. 22 and 23 show that high indices of agreement can be obtained between measured LAI and LAI estimated from VIs at all eleven VZAs using the regression equation established with nadir data. The overall mean relative error is 11% for estimation of LAI by SRVI and 6% for estimation by NDVI. The inability of NDVI to estimate LAIs greater than 4.0 is evident in Fig. 22. The mean relative error

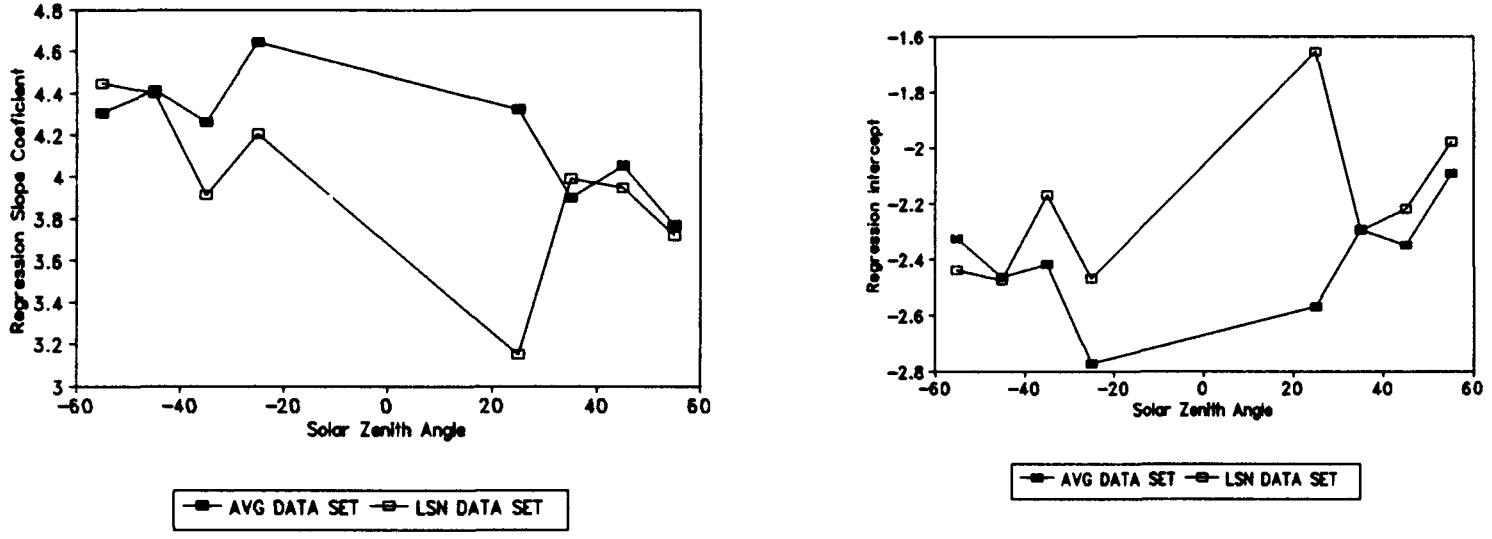

(a) (b)

Fig. 19. Regression coefficients as a function of solar zenith angle for NDVI vs LAI relationship. Solar zenith angles prior to solar noon are negative. a) Regression slope coefficient. b) Regression intercept.

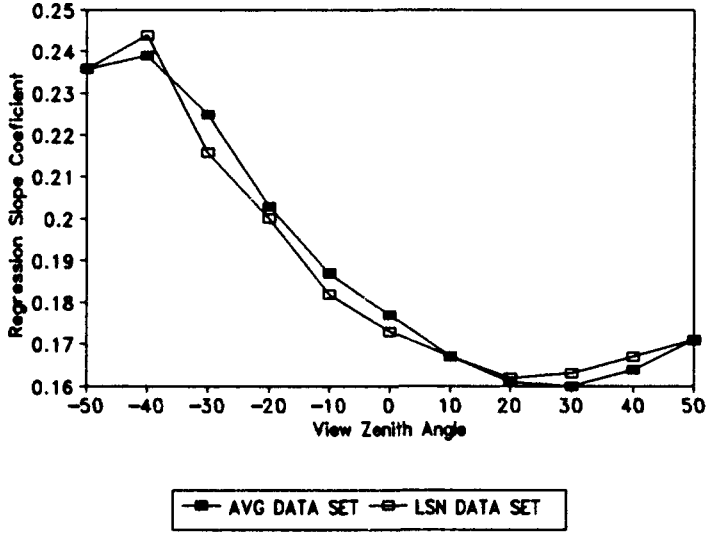

(a)

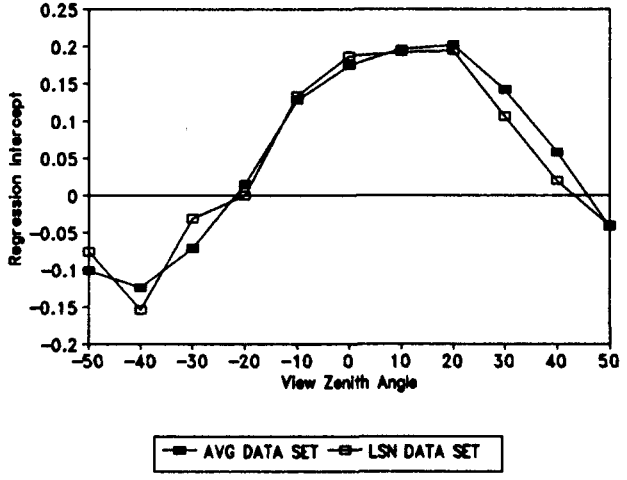

(b)

Fig. 20. Regression coefficients as a function of view zenith angle for SRVI vs LAI relationship. Negative View zenith angle indicates backscattering. a) Regression slope coefficient. b) Regression intercept.

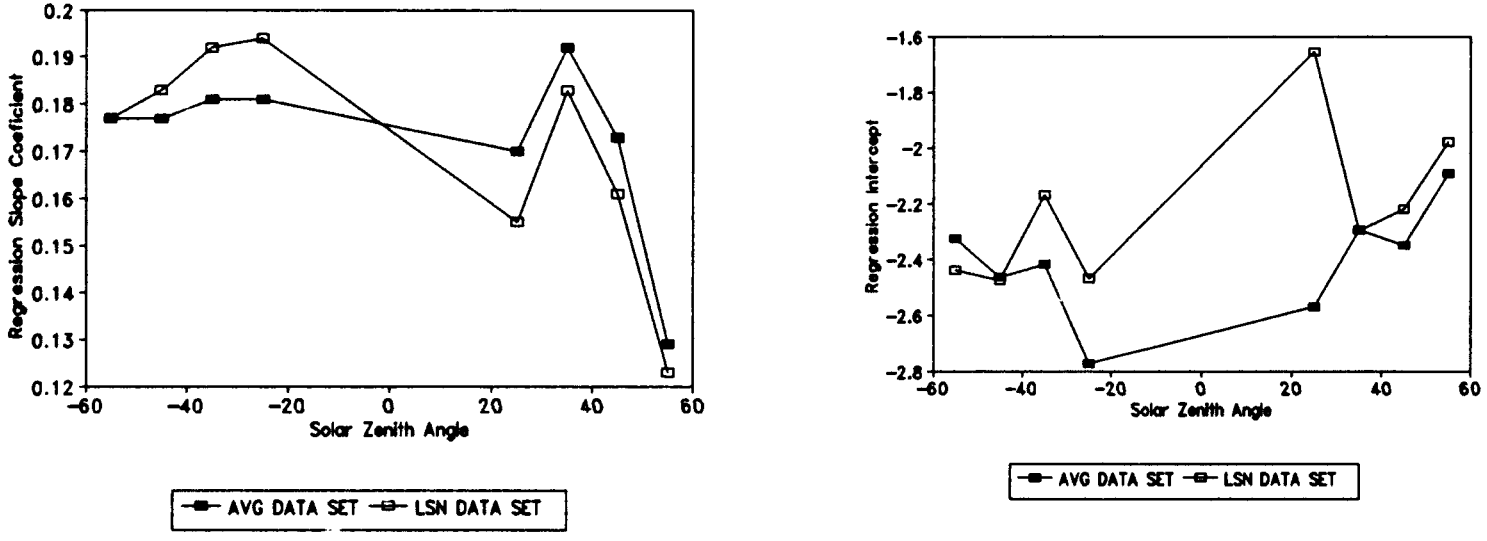

(a) (b)

Fig. 21. Regression coefficients as a function of solar zenith angle for SRVI vs LAI relationship. Solar zenith angles prior to solar noon are negative. a) Regression slope coefficient. b) Regression intercept.

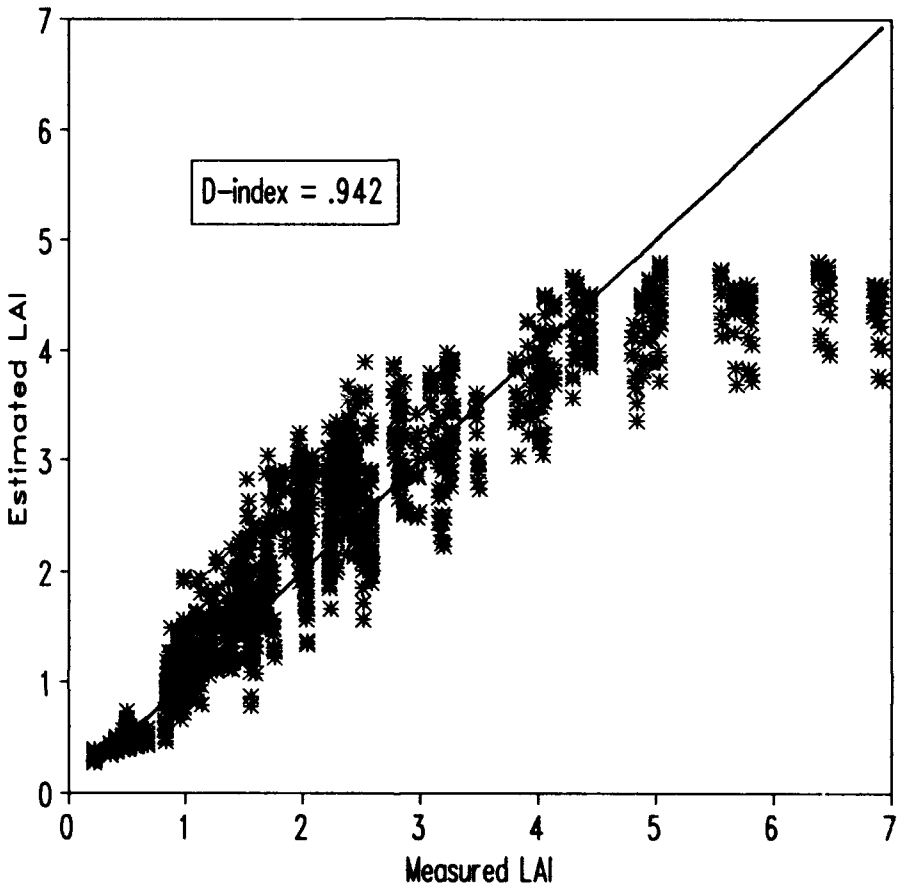

Fig. 22. Measured LAI versus LAI estimated with NDVI from all view zenith angles used in regression equation established using only nadir data.

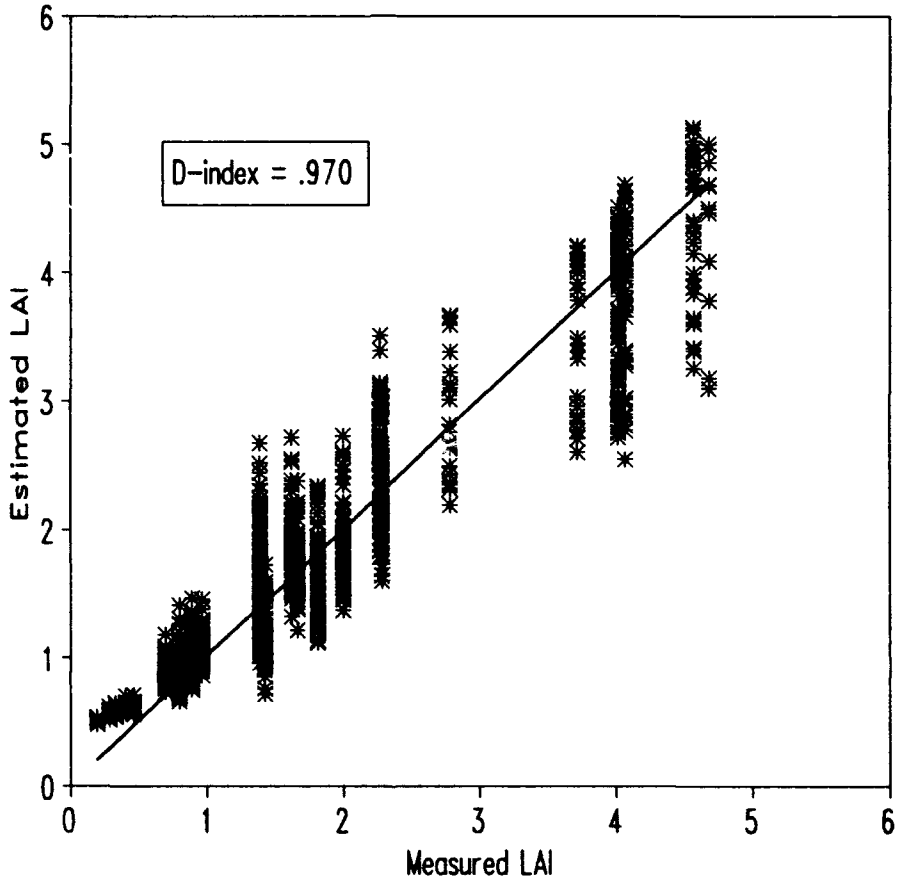

Fig. 23. Measured LAI versus estimated LAI with SRVI from all view zenith angles used in regression equation established using only nadir data.

between estimated (using off-nadir data with nadir derived equations) and measured LAI changes with VZA in a manner similar to the VIs themselves, increasing from far backscattering to far forward scattering VZAs (Fig. 24). This suggest that when using off-nadir spectral data in nadir derived equations to estimate LAI of alfalfa, LAI is best estimated using spectral data at off-nadir angles in the backscatter direction.

Estimation of APAR

Scatter plots of VIs and LAI vs APAR (Figs. 25-27) indicate that the relationship between SRVI or LAI and APAR takes a limited growth (monomolecular) form while the relationship between NDVI and APAR is nearly linear. Some researchers have used a quadratic equation to describe the NDVI vs APAR relationship (eg. Gallo et al., 1985) but since there is no physical basis behind doing this, a linear equation was used here. Therefore, the estimation equations for APAR took the following forms:

$$APAR = \beta_0 + \beta_1 * NDVI$$

$$\ln(1 - APAR) = \beta_0 + \beta_1 * SRVI$$

$$\ln(1 - APAR) = \beta_0 + \beta_1 * LAI/\cos(\theta_s)$$

The strength of the linear relationship between VIs and APAR is best for near-nadir VZAs and decreases as VZA increases beyond ± 20° (Fig. 28). No consistent trend is seen for the Pearson correlation coefficient values as a function of SZA for the relationships between APAR, NDVI and LAI (Fig. 29). Except for a drop off at a SZA of 25°, there is an increase in the correlation coefficient as SZA decreases for the SRVI vs APAR

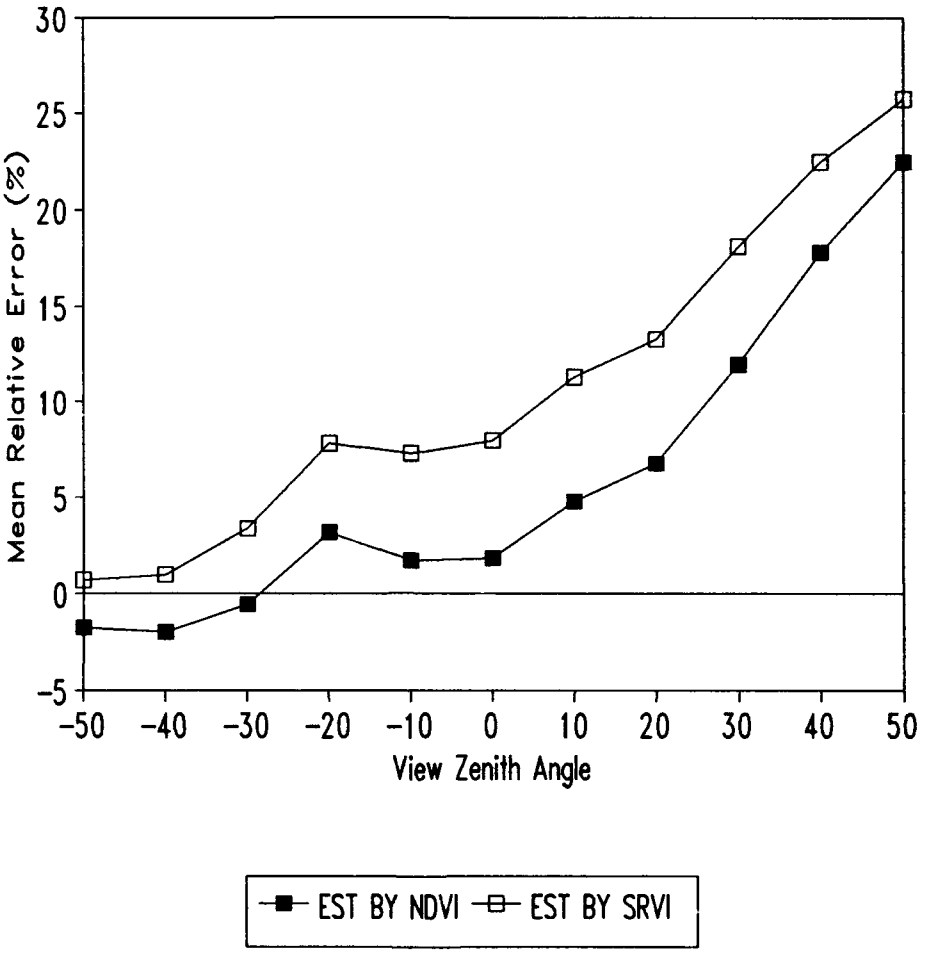

Fig. 24. Mean relative error for estimation of LAI by normalized difference and simple ratio vegetative indices (NDVI, SRVI) as function of view zenith angle. Negative view zenith angle indicates backscattering.

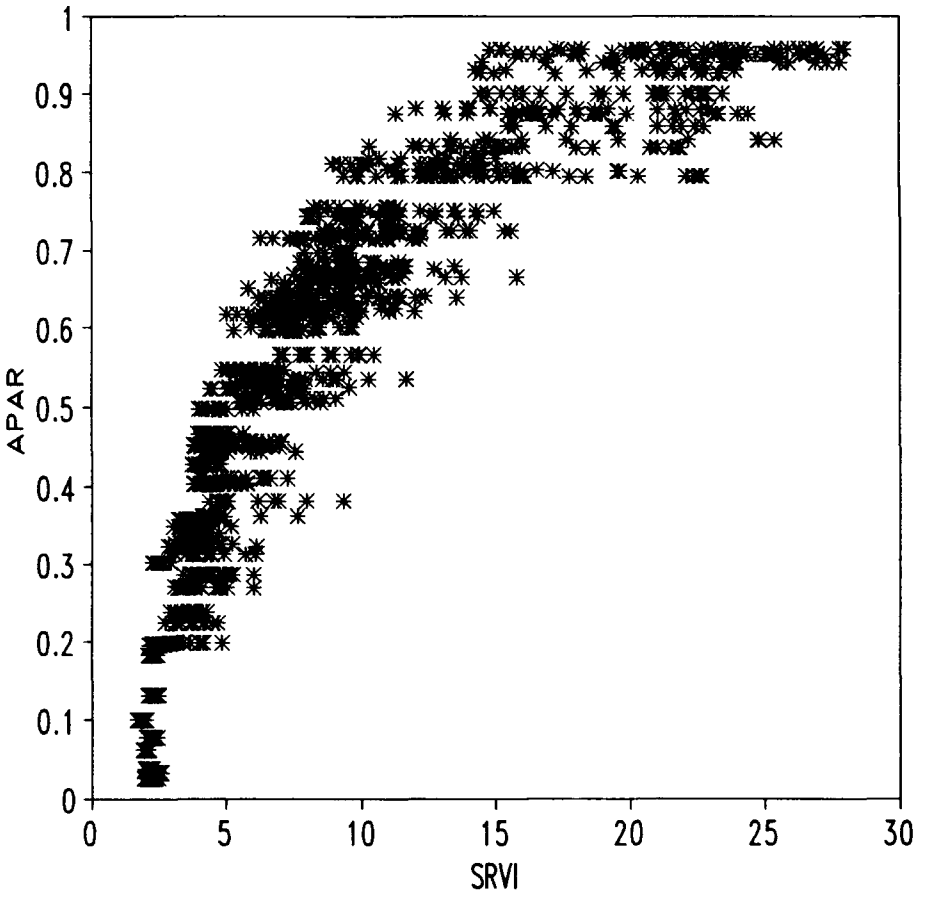

Fig. 25. Scatter plot of simple ratio vegetative index (SRVI) versus fraction of absorbed photosynthetically active radiation (APAR). Data averaged by run (AVG data set).

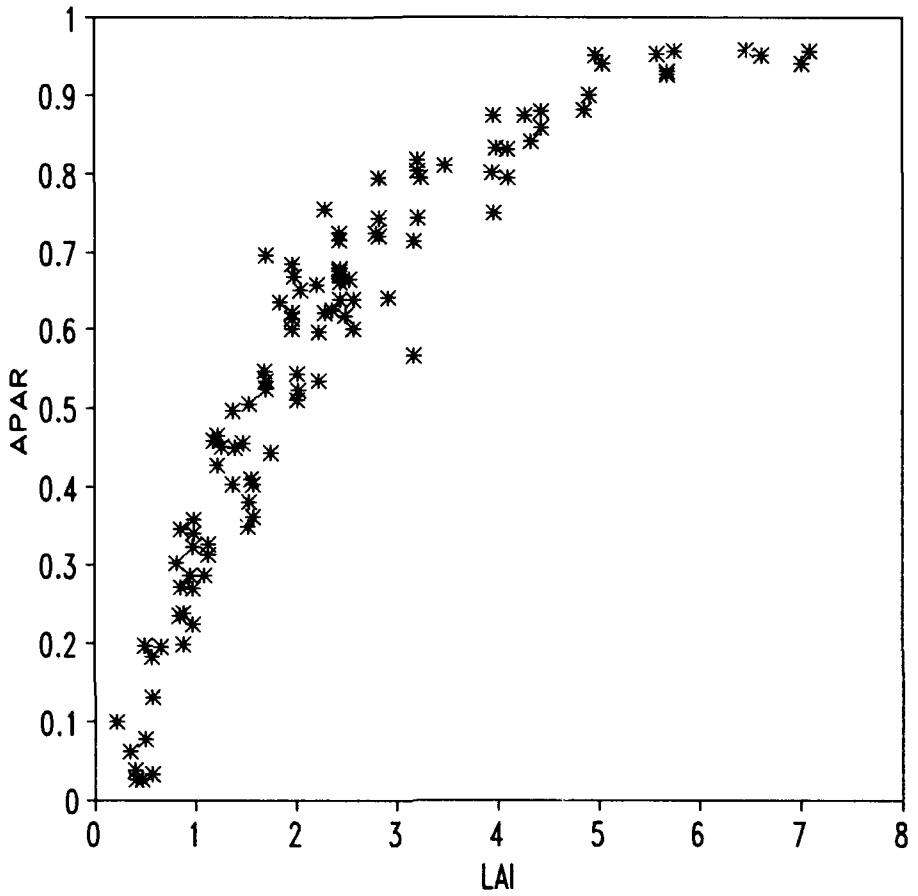

Fig. 26. Scatter plot of leaf area index (LAI) versus fraction of absorbed photosynthetically active radiation (APAR). Data averaged by run (AVG data set).

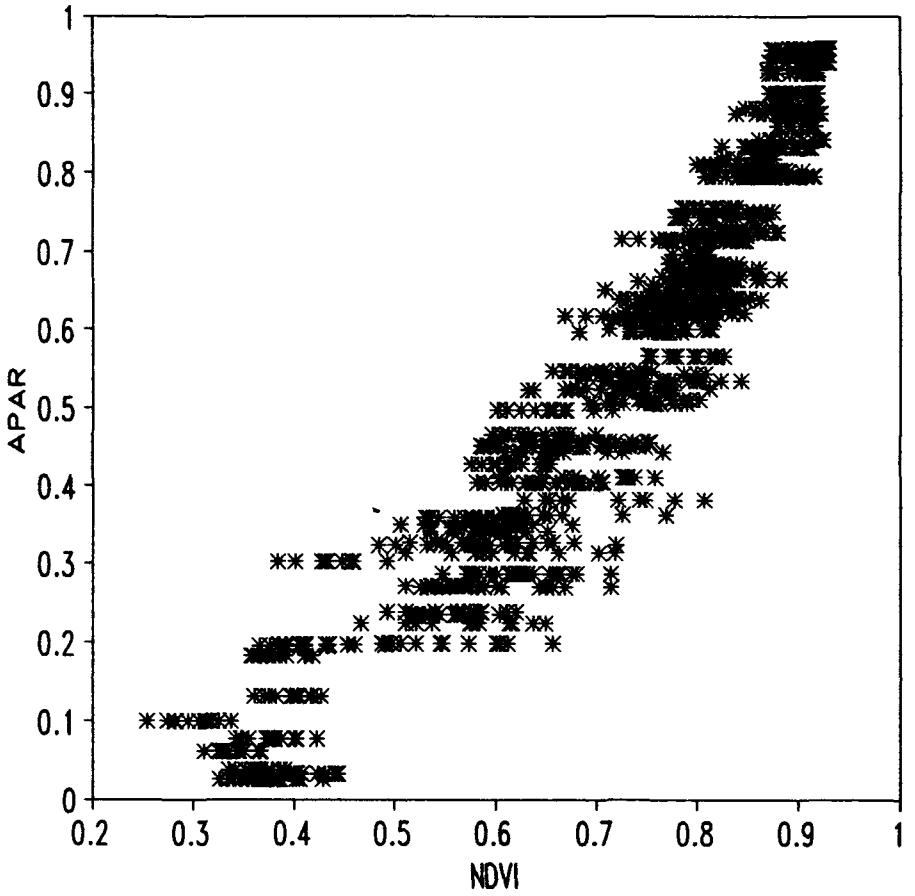

Fig. 27. Scatter plot of normalized difference vegetative index (NDVI) versus fraction of absorbed photosynthetically active radiation (APAR). Data averaged by run (AVG data set).

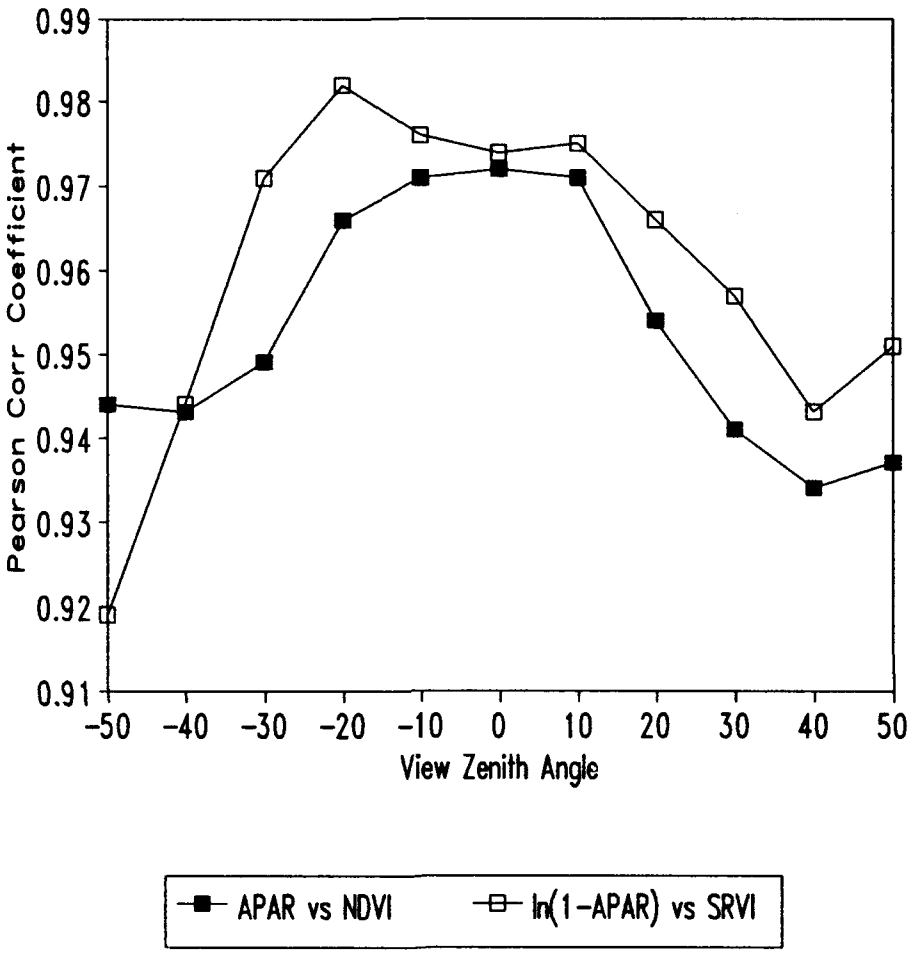

Fig. 28. Absolute value of Pearson correlation coefficient for normalized difference and simple ratio vegetative indices (NDVI, SRVI) vs APAR as function of view zenith angle. SRVI and ln(1-APAR) are negatively correlated. Negative view zenith angle indicates backscattering.

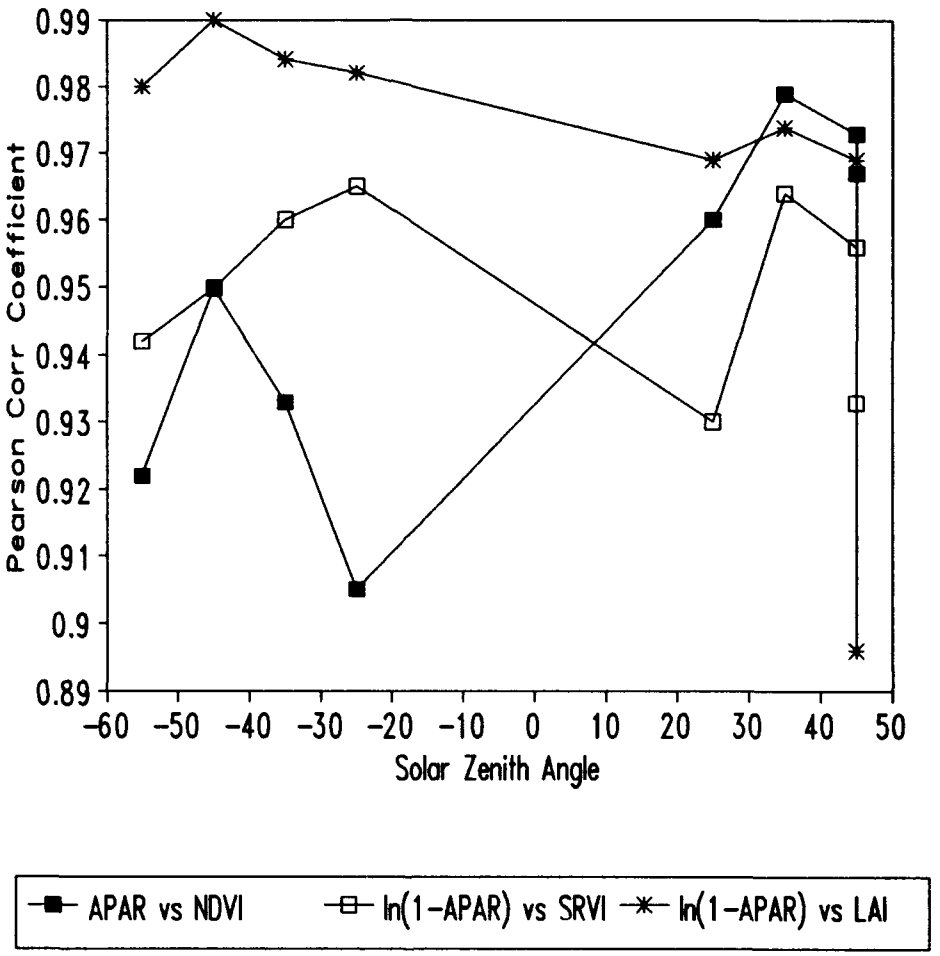

Fig. 29. Absolute value of Pearson correlation coefficient between APAR and NDVI, SRVI and LAI as a function of solar zenith angle. SRVI and LAI are negatively correlated to ln(1-APAR). Solar zenith angles prior to solar noon are negative.

relationship. Results from the ANOVA on the regression parameters show the significance of view and solar zenith angle changes on the relationships (Table 11). The AMPM main effect was significant for the estimation of APAR by NDVI and LAI regression parameters but not for the APAR vs SRVI regression parameters. However, the VZA * AMPM interaction term was significant for the SRVI vs APAR regression parameters. The effect of SZA was significant for all tested estimators of APAR. VZA effects were highly significant for SRVI vs APAR regression parameters but not for NDVI using the LSN data set. However, the NDVI vs APAR regression parameters were significantly (Prob > F = 0.00) dependent on VZA for both the SYM and AMBAL data sets.

The change in regression parameters for the SRVI vs APAR relationship, like those for the SRVI vs LAI relationship, show a smooth trend with changing VZA (Fig. 30). These trends are mirror images of those exhibited for the SRVI vs LAI relationship (Fig. 20). This is a result of SRVI being positively correlated to LAI but negatively correlated to the transformed APAR (ln(1-APAR)) required for the linear regression of SRVI and APAR. Regression parameters for the NDVI vs APAR relationship as a function of VZA (Fig. 31) change in a similar manner to the regression parameters for the NDVI vs LAI relationship (Fig. 18). No functional relationship appears to exist between SZA and any of the regression parameters for the estimation of APAR (Figs. 32-34). Appendix C provides a complete listing of the regression parameters of the VIs and LAI vs APAR relationships, the coefficients of determination (r^2), and the RMSEs for each combination of SZA and VZA for both the LSN and AVG data sets. These results indicate that, for all SZAs, APAR is best estimated from VIs

TABLE 11.
Probability of a larger F value for ratio of appropriate mean square error to test significance of source of variation. Probability < 0.05 indicates differences in regression slope coefficients for stated relationship (from LSN data set) as a result of source of variation are significant.

	Probability > F		
Source of Variation	APAR vs NDVI	APAR vs SRVI	APAR vs LAI
AMPM	0.03	0.36	0.04
SZA	0.00	0.00	0.00
SZA * AMPM	0.00	0.64	
VZA	0.19	0.00	
VZA * AMPM	0.99	0.00	
VZA * SZA	0.99	0.32	
VZA * SZA * AMPM	0.99	0.95	

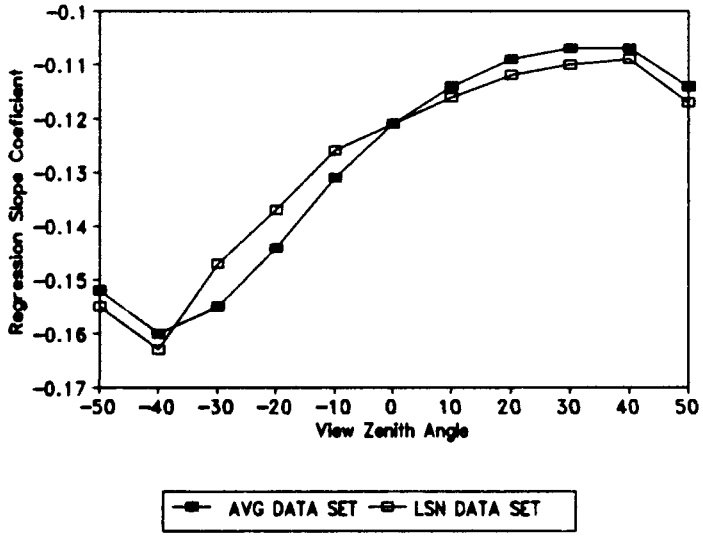

(a)

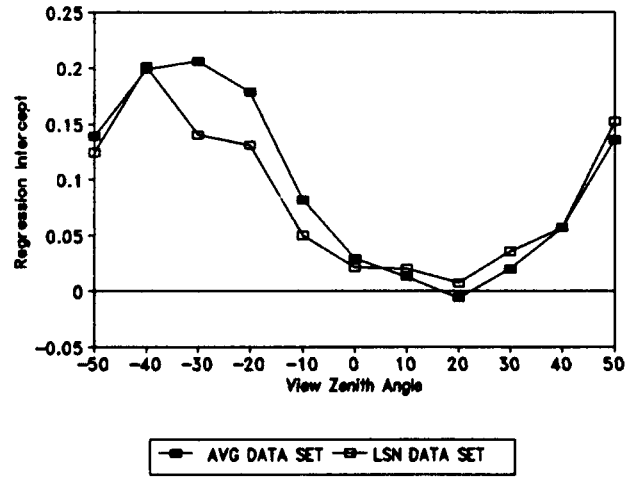

(b)

Fig. 30. Regression coefficients as a function of view zenith angle for SRVI vs APAR relationship. Negative view zenith angle indicates backscattering. a) Regression slope coefficient. b) Regression intercept.

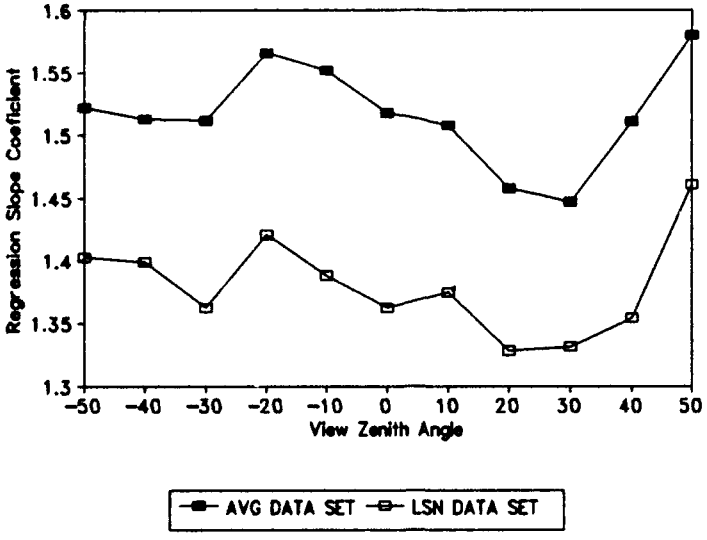

(a)

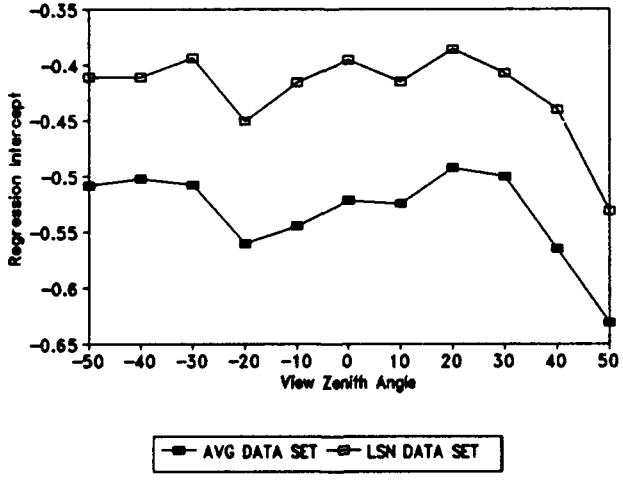

(b)

Fig. 31. Regression coefficients as a function of view zenith angle for NDVI vs APAR relationship. Negative view zenith angle indicates backscattering. a) Regression slope coefficient. b) Regression intercept.

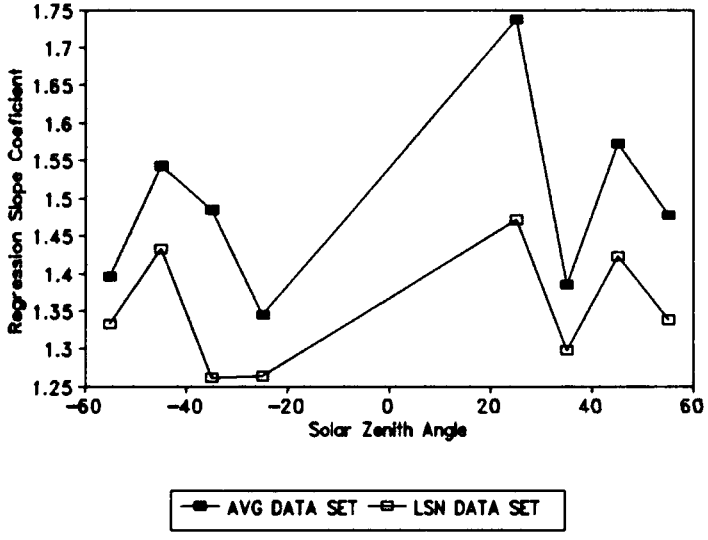

(a)

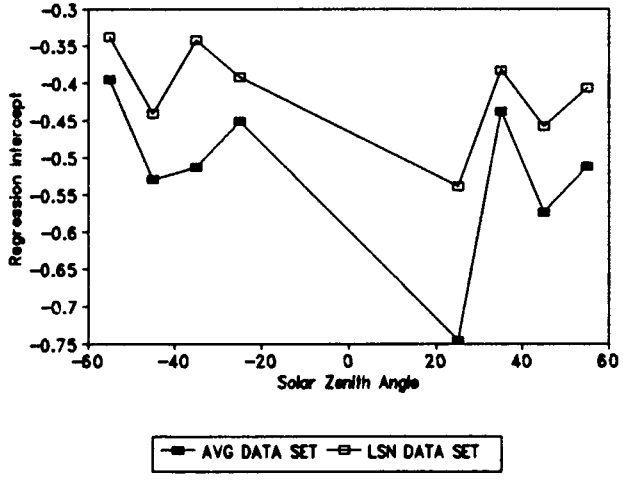

(b)

Fig. 32. Regression coefficients as a function of solar zenith angle for NDVI vs APAR relationship. Solar zenith angles prior to solar noon are negative. a) Regression slope coefficient. b) Regression intercept.

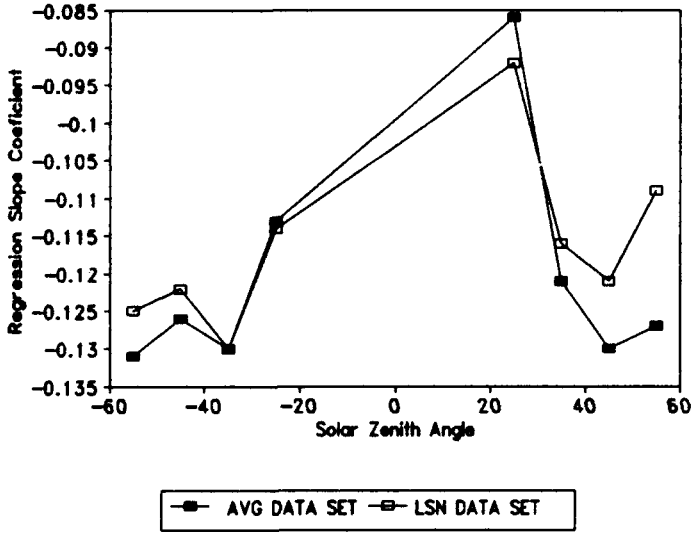

(a)

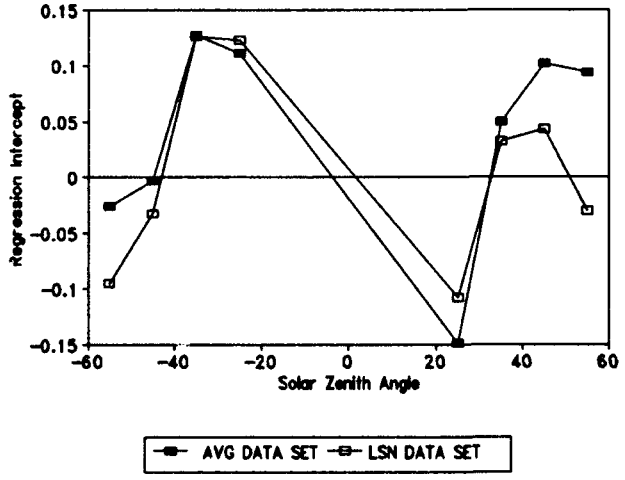

(b)

Fig. 33. Regression coefficients as a function of solar zenith angle for SRVI vs APAR relationship. Solar zenith angles prior to solar noon are negative. a) Regression slope coefficient. b) Regression intercept.

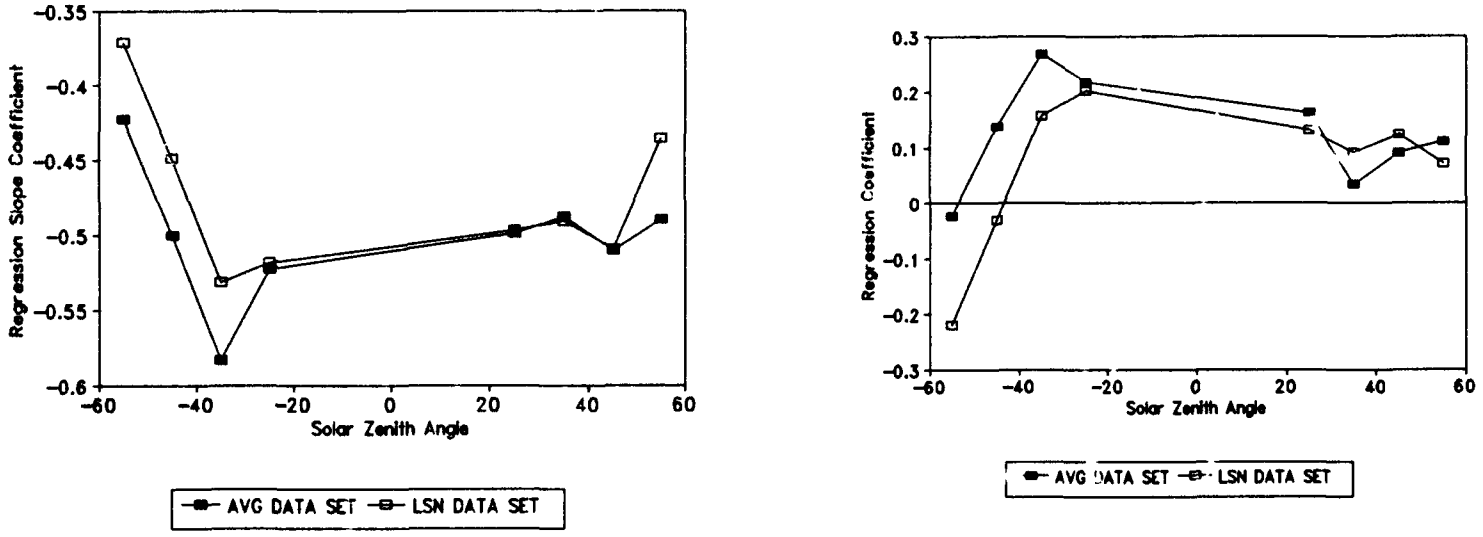

(a) (b)

Fig. 34. Regression coefficients as a function of solar zenith angle for LAI vs APAR relationship. Solar zenith angles prior to solar noon are negative. a) Regression slope coefficient. b) Regression intercept.

derived from BRFs at nadir or slightly off nadir VZAs. Similarly, Novo et al. (1989), in a laboratory experiment, found the relationship between spectral reflectance and suspended sediment concentration (SCC) was "best" when reflectance measurements were made with a nadir view zenith angle. There does not appear to be any "best" SZA for estimation of APAR from VIs. The overall regression parameters for the estimation of APAR by NDVI from the AVG data set (β_0 = -0.52, β_1 = 1.50) are very similar to those found by Wiegand et al. (1990) (β_0 = -0.49), β_1 = 1.52) from pooled spectral data taken over corn at different experimental sites. LAI best estimated APAR at small SZAs.

Figs. 35 and 36 provide a measure of the error involved with using data from all measured VZAs in a regression equation based on nadir BRF data. With both VIs mean relative error for the estimation of APAR is less than 7%. As with the estimation of LAI, it appears that the ability for NDVI to estimate APAR drops off at high values of APAR (Fig. 35) while SRVI estimates APAR poorly at very low values of APAR (Fig. 36). Mean relative error for the estimation of APAR with VIs computed from nadir and off-nadir data with a nadir-derived regression equation is greater for oblique view angles in the forward scatter view direction than oblique angles in the backscatter view direction (Fig. 37). This follows from the way in which the VIs change as a function of VZA (Figs. 8-9), i.e. mean relative change from nadir is less in the backscatter direction than in the forward scatter direction. For estimation of APAR by LAI, mean relative error is somewhat higher at 12.8% with a 0.986 D-index of agreement (Fig. 38).

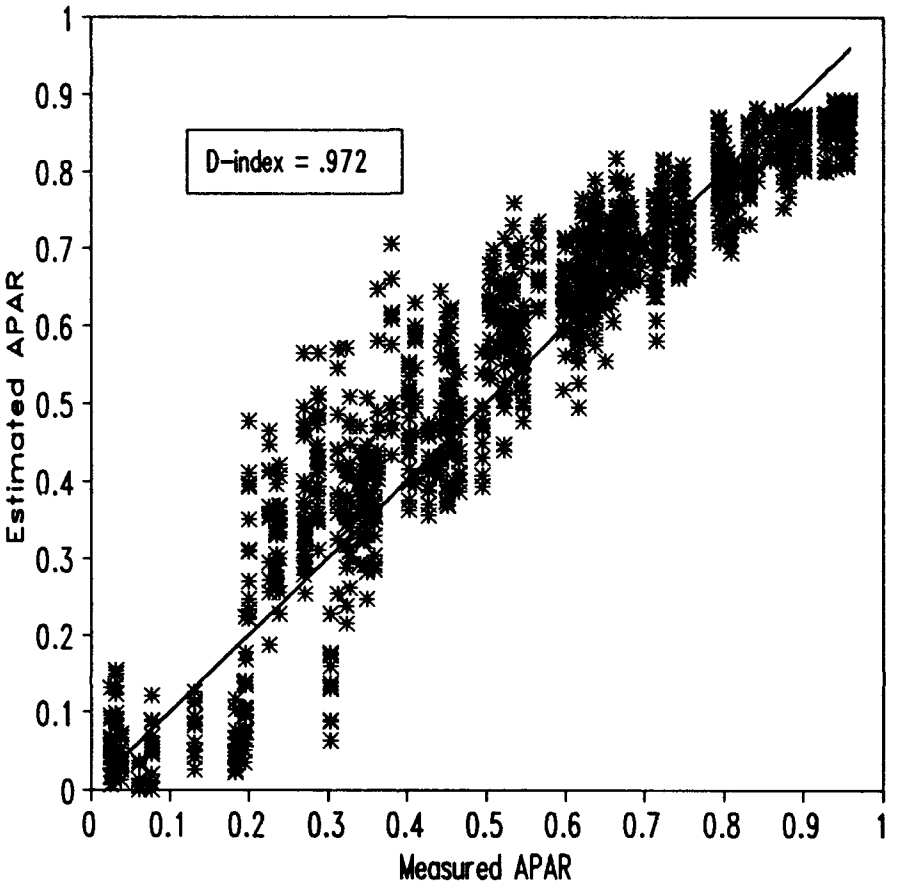

Fig. 35. Measured APAR versus estimated APAR with NDVI from all view zenith angles used in regression equation established using only nadir data.

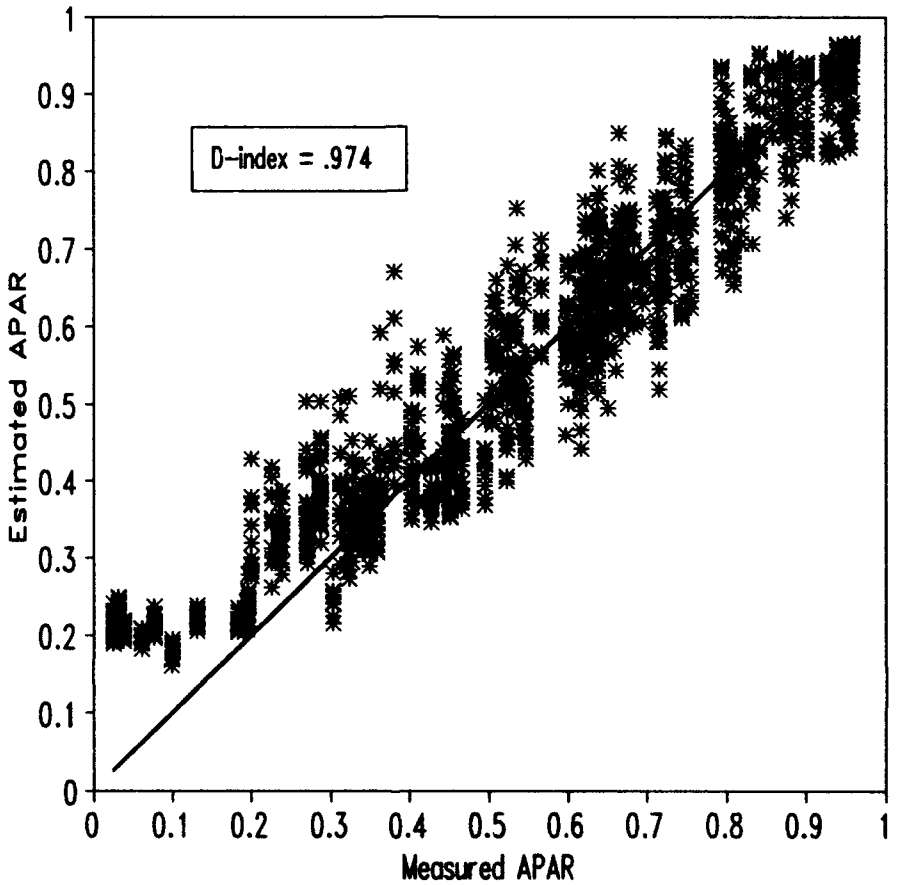

Fig. 36. Measured APAR versus estimated APAR with SRVI from all view zenith angles used in regression equation established using only nadir data.

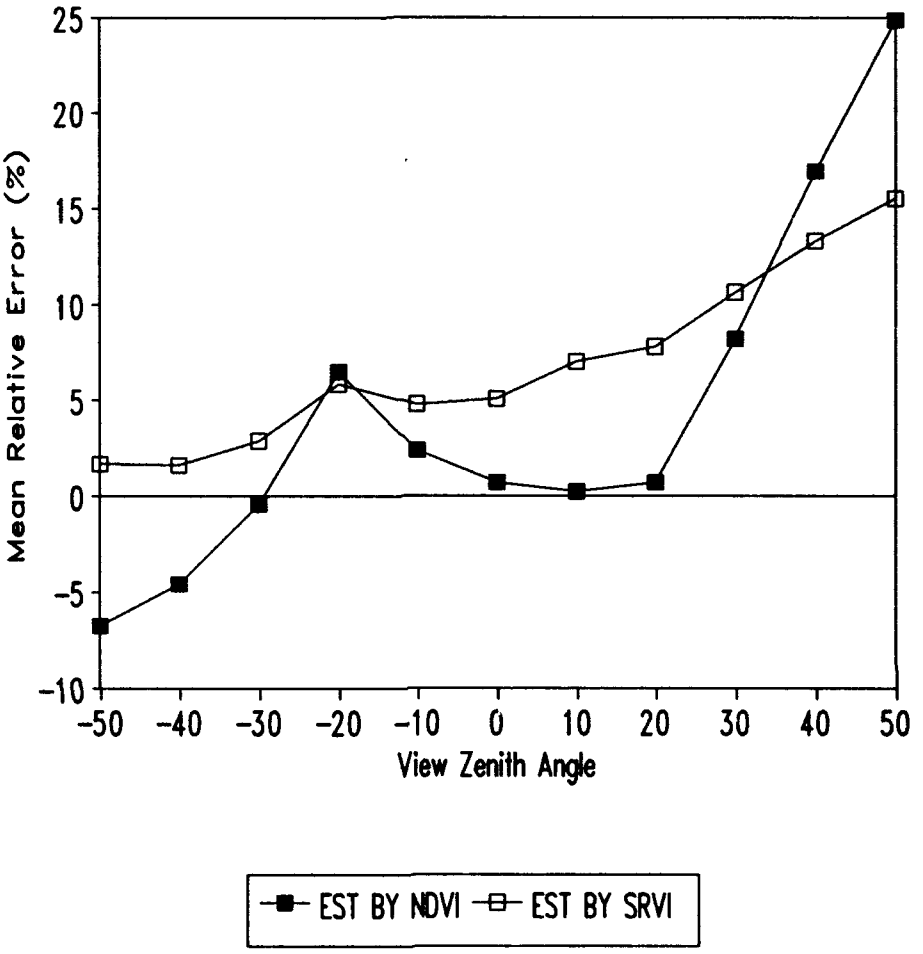

Fig. 37. Mean relative error of estimation of APAR by normalized difference and simple ratio vegetative indices (NDVI, SRVI) as function of view zenith angle. Negative view zenith angle indicates backscattering.

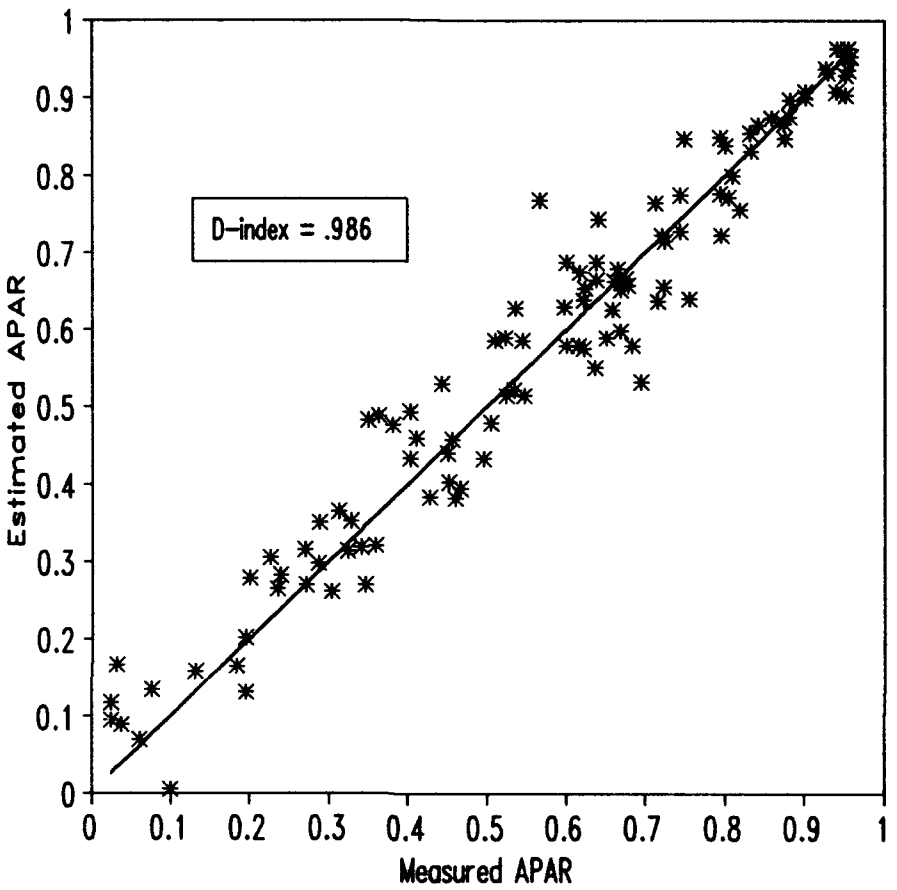

Fig. 38. Measured APAR versus APAR estimated from LAI.

Estimation of above ground dry weight

Two approaches can be taken to use spectral reflectance data and leaf area measurements to estimate above ground dry phytomass weight (ABGDWT): 1) The VIs and LAI can be used to estimate APAR which in turn is used to estimate ABGDWT in a manner similar to that used to estimate total (above and below ground) dry matter (DM):

$$DM = \Sigma \, APAR * I_{par} * E_c \, \Delta t$$

where, APAR = Daily fraction of absorbed photosynthetically active radiation;

I_{par} = Quantity of incoming PAR radiation, $MJm^{-2}day^{-1}$;

E_c = Efficiency of radiant energy conversion to dry matter, gMJ^{-1} (a function of the availability of water and nitrogen);

Δt = time interval, days;

and 2) A direct relationship can be established between the spectral data in the form of VIs or LAI measurement and ABGDWT.

Since both APAR and VIs such as NDVI are functions of SZA (Fig. 39) estimating daily values for these parameters can be complex. Ideally, values are measured throughout the day to establish a relationship for APAR/VI as a function of time of day which when integrated provides a daily value for APAR. In this study, linear regression was used to get expressions for APAR, VIs, and LAI as functions of DOY. Daily values of APAR/VIs could be roughly approximated since instantaneous values of APAR/VIs were measured at different SZAs. Separate regression lines were fit for VIs derived from nadir and ± 50° VZAs as a means of accounting for

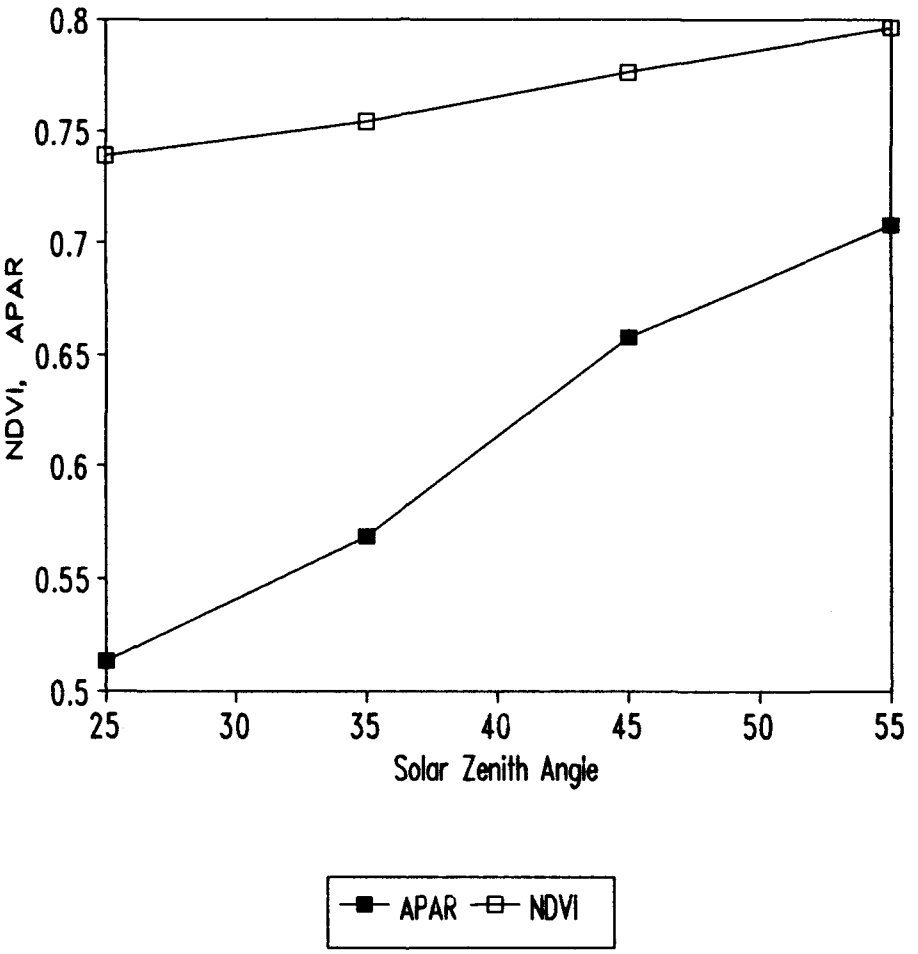

Fig. 39. APAR and NDVI as a function of solar zenith angle. Data from days in which all solar zenith angles (25,35,45,55°) prior to solar noon was represented (AMBAL data set).

the VZA effect (Table 12). By using regression equations between APAR and nadir-derived VIs (from the AVG data set) to estimate APAR the effect of using off-nadir spectral data with an equation that was derived from nadir data can be seen. The overall regression (all SZAs) between LAI and instantaneous APAR was used to estimate daily APAR from LAI as a function of DOY. From these daily APAR estimates, cumulative APAR was calculated.

The slope of the best fit line for the linear relationship between daily ABGDWT and accumulated APAR was used as the efficiency of radiant energy conversion to ABGDWT, E_c, (Fig. 40). As can be expected, E_c differed between growth cycles with a value of 1.58 g MJ^{-1} for growth cycle three and a value of 1.84 g MJ^{-1} for growth cycle four. Experimental evidence indicates that a healthy green crop not limited by disease or water stress has an E_c in the range 1.5 - 2.0 g MJ^{-1} (Steven et al., 1983). Combined data from the third and fourth growth cycles were used to estimate E_c. The third and fourth growth cycles were used because oven-drying of phytomass was done more consistently during these two growth cycles.

Differences in the ability to estimate ABGDWT from APAR from one growing cycle to the next may be due to changes in E_c. Some researchers believe that VIs may actually be able to reflect these changes, so VIs may be better correlated to the product of APAR and E_c than to APAR alone (Steven et al., 1983).

To calculate ABGDWT directly from the VIs, a regression line was fit to the ABGDWT data and the accumulated nadir derived VI through time (Table 13). The regression equation derived from the fourth growth cycle was used to estimate ABGDWT for the third growth cycle and vice versa.

TABLE 12.
Regression parameters for linear regressions between day of year (DOY) and APAR, normalized difference and simple ratio vegetative indices (NDVI, SRVI), and LAI for third and fourth growth cycles. View zenith angle given in parentheses for vegetative indices.

Dependent Variable	Third Growth Cycle				Fourth Growth Cycle			
	β_0	β_1	r^2	RMSE	β_0	β_1	r^2	RMSE
APAR	-4.90	0.025	0.86	0.066	-7.02	0.030	0.85	0.107
NDVI(50)	-2.97	0.017	0.83	0.048	-4.25	0.020	0.80	0.082
NDVI(0)	-3.37	0.019	0.86	0.047	-4.37	0.020	0.82	0.077
NDVI(-50)	-3.18	0.018	0.90	0.038	-4.40	0.020	0.82	0.078
SRVI(50)	-98.0	0.494	0.89	1.070	-132	0.555	0.90	1.490
SRVI(0)	-82.8	0.416	0.82	1.230	-114	0.480	0.87	1.500
SRVI(-50)	-72.0	0.364	0.88	0.846	-86.5	0.367	0.93	0.856
LAI	-15.4	0.079	0.93	0.452	-18.5	0.078	0.99	0.163

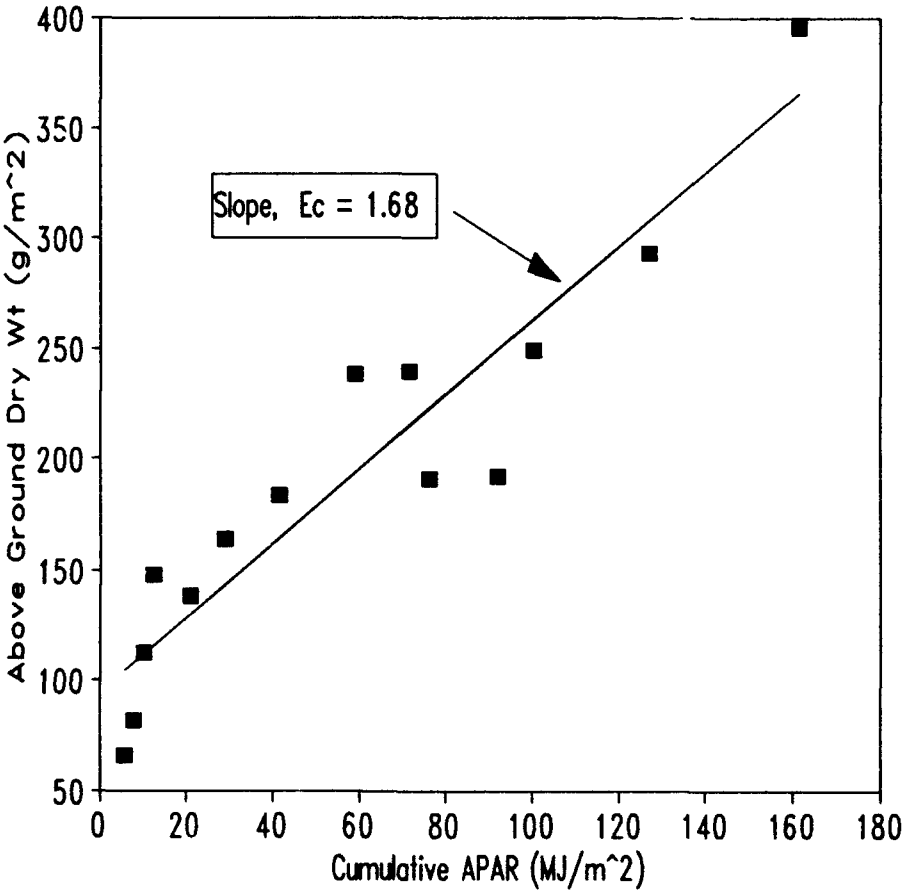

Fig. 40. Relationship between measured above ground dry phytomass weight (ABGDWT) and accumulated absorbed photosynthetically active radiation (APAR). Slope of regression line represents the efficiency of conversion of light to ABGDWT, Ec.

TABLE 13.
Regression parameters for linear regression between acummulated nadir normalized difference and simple ratio vegetative indices (NDVI, SRVI), LAI, and above ground dry weight (ABGDWT) for third and fourth growth cycles.

ABGDWT Estimator	Third Growth Cycle				Fourth Growth Cycle			
	β_0	β_1	r^2	RMSE	β_0	β_1	r^2	RMSE
ΣNDVI	52.75	12.45	0.75	36.2	62.73	12.26	0.89	24.10
ΣSRVI	126.70	1.30	0.85	28.3	107.30	1.02	0.79	32.60
LAI	58.95	99.35	0.69	40.2	49.98	114.90	0.97	12.25

This same approach was taken with the relationship between ABGDWT and LAI. Only the third and fourth growth periods had enough measurements to get the full range of APAR/VIs values.

For the most part, estimates of ABGDWT from measured or estimated APAR were less than the mean measured ABGDWT (Table 14). Regressions of VIs vs APAR for all growth cycles showed that the regression parameters for these relationships were just as variable between growth periods (Table 15) as they were due to changes in solar or view zenith angles (Appendix C). The consistent underestimation of ABGDWT from measured and estimated APAR could be the result of: 1) the method in which daily APAR was calculated; 2) fitting a line rather than a curve to the relationship between APAR and DOY resulting in the underestimation of daily APAR and 3) the use of the overall regression relationship (i.e. from all 107 runs) between VIs/LAI and APAR to estimate APAR from the VIs/LAI.

Estimates of ABGDWT from accumulated VIs underestimated ABGDWT for growth cycle three and overestimated ABGDWT for growth cycle four. SZA influence on the VIs is the most likely reason for this. The average SZA is larger for growth cycle four as compared to growth cycle three (44 vs 38°) and since the relationship between accumulated VIs and ABGDWT from growth cycle four was used to estimate the ABGDWT for growth cycle three and vice versa the same amount of vegetation can be expected to be associated with a higher VI for growth cycle four as compared to three. LAI was the most consistent estimator of ABGDWT over the two growth cycles.

TABLE 14.
Estimated and mean measured above ground dry weight (ABGDWT) and mean relative error (MRE) of estimated ABGDWT with respect to measured mean. View zenith angle for normalized difference and simple ratio vegetative indices (NDVI, SRVI) given in parentheses.

ABGDWT Estimator	Third Growth Cycle		Fourth Growth Cycle	
	ABGDWT (gm^{-2})	MRE (%)	ABGDWT (gm^{-2})	MRE (%)
APAR	271	-32	214	-27
APAR by NDVI(-50)	272	-31	193	-34
APAR by NDVI(0)	291	-27	217	-26
APAR by NDVI(50)	270	-32	311	6
APAR by SRVI(-50)	246	-38	204	-30
APAR by SRVI(0)	252	-36	222	-24
APAR by SRVI(50)	288	-27	241	-17
APAR by LAI	241	-39	155	-47
ΣNDVI (-50)	343	-13	306	4
ΣNDVI (0)	352	-11	320	9
ΣNDVI (50)	343	-13	371	27
ΣSRVI (-50)	341	-14	368	26
ΣSRVI (0)	294	-26	411	40
ΣSRVI (50)	288	-27	454	55
LAI	369	-7	275	-6
Measured Mean	396	-	293	-

TABLE 15.
Results of linear regression for normalized difference and simple ratio vegetative indices (NDVI, SRVI) vs APAR for growth cycles two through four. Includes data from all view and solar zenith angles from AVG data set.

Growth Cycle	NDVI vs APAR				SRVI vs APAR			
	β_0	β_1	r^2	RMSE	β_0	β_1	r^2	RMSE
2	-0.62	1.56	0.810	0.083	0.07	-0.12	0.821	0.180
3	-0.33	1.23	0.828	0.072	-0.05	-0.11	0.760	0.210
4	-0.45	1.42	0.955	0.057	0.09	-0.13	0.922	0.159

SUMMARY AND CONCLUSION

A field experiment was conducted to examine the relationships between two commonly used VIs, the simple ratio vegetative index (SRVI) and the normalized difference vegetative index (NDVI), and the biophysical parameters of leaf area index (LAI) and fraction of absorbed photosynthetically active radiation (APAR) for alfalfa. Statistical tests were run to determine if significant differences (at $\alpha = 0.05$) existed for the regression coefficients from relationships established using VIs calculated at different solar and view zenith angles. The results of these statistical tests showed that the regression coefficients (slope and intercept) for the relationships between VIs and APAR/LAI were significantly different for different solar and view zenith angles. Additionally, the relationships were not symmetrical about solar noon and significant interaction existed between the main effects. This was attributed to changes in canopy geometry which occurred throughout the day as the result of alfalfa's diaheliotropism. In most cases, regression coefficients did not appear to have a functional relationship to view or solar zenith angle. However, in the cases of SRVI vs LAI and SRVI vs APAR, regression coefficients exhibited a smooth trend as a function of VZA indicating that the VZA effect may be modelled and corrected for in these cases. No one combination of view and solar zenith angles best predicted LAI from the VIs while APAR was best estimated from VIs calculated from bidirectional reflectance factors with nadir/near-nadir view zenith angles. Despite the statistical significance of the view and solar zenith angle effects, D-indices of agreement between measured and

estimated APAR/LAI were very high when VI data from all view and solar zenith angles were used in regressions established with nadir VI data. As reported by other researchers, NDVI lost its sensitivity to changes in vegetation amount as LAI approached 4.0 while SRVI was fairly insensitive to changes in vegetative amount at low LAIs. Similarly, when estimating APAR, NDVI was a poor estimator at high values of APAR and SRVI was a poor estimator at low values of APAR. NDVI was less affected by changes in solar and view zenith angles than SRVI and subsequently had about half as much variation in the regression coefficients as a result of changes in view and solar zenith angle than SRVI.

Both measured and estimated APAR (by VIs and LAI) accumulated over time consistently underestimated above ground dry weight (ABGDWT). This may have been the result of error involved in determining daily APAR and using a linear model to describe daily APAR as a function of day of year. Estimates of ABGDWT from accumulated VIs and LAI had lower overall mean relative errors than APAR estimates of ABGDWT. This could be a result of VIs and LAI being able to reflect some of the changes in the efficiency of radiant energy conversion to dry matter exhibited from growth cycle to growth cycle. Using VIs calculated from off-nadir ($\theta_v = \pm 50°$) spectral data in nadir-derived relationships, changed ABGDWT estimates by at most 15%. The mean relative error for the estimation of ABGDWT when averaged over the two growth cycles tested was lowest for accumulated nadir-derived NDVI estimates of ABGDWT.

Suggestion for future research

Similar studies should be conducted with other canopies. However, because the assumptions underlying the analysis of a split-plot in time: 1) homogeneity of error variance among levels of the independent variable and 2) identical correlations between measurements for any two periods are unrealistic in these studies, a repeated measures experimental design is recommended (Eskridge and Stevens, 1987). Since current measurement techniques limit the number of experimental plots that can be measured in the 20 - 30 minutes required to limit changes in SZA, fewer treatment levels would have to be used to get the needed degrees of freedom for error in a repeated measure analysis. This can be done by making spectral measurements in just three VZAs (at nadir and extreme off-nadir values in the forward and backscattered directions rather than the eleven VZAs used in this experiment.) This would also result in less correlation of random error between experimental units since the experimental units would not overlap as they did in this experiment. The architectural changes in the alfalfa canopy as a result of its diaheliotropic nature was a contributing factor in the regression coefficients being nonsymmetrical with respect to solar noon. These same kind of results can be expected for row crops, requiring measurements before and after solar noon.

The data set generated by this experiment could be used with a radiative transfer model to simulate what effect differing atmospheric conditions may have. Holben et al. (1986) reported that off-nadir reflectances were approximately maintained when factoring in the atmosphere, the magnitude of response across the VZAs changed but the

shape of the reflectance vs VZA curve did not. Other researchers have indicated that interpretable spectral results may not be obtainable from satellites without prior atmospheric corrections (Dave, 1980; Jackson et al., 1983).

In this study the non-Lambertian aspects of leaf reflectance played a major role in explaining observed canopy reflectance. If view or solar zenith angle correction factors are going to be applied to spectral data, more research is needed to determine the spatial resolution and canopy architecture at which non-Lambertian effects are of concern.

The technology of remote sensing is advancing at a rapid pace. The ability to process and transmit data at ever increasing speeds is making the move toward narrow-band sensors more practical. Spectral curve analysis may prove to be a more repeatable and subsequently more standardized method to estimate the quantity and quality of vegetation than broad-band VIs (see for eg. Demetriades-Shah et al., 1990; Hall et al., 1990). This would conveniently settle the current quandary over the "best" vegetative index. If not, the question of what radiometric precision is most appropriate for the task at hand must be addressed.

REFERENCES

Aase, J.K. and F.H. Siddoway. 1980. Determining winter wheat stand densities using spectral reflectance measurements. Agron. J., 72:149-152.

Ahlrichs, J.S., and M.E. Bauer. 1983. Relation of Agronomic Multispectral Reflectance Characteristics of Spring Wheat Canopies. Agron. J., 75:987-993.

Ajai, D.S. Kamat, G.S. Chaturvedi, A.K. Singh, and S.K. Singh. 1983. Spectral assessment of leaf area index, chlorophyll content, and biomass of chickpea. Photogram. Engr. Remote Sens., 49:1721-1727.

Anderson, M.C. 1966. Stand structure and light penetration II. A theoretical analysis. J. Appl. Ecol., 3:41-54

Ashley, M.D. and J. Rhea. 1975. Remote sensing seasonal vegetation differences from ERTS imagery. Photogram. Engr. Remote Sens., 41:713-719.

Asrar, G., M. Fuchs, E.T. Kanemasu, and J.L. Hatfield. 1984. Estimating absorbed photosythetic radiation and leaf area index from spectral reflectance in wheat. Agron J., 76:300-306.

Asrar, G., E.T. Kanemasu, and M.Yoshida. 1985a. Estimation of leaf area index from spectral reflectance of wheat under different cultural practices and solar angle. Remote Sens. Environ., 17:1-12.

Asrar, G., E.T. Kanemasu, R.D. Jackson, P.J. Pinter, Jr. 1985b. Estimation of total above-ground phytomass using remotely sensed data. Remote Sens. Environ., 17:211-220.

Badwar, G.D., W. Verhoef, and N.J.J. Bunnick. 1985. Comparative study of Suits and SAIL canopy reflectance models. Remote Sens. Environ., 17:179-195.

Baret, F., I. Champion, G. Guyot, and A. Podaire. 1987. Monitoring wheat canopies with a high spectral resolution radiometer. Remote Sens. Environ., 22:367-378.

Barnsley, M.J. 1984. Effects of off-nadir view angles on the detected spectral response of vegetation canopies. Intl J. Remote Sens., 5:715-728.

Barnsley, M.J. and S.A.W. Kay. 1990. The relationship between sensor geometry, vegetation-canopy geometry and image variance. Intl. J. Remote Sens., 11:1075-1083.

Bartlett, D.S., R.W. Johnson, M.A. Hardisky, and V. Klemas. 1986. Assessing impacts of off-nadir observations on remote sensing of vegetation: use of the Suits model. Intl J. Remote Sens., 7:247-264.

Bartlett, D.S., G.J. Whiting, J.M. Hartman. 1990. Use of vegetation indices to estimate intercepted solar radiation and net carbon dioxide exchange of a grass canopy. Remote Sens. Environ., 30:115-128.

Bauer, M.E., B.F. Robinson, C.S. Daughtry, and C.C. Biehl. 1981. Field measurement workshop, Oct 14-16. Laboratory of apllications of remote sensing, Purdue Univ., Lafayette, IN.

Best, R.G. and J.C. Harlan. 1985. Spectral estimation of green leaf area index of oats. Remote Sens. Environ., 17:27-36.

Brakke, T.W. and J. Otterman. 1990. Canopy bidirectional reflectance dependence on leaf orientation. Intl. J. Remote Sens., 11:1023-1032.

Breece, H.T. and R.A. Holmes. 1971. Bidirectional scattering characteristics of healthy green soybean and corn leaves in vivo. Applied Optics, 10:119-127.

Campbell, J.B. 1987. Introduction to remote sensing. Guilford Press, New York.

Chance, J.E., and E.W. LeMaster. 1978. Plant canopy light absorption model with application to wheat. Applied Optics, 17:2629-2636.

Choudhury, B.J. 1987. Relationships between vegetation indices, radiation absorption, and net photosynthesis evaluated by a sensitivity analysis. Remote Sens. Environ., 22:209-233.

Clevers, J.G.P.W. 1989. The application of a weighted infrared-red vegetation index for estimating leaf area index by correcting for soil moisture. Remote Sens. Environ., 29:25-37.

Colwell, J.E. 1974. Vegetation Canopy Reflectace. Remote Sens. Environ., 3:175-183.

Cowan, I.R. 1968. The interception and absorption of radiation in plant stands. J Appl. Ecol., 5:367-379.

Crist, E.P. 1984. Effects of cultural and environmental factors on corn and soybean spectral development patterns. Remote Sens. Environ., 14:3-13.

Curran, P.J. and A.M. Hay. 1986. The importance of measurement error for certain procedures in remote sensing at optical wavelengths. Photogram. Engr. Remote Sens., 52:229-241.

Daughtry, C.S.T., M.E. Bauer, D.W. Crecelius, and M.M. Hixson. 1980. Effects of management practices on reflectance of spring wheat canpoies. Agron. J., 72:1055-1060.

Daughtry, C.S.T., K.P. Gallo, and M.E. Bauer. 1983. Spectral estimates of solar radiation intercepted by corn canopies. Agron J., 75:527-531.

Dave, J.V. 1980. Effect of atmospheric conditions on remote sensing of vegetation parameters. Remote sens. Environ., 10:87-90.

Deering, D.W. and T.F. Eck. 1987. Atmospheric optical depth effects on angular anisotropy of plant canopy reflectance. Intl J. Remote Sens., 8:893-916

Deering, D.W. and E.M. Middleton. 1990. Spectral bidirectional reflectance and effects on vegetation indices for a prairie grassland. Symposium on FIFE, Feb 7-9. Anaheim, CA.

Demetriades-Shah, T.H., M.D. Steven, and J.A. Clark. 1990. High resolution derivative spectra in remote sensing. Remote Sens. Environ., 33:55-64.

Duggin, M.J. 1977. Likely effects of solar elevation on the quantification of changes in vegetation with maturity using sequential Landsat imagery. Applied Optics, 16:521-522.

Duggin, M.J. and T. Cunia. 1983. Ground reflectance measurements techniques: a comparison. Applied Optics, 22:3771-3777.

Duggin. M.J. and W.R. Philipson. 1982. Field measurement of reflectance: some major considerations. Applied Optics, 21:233-2840.

Duggin, M.J. and D. Piwinski. 1984. Recorded radiance indices for vegetation monitoring using NOAA-AVHRR data; atmospheric and other effects in multitemporal data sets. Applied Optics, 23:2620-2623.

Duggin. M.J., D. Piwinski, V. Whitehead, and G. Ryland. 1982. Evaluation of NOAA-AVHRR data for crop assessment. Applied Optics, 21:1873-1875.

Dusek, D.A., R.D Jackson, and J.T. Musick. 1985. Winter wheat vegetation indices calculated from combinations of seven spectral bands. Remote Sens. Environ., 18:255-267.

Egbert, D.D. and F.T. Ulaby. 1972. Effect of angles on reflectivity. Photogram. Engr. Remote Sens., 38:556-565.

Eskridge, K.M. and E.J. Stevens. 1987. Growth curve analysis of temperature-dependent phenology models. Agron. J., 79:291-297.

Gallo, K.P. and C.S.T. Daughtry. 1986. Techniques for measuring intercepted and absorbed photosynthetically active radiation in corn canopies. Agron J., 78:752-756.

Gallo, K.P. and J.C. Eidenshink. 1988. Differences in visible and near-ir responses, and derived vegetation indices, for the NOAA-9 and NOAA-10 AVHRRs: A case study. Photogram. Eng. Remote Sens., 54:485-490.

Gallo, K.P., C.S.T. Daughtry, and M.E. Bauer. 1985. Spectral estimation of absorbed photosynthetically active radiation in corn canopies. Remote Sens. Environ., 17:221-232.

Gardner, B.R., B.L. Blad, D.R. Thompson, and K.E. Henderson. 1985. Evaluation and interpretation of thermatic mapper ratios in equations for estimating corn growth parameters. Remote Sens. Environ., 18:225-234.

Gerstl, S.A.W. and C. Simmer. 1986. Radiation physics and modelling for off-nadir satellite-sensing of non-lambertian surfaces. Remote Sens. Environ., 20:1-29.

Goel, N.S. and N.E. Reynolds. 1989. Bidirectional canopy reflectance and its relationship to vegetation characteristics. Intl. J. Remote Sens., 10:107-132.

Goel, N.S. and R.L. Thompson. 1985. Optimal solar/viewing geometry for an accurate estimation of leaf area index and leaf angle distribution from bidirectional canopy reflectance data. Intl J. Remote Sens., 6:1493-1520.

Gomez, K.A. and A.A. Gomez. 1983. Statistical procedures for agricultural research. John Wiley and Sons, New York.

Goudriaan, J. 1988. The bare bones of leaf-angle distribution in radiation models for canopy photosynthesis and energy exchange. Agric. For. Meteorol., 43:155-169.

Hall, F.G., K.F. Huemmrich, and S.N. Goward. 1990. Use of narrow-band spectra to estimate the fraction of absorbed photosynthetically active radiation. Remote Sens. Environ., 32:47-53.

Hatfield, J.L., G. Asrar, and E.T. Kanemasu. 1984. Intercepted photosynthetically active radiation estimated by spectral reflectance. Remote Sens. Environ., 14:65-75.

Heilman, J.L. and M.R. Kress. 1987. Effects of vegetation on spectral irradiances at the soil surface. Agron. J., 79:765-768.

Hipps, L.E., G. Asrar, and E.T. Kaemasu. 1983. Assessing the interception of photosynthetically active radiation in winter wheat. Agric. Meteo., 28:253-259.

Hinzman, L.D., M.E. Bauer, and C.S.T. Daughtry. 1986. Effects of nitrogen fertilization on growth and reflectance characteristics of winter wheat. Remote Sens. Environ., 19:47-61.

Holben, B.N. 1986. Characteristics of maximum-value composite images from temporal AVHRR data. Intl. J. Remote Sens., 8:1417-1434.

Holben, B.N., D.S. Kimes, and R.S. Fraser. 1986. Directional reflectance response in AVHRR red and near-IR bands for three cover types and varying atmospheric conditions. Remote Sens. Environ., 19:213-236.

Holben, B.N., C.J. Tucker and C. Fan. 1980. Spectral assessment of soybean leaf area and leaf biomass. Photogram. Engr. Remote Sens., 46:651-656.

Huete, A.R. 1987. Soil and sun angle interactions on partial canopy spectra. Intl. J. Remote Sens., 8:1307-1317.

Huete, A.R. 1988. A soil adjusted vegetation index (SAVI). Remote Sens. Environ., 25:295-309.

Huete, A.R. and R.D. Jackson. 1988. Soil and atmosphere influences on the spectra of partial canopies. Remote Sens. Environ., 25:89-105.

Huete, A.R., R.D. Jackson, and D.F. Post. 1985. Spectral response of a plant canopy with different soil backgrounds. Remote Sens. Environ., 17:37-53.

Irons, J.R., R.A. Weismiller, and G.W. Peterson. 1989. Soil Reflectance. p. 66-106. *In* Ghassem Asrar (ed.) Theory and applications of optical remote sensing.John Wiley & Sons, Inc., New York, New York

Jackson, R.D., P.N. Slater, and P.J.Pinter, Jr. 1983. Discrimination of growth and water stress in wheat by various vegetation indices through clear and turbid atmospheres. Remote Sens. Environ., 13:187-208.

Jackson, R.D., C.A. Jones, G. Uehara, and L.T. Santo. 1980. Remote detection of nutrient and water deficiences in sugarcane under variable cloudiness. Remote Sens. Environ., 11:327-331.

Jackson, R.D., M.S. Moran, P.N. Slater, and S.F. Biggar. 1987. Field calibration of reference reflectance panels. Remote Sens. Environ., 22:145-158.

Jackson, R.D., R.J. Reginato, P.J. Pinter, Jr., and S.B. Idso. 1979. Plant canopy information extraction from composite scene reflectance of row crops. Applied Optics, 18:3775-3782.

Kanemasu, E.T. 1974. Seasonal canopy reflectance patterns of wheat, sorghum, and soybean. Remote Sens. Environ., 3:43-47.

Kauth, R.J., and G.S. Thomas. 1976. The tassel cap - A graphic description of the spectral-temporal development of agricultural crops as seen by Landsat. Proceedings of the symposium on machine processing of

remotely sensed data, IEEE catologue No. 76, Ch 1103-1 MPRSD, LARS, Purdue, Univ., Lafayette, IN.

Kimes, D.S. 1983. Dynamics of Directional Reflectance factor distributions for vegetation canopies. Applied Optics, 22:1364-1372.

Kimes, D.S. 1984. Modeling the directional reflectance from complete homogeneous vegetation canopies with various leaf-orientation distributions. J. Opt. Soc. Am. A., 1:725.

Kimes, D.S. and J.A. Kirchner. 1982. Irradiance measurement error due to the assumption of a Lambertian reference panel. Remote Sens. Environ., 12:141-149.

Kimes, D.S., B.L. Markham, C.J. Tucker, and J.E. McMurtrey III. 1980a. Temporal relationships between spectral response and agronomic variables of a corn canopy. Remote Sens. Environ., 11:401-411.

Kimes, D.S., J.A. Smith, and K.J. Ranson. 1980b. Vegetation reflectance measurements as a function of solar zenith angle. Photogram. Eng. Remote Sens., 46:1563-1573.

Kirchner, J.A., D.S. Kimes, and J.E. McMurtrey III. 1982. Variation of directional reflectance factors with structural changes of a developing alfalfa canopy. Applied Optics, 21:3766-3774.

Kirchner, J.A., C.C. Schnetzler, and J.A. Smith. 1981. Simulated directional radiances of vegetation from satellite platforms. Intl. J. Remote Sens., 2:253-264.

Kogan, F.N. 1990. Remote sensing of weather impacts on vegetation in non-homogeneous areas. Intl. J. Remote Sens., 11:1405-1419.

Knipling, E.B. 1970. Physical and physiological basis for the reflectance of visible and near-infrared radiation from vegetation. Remote Sens. Environ., 1:155-159.

Kollenkark, J.C., C.S.T. Daughtry, M.E. Bauer, and T.L. Housley. 1982a. Effects of cultural practices on agronomic and reflectance characteristics of soybean canopies. Agron. J., 74:751-758.

Kollenkark, J.C., V.C. Vanderbilt, C.S.T. Daughtry, and M.E. Bauer. 1982b. Influence of solar illumination angle on soybean canopy reflectance. Applied Optics, 21:1179-1184.

Kriebel, K.T. 1976. On the variability of the reflected radiation field due to differing distributions of the irradiation. Remote Sens. Environ., 4:257-264.

Kriebel, K.T. 1978. Measured spectral bidirectional reflection properties of four vegetated surfaces. Applied Optics, 17:253-259.

Kumar, M. 1988. Crop canopy spectral reflectance. Intl. J. Remote Sens., 9:285-294.

Kumar, M., and J.L. Monteith. 1981. Remote sensing of crop growth. In: H. Smith (Editor), Plants and the daylight spectrum, Academic Press, London, pp133-144.

Lord, D., and R.J. Desjardins. 1985. Influence of wind on crop canopy reflectance measurements. Remote Sens. Environ., 18:113-123.

Lord, D., R.J. Desjardins, P.A. Dube, and E.J. Branch. 1985. Variations of crop canopy spectral reflectance measurements under changing sky conditions. Photogram. Engr. Remote Sens., 51:689-695.

Millard, P., G.G. Wright, M.J. Adams, R.V. Birnie, and P.Whitworth. 1990. Estimation of light interception and biomass of the potato (*Solanum tuberosum* L.) from reflection in the red and near-infrared spectral bands. Agric. For. Meteorol., 53:19-31.

Moran, M.S., R.D. Jackson, G.F. Hart, P.N. Slater, R.J. Bartell, S.F. Biggar, D.I. Gellman, and R.P. Santer. 1990. Obtaining surface reflectance factors from atmospheric and view angle corrected SPOT-1 HRV data. Remote Sens. Environ., 32:203-214.

Moran, M.S., P.J. Pinter, Jr., B.E. Clothier, and S.G. Allen. 1989. Effect of water stress on the canopy architecture and spectral indices of irrigated alfalfa. Remote Sens. Environ., 29:251-261.

Myneni, R.B., R.B. Burnett, and E.T. Kanemasu. 1987. Radiative transfer in an anisotropically scattering vegetative medium. Agric. For. Meteorol., 41:97-121.

Novo, E.M.M., J.D. Hansom, and P.J. Curran. 1989. The effect of viewing geometry and wavelength on the relationship between reflectance and suspended sediment concentration. Intl J. Remote Sens., 10:1357-1372.

Ohring, G., K. Gallo, A. Gruber, W. Planet, L. Stowe, and J.D. Tarpley. 1989. Characteristics of NOAA Satellite data. Climate and Global Change, 70:889-901.

Paltridge, G.W. and R.M. Mitchell. 1990. Atmospheric and viewing angle correction of vegetation indices and grassland fuel moisture content derived from NOAA/AVHRR. Remote Sens. Environ., 31:121-135.

Perry C.R., Jr. and L.F. Lautenschlager. 1984. Funtional equivalence of spectral vegetation indices. Remote Sens. Environ., 14:169-182.

Pinker, R.T., and L.L. Stowe. 1990. Modelling planetary bidirectional refelectance over land. Intl. J. Remote Sens., 11:113-123.

Pinter, P.J., Jr. 1986. Effect of dew on canopy reflectance and temperature. Remote Sens. Environ., 19:187-205.

Pinter, P.J., Jr., R.D. Jackson, C.E. Ezra, and H.W. Gausman. 1985. Sun-angle and canopy-architecture effects on the spectral reflectance of six wheat cultivars. Intl. J. Remote Sens., 6:1813-1825.

Pinter, P.J., Jr., R.D. Jackson, and M.S. Moran. 1990. Bidirectional reflectance factors of agricultural targets: A comparison of ground-, aircraft-, and satellite-based observations. Remote Sens. Environ., 32:215-228.

Pinter, P.J., Jr., H.L. Kelly, Jr., and S. Schell. 1987a. Spectral estimation of alfalfa biomass under conditions of variable cloud cover. p83-86. In 18th Conf. on Agric. and Forest Meteor. W. Lafayette, IN. 14-18 Sept. 1987. Am. Meteor. Soc., Boston, MA.

Pinter, P.J., Jr., G. Zipoli, G. Maraacchi, and R.J. Reginato. 1987b. Influence of topography and sensor view angle on NIR/Red ratio and greeness vegetation indices of wheat. Intl. J. Remote Sens., 8:953-957.

Ranson, K.J., L.L. Biehl, and M.E. Bauer. 1985a. Variation in spectral response of soybeans with respect to illumination, view and canopy geometry. Intl J. Remote Sens., 6:1827-1842.

Ranson, K.J., C.S.T.Daughtry, L.L. Bielhl., and M.E. Bauer. 1985b. Sun-View angle effects on reflectance factors of corn canopies. Remote Sens. Environ., 18:147-161.

Rao, V.R., E.J. Branch, A.R. Mack. 1979. Bidirectional reflectance of crops and the soil contribution. Remote Sens. Environ., 8:115-126.

Redelfs, M.S., L.R. Stone, E.T. Kanemasu, and M.B. Kirkham. 1987. Greeness-leaf area index relationships of seven row crops. Agron. J., 79:254-259.

Richardson, A.J. and C.L. Wiegand. 1977. Distinquishing vegetation from soil-background information. Photogram. Eng. Remote Sens., 43:1541-1552.

Richardson, A.J., and C.L. Wiegand. 1989. Canopy leaf display effects on absorbed, transmitted and reflected solar radiation. Remote Sens. Environ., 29: 15-24.

Ripple, W.J. 1985. Asymptotic reflectance characteristics of grass vegetation. Photogram. Engr. Remote Sens., 51:1915-1921.

Robinson, B.F., and L.L. Biehl. 1979. Calibration procedues for measurement of reflectance factor in remote sensing field research. Proc. Soc. Photo-Optical Instr.. Eng., 196:16-26.

Ross, J. and A. Marshak. 1989. The influence of leaf orientation and the specular component of leaf reflectance on the canopy bidirectional reflectance. Remote Sens. Environ., 27:251-260.

Royer, A., P. Vincent, and F. Bonn. 1985. Evaluation and correction of viewing angle effects on satellite measurements of bidirectional reflectance. Photogram. Eng. Remote Sens., 51:1899-1913.

Rudorff, B.F.T and G.T. Batista. 1990. Yield estimation of sugarcane based on agrometeorological-spectral models. Remote Sens. Environ., 33:183-192

Sellers, P.J. 1985. Canopy reflectance, photosynthesis and transpiration. Intl. J. Remote Sens., 6:1335-1372.

Sellers, P.J. 1987. Canopy reflectance, photosynthesis, and transpiration. II. The role of biophysics in the linearity of their interdependance. Remote Sens. Environ., 21:143-183.

Sharratt, B.S., D.G. Baker, and C.C. Sheaffer. 1987. Climatic effect on alfalfa dry matter production part II. Summer harvests. Agric. For. Meteorol., 39:121-129.

Shibayama, M. and C.L. Wiegand. 1985. View azimuth and zenith, and solar angle effects on wheat canopy reflectance. Remote Sens. Environ., 18:91-103.

Shibayama, M., C.L. Wiegand and A.J. Richardson. 1986. Diurnal patterns of bidirectional vegetation indices for wheat canopies. Intl J. Remote Sens., 7: 233-246.

Sinclair, T.R. and E.R. Lemon. 1974. Penetration of photosynthetically active radiation in corn canopies. Agron. J., 66:201-205.

Singh, S.M. 1987. Simulation of solar zenith angle effect on global vegetation index (GVI). Intl. J. Remote Sens., 9:237-248.

Singh, S.M. 1988. Lowest order correction for solar zenith angle to global vegetation index (GVI) data. Intl. J. Remote Sens., 9:1565-1572.

Slater, P.N. and R.D. Jackson. 1982. Atmospheric effects on radiation reflected from soil and vegetation as measured by orbital sensors using various scanning directions. Applied Optics, 21:3923-3931.

Smith, H. 1981. Plants and the daylight spectrum. Academic Press, London.

Steven, M.D., P.V. Biscoe, and K.W. Jaggard. 1983. Estimation of sugar beet productivity from reflection in the red and infrared spectral bands. Intl. J. Remote Sens., 4:325-334.

Stohr, C.J. and T.R. West. 1985. Terrain and look angle effects upon multispectral scanner response. Photogram. Eng. Remote Sens., 51:229-235.

Tarpley, J.D., S.R. Schneider and R.L. Money. 1984. Global vegetation indices from NOAA-7 meteorological satellite. J. Clim. Appl. Meteo., 23:491-494.

Travis, R.L. and R. Reed. 1983. The solar tracking pattern in a closed alfalfa canopy. Crop Science, 23:664-668.

Tucker, C.J. 1977. Asymptotic nature of grass canopy spectral reflectance. Applied Optics. 16:1151-1156.

Tucker, C.J. 1979. Red and photographic infrared linear combinations for monitoring vegetation. Remote Sens. Environ., 8:127-150.

Tucker, C.J. 1980. Remote sensing of leaf water content in the near infrared. Remote Sens. Environ., 10:23-32.

Tucker, C.J. and P.J. Sellers. 1986. Satellite remote sensing of primary production. Intl J. Remote Sens.. 7:1395-1416.

Tucker, C.J., J.H. Elgin,Jr. and J.E. McMurtrey, III. 1980. Relationships of crop radiance to alfalfa agronomic values. Intl J. Remote Sens., 1:69-75.

Van Dijk, A., S.L. Callis, C.M. Sakamoto, and W.L. Decker. 1987. Smoothing vegetation index profiles: An alternative method for reducing radiometric disturbance in NOAA/AVHRR Data. Photogram. Eng. Remote Sens., 53:1059-1067.

Vygodskaya, N.N., I.I. Gorshkova and Y.V. Fadeyeva. 1989. Theoretical estimates of sensitivity in some vegetation indices to variation in canopy condition. Intl. J. Remote Sens., 10:1857-1872.

Walburg, G., M.E. Bauer, C.S.T. Daughtry, and T.L. Housley. 1982. Effects of nitrogen on the growth, yield, and reflectance characteristics of corn canopies. Agron. J., 74:677-683.

Walter-Shea, E.A. 1987. Laboratory and field measurements of leaf spectral properties and their effects on canopy reflectance. Ph.D. Dissertation. Univer. of Nebraska - Lincoln.

Walter-Shea, E.A., J.M. Norman and B. Blad. 1989. Leaf birectional reflectance and transmittance in corn and soybean. Remote Sens. Environ., 29:161-174.

Wardley, N.W. 1984. Vegetation index variability as a function of viewing geometry. Intl J. Remote Sens., 5:861-870.

Weiser, R.L., G. Asrar, G.P. Miller, and E.T. Kanemasu. 1986. Assessing grassland biophysical characteristics from spectral measurements. Remote Sens. Environ., 20:141-152.

Wiegand, C.L., and A.J. Richardson. 1984. Leaf area, Light Inteception, and Yield Estimates from Spectral Component Analysis. Agron J., 76:543-547.

Wiegand, C.L. and A.J. Richardson. 1987. Spectral components analysis rationale, and results from three crops. Intl. J. Remote Sens., 8:1011-1032.

Wiegand, C.L., and A.J. Richardson. 1990a. Use of spectral vegetation indices to infer leaf area, evapotranspiration and yield I. Rationale. Agron J., 82:623-629.

Wiegand, C.L. and A.J. Richardson. 1990b. Use of spectral vegetation indices to infer leaf area, evapotranspiration and yield: II. Results. Agron. J., 82:630-636.

Wiegand, C.L., A.H. Gerbermann, K.P. Gallo, B.L. Blad, and D. Dusek. 1990. Multisite analyses of spectral-biophysical data for corn. Remote Sens. Environ., 33:1-16.

Wiegand, C.L., A.J. Richardson, and P.R. Nixon. 1986. Spectral components analysis: a bridge between spectal observations and agrometeorological crop models. IEEE Transactions on Geoscience and Remote Sensing., 24:83-88.

Willmott, C.J. 1981. On the validation of models. Phy. Geog., 2:184-194.

Wright, G.G. 1986. Some observations of the effect of wind turbulence on the near-infrared/red ratio. Intl J. Remote Sens., 7:173-178.

Appendix A. Mean environmental conditions and coefficients of variation (CV) for BRFs and VIs for each data run. %QDIF is percent diffuse irradiance in PAR wavelengths; RH is relative humidity; WS,WD are wind speed and direction; MTA is mean tilt angle.

DOY	SZA	B3CV	B4CV	NDCV	SRCV	%QDIF	RH	WS	WD	MTA
130	-25	21	8	2	19	17	46	6.0	209	
130	25	23	9	2	18	19	45	5.4	285	47
137	-55	30	13	2	15	19	48	7.6	290	48
137	-45	29	12	2	17	12	42	7.7	291	
137	-35	23	11	2	17	17	37	7.5	288	
137	-25	18	10	2	16	14	34	6.9	292	
137	22	17	6	2	16	13	28	6.7	280	
137	25	21	9	2	15	12	23	6.3	260	
137	35	28	13	2	15	14	21	6.1	252	50
137	45	30	13	2	16	15	21	5.5	256	
148	-45	26	9	1	15	25	68	3.7	240	44
148	-35	23	9	1	15	22	59	3.9	244	
148	-25	18	7	1	13	22	55	4.1	175	
149	-45	28	10	2	16	30	59	4.2	108	45
155	-55	28	15	2	14	16	73	2.5	140	48
155	-45	28	13	2	16	14	68	2.8	129	
155	-35	26	12	2	18	13	60	2.9	139	
155	19	26	8	3	24	12	44	4.9	106	
171	-45	31	24	16	31	13	63	4.1	323	90
171	-35	26	21	17	32	11	56	4.5	321	
171	-25	23	19	20	37	11	47	4.5	292	39
171	18	17	11	9	15	11	42	3.9	307	
171	25	29	17	20	37	12	38	3.6	288	
171	35	32	19	21	39	11	34	4.5	290	
171	45	36	22	19	40	13	32	3.3	284	90
171	55	39	25	17	40	16	31	2.6	285	
173	-52	32	25	12	31	19	80	5.1	297	

Appendix A cont. Mean environmental conditions and coefficients of variation (CV) for BRFs and VIs for each data run. %QDIF is percent diffuse irradiance in PAR wavelengths; RH is relative humidity; WS,WD are wind speed and direction; MTA is mean tilt angle.

DOY	SZA	B3CV	B4CV	NDCV	SRCV	%QDIF	RH	WS	WD	MTA
173	-45	29	22	13	30	16	78	5.1	289	61
173	-35	24	18	13	29	15	74	5.2	288	62
173	-25	20	17	16	36	14	66	6.1	296	59
173	18	16	12	9	18	17	57	6.6	289	67
176	-55	36	22	7	27	16	77	1.7	286	62
176	-45	33	19	8	29	14	70	1.5	276	62
176	-35	28	16	9	30	13	67	2.0	228	63
176	-25	28	14	11	37	13	65	2.5	248	55
176	18	17	9	7	21	13	57	2.4	118	63
176	25	28	13	9	32	15	51	1.7	121	53
176	35	28	16	9	34	17	45	1.9	105	60
176	45	31	18	8	31	18	37	2.0	116	61
176	55	34	20	7	28	28	44	2.6	81	
179	-55	31	20	3	17	27	80	6.2	134	61
179	-45	31	18	3	20	22	71	7.0	147	56
179	-35	25	16	4	22	20	61	6.9	152	56
179	-25	24	14	5	27	18	55	6.3	153	57
179	18	20	10	4	22	18	50	5.8	157	47
198	-25	17	15	14	11	17	47	7.5	180	90
204	-35	24	18	9	15	22	52	2.0	175	72
212	-55	37	20	8	24	19	79	1.6	70	54
212	-45	37	17	11	28	16	71	1.6	68	59
212	-35	32	15	12	30	15	58	1.7	107	57
212	-25	26	13	13	29	17	52	2.1	141	53
212	23	24	12	11	22	19	51	2.3	129	59
212	25	26	12	11	22	26	50	2.3	123	60
218	-55	41	23	9	32	16	75	1.2	223	62

Appendix A cont. Mean environmental conditions and coefficients of variation (CV) for BRFs and VIs for each data run. %QDIF is percent diffuse irradiance in PAR wavelengths; RH is relative humidity; WS,WD are wind speed and direction; MTA is mean tilt angle.

DOY	SZA	B3CV	B4CV	NDCV	SRCV	%QDIF	RH	WS	WD	MTA
218	-45	42	21	12	38	14	57	1.2	122	55
218	-35	39	19	14	40	13	45	1.6	117	58
218	-25	35	17	15	39	18	43	1.9	139	54
218	25	29	13	10	34	22	41	2.2	210	46
218	35	28	16	8	25	17	35	2.3	139	55
218	45	35	19	9	28	19	36	2.5	77	61
218	55	33	22	8	29	31	36	2.5	98	58
220	25	27	15	8	33	14	57	5.4	108	49
220	35	29	17	8	26	18	56	5.1	126	55
220	45	35	19	8	28	23	55	5.3	118	53
220	55	34	23	7	28	28	55	5.4	113	64
221	-55	39	24	8	32	26	81	3.4	137	67
221	-45	42	22	11	38	24	73	2.1	168	48
221	-35	41	21	13	41	22	67	1.8	142	46
221	25	28	16	8	35	22	60	2.6	111	47
221	35	29	16	7	28	28	60	3.0	138	57
229	-55	35	24	5	27	18	76	6.1	165	54
229	-45	37	21	6	32	15	71	5.9	166	61
241	35	18	17	9	7	26	40	4.3	206	66
241	45	23	20	10	9	21	38	4.8	223	90
241	55	27	23	10	9	18	36	5.0	253	90
242	35	19	18	11	9	16	43	4.9	130	79
242	45	23	20	10	9	21	44	4.7	107	90
242	55	28	23	12	12	22	43	5.0	109	83
243	-55	30	23	12	14	19	49	4.9	172	90
243	-45	25	21	12	12	17	42	5.5	199	90
243	-35	21	17	12	11	14	37	5.0	206	64

Appendix A cont. Mean environmental conditions and coefficients of variation (CV) for BRFs and VIs for each data run. %QDIF is percent diffuse irradiance in PAR wavelengths; RH is relative humidity; WS,WD are wind speed and direction; MTA is mean tilt angle.

DOY	SZA	B3CV	B4CV	NDCV	SRCV	%QDIF	RH	WS	WD	MTA
243	33	19	17	12	11	14	35	3.7	200	65
247	-55	34	27	14	28	16	56	4.8	213	88
247	-45	30	25	16	27	13	48	5.2	204	59
247	-35	27	21	18	30	11	36	5.6	222	64
247	35	25	19	12	19	12	34	5.1	225	66
247	45	27	23	10	20	14	32	5.4	204	72
247	55	33	24	11	23	18	32	3.9	199	62
249	-45	32	25	17	36	11	45	4.7	185	74
249	35	27	19	12	23	11	37	3.5	193	51
249	45	27	21	9	22	14	34	3.6	249	61
249	55	32	24	9	26	17	34	3.9	267	74
255	-55	38	26	10	38	17	59	4.1	208	61
255	-45	37	25	13	41	15	49	4.1	192	54
255	38	28	18	8	30	14	36	4.3	174	59
255	45	29	20	6	27	15	30	4.4	179	59
255	55	36	22	6	26	18	28	4.6	161	51
257	-55	36	26	8	34	17	63	5.8	313	70
257	-45	38	26	13	43	13	52	5.2	315	53
257	39	31	18	7	30	12	41	6.0	300	57
257	45	29	19	5	25	12	29	6.1	306	55
257	55	36	22	5	23	14	27	5.5	308	60
267	-55	32	25	7	33	12	42	5.8	184	50
267	-45	34	24	9	40	11	36	6.8	179	
267	43	32	17	5	26	11	33	6.7	174	49
267	45	33	16	4	21	11	32	6.5	183	56
267	55	37	21	3	17	13	32	6.2	170	58

Appendix B-1. Results of NDVI vs LAI regression. Minus signs indicate a SZA prior to solar noon or a VZA in the backscatter direction.

Model: $\ln(LAI/Cos(\theta_s)) = \sigma_0 + \sigma_1 * NDVI$

		From LSN data set				From AVG data set			
SZA	VZA	σ_0	σ_1	r^2	RMSE	σ_0	σ_1	r^2	RMSE
-55	-50	-2.26	4.43	0.71	0.38	-2.15	4.30	0.86	0.23
-55	-40	-2.35	4.41	0.72	0.38	-2.04	4.03	0.80	0.29
-55	-30	-2.57	4.62	0.76	0.35	-2.42	4.43	0.82	0.26
-55	-20	-2.78	4.90	0.87	0.26	-2.67	4.76	0.91	0.18
-55	-10	-2.41	4.51	0.76	0.35	-2.75	4.94	0.92	0.17
-55	0	-2.26	4.27	0.73	0.37	-2.64	4.75	0.94	0.17
-55	10	-2.53	4.50	0.75	0.36	-2.32	4.25	0.83	0.25
-55	20	-2.25	4.14	0.73	0.37	-2.05	3.89	0.79	0.28
-55	30	-2.74	4.70	0.78	0.33	-2.34	4.22	0.82	0.26
-55	40	-2.62	4.63	0.76	0.35	-2.61	4.61	0.87	0.23
-55	50	-2.76	4.73	0.71	0.38	-2.52	4.44	0.81	0.27
-45	-50	-2.54	4.63	0.78	0.35	-2.42	4.54	0.90	0.21
-45	-40	-2.62	4.76	0.79	0.37	-2.36	4.44	0.89	0.23
-45	-30	-2.61	4.59	0.77	0.37	-2.53	4.51	0.85	0.26
-45	-20	-2.87	4.89	0.88	0.27	-2.71	4.72	0.92	0.19
-45	-10	-2.49	4.49	0.87	0.28	-2.56	4.61	0.95	0.14
-45	0	-2.01	3.88	0.71	0.42	-2.49	4.54	0.94	0.16
-45	10	-2.33	4.19	0.75	0.39	-2.61	4.58	0.92	0.19
-45	20	-2.30	4.13	0.77	0.37	-2.29	4.15	0.85	0.26
-45	30	-2.43	4.23	0.77	0.38	-2.33	4.12	0.83	0.28
-45	40	-2.74	4.64	0.84	0.31	-2.63	4.53	0.91	0.21
-45	50	-3.15	5.08	0.77	0.37	-2.96	4.86	0.87	0.24
-35	-50	-2.12	4.08	0.83	0.36	-2.38	4.32	0.95	0.18
-35	-40	-2.17	4.01	0.81	0.40	-2.34	4.27	0.93	0.22
-35	-30	-2.19	4.03	0.82	0.38	-2.41	4.35	0.90	0.25
-35	-20	-2.38	4.28	0.89	0.30	-2.65	4.66	0.96	0.15
-35	-10	-2.15	4.02	0.90	0.27	-2.64	4.33	0.97	0.13

Appendix B-1 cont. Results of NDVI vs LAI regression. Minus signs indicate a SZA prior to solar noon or a VZA in the backscatter direction.

Model: $\ln(LAI/\cos(\theta_s)) = \delta_0 + \delta_1 * NDVI$

		From LSN data set				From AVG data set			
SZA	VZA	δ_0	δ_1	r^2	RMSE	δ_0	δ_1	r^2	RMSE
-35	0	-1.93	3.73	0.82	0.38	-2.26	4.22	0.97	0.13
-35	10	-2.01	3.76	0.77	0.42	-2.50	4.45	0.97	0.13
-35	20	-2.21	3.90	0.81	0.38	-2.46	4.25	0.93	0.21
-35	30	-2.29	3.89	0.80	0.39	-2.53	4.21	0.88	0.28
-35	40	-2.32	3.92	0.85	0.34	-2.64	4.33	0.91	0.24
-35	50	-2.40	4.10	0.85	0.34	-2.72	4.52	0.94	0.20
-25	-50	-2.72	4.52	0.83	0.38	-2.96	4.87	0.97	0.15
-25	-40	-2.80	4.60	0.80	0.41	-3.12	5.05	0.96	0.18
-25	-30	-2.80	4.63	0.87	0.34	-2.95	4.86	0.96	0.20
-25	-20	-2.57	4.51	0.93	0.24	-2.73	4.75	0.99	0.09
-25	-10	-2.35	4.28	0.91	0.28	-2.65	4.73	0.98	0.13
-25	0	-2.26	4.15	0.89	0.31	-2.51	4.52	0.97	0.18
-25	10	-2.15	3.93	0.75	0.46	-2.62	4.64	0.96	0.20
-25	20	-2.08	3.76	0.70	0.51	-2.74	4.73	0.97	0.17
-25	30	-2.60	4.31	0.82	0.39	-2.88	4.70	0.96	0.19
-25	40	-3.05	4.65	0.83	0.38	-3.37	5.07	0.94	0.23
-25	50	-2.93	4.56	0.89	0.31	-3.24	4.96	0.97	0.17
25	-50	-1.68	3.17	0.62	0.30	-2.58	4.33	0.80	0.24
25	-40	-1.48	2.98	0.61	0.31	-2.68	4.54	0.87	0.19
25	-30	-1.51	3.15	0.80	0.22	-2.05	3.88	0.90	0.17
25	-20	-1.74	3.41	0.83	0.21	-2.34	4.20	0.93	0.15
25	-10	-1.99	3.65	0.83	0.21	-2.60	4.45	0.94	0.13
25	0	-1.87	3.41	0.67	0.28	-2.95	4.78	0.92	0.15
25	10	-1.64	3.09	0.61	0.31	-3.05	4.89	0.96	0.11
25	20	-1.44	2.82	0.58	0.32	-2.89	4.65	0.93	0.14
25	30	-1.39	2.75	0.53	0.34	-3.09	4.86	0.90	0.17
25	40	-2.16	3.72	0.82	0.21	-2.68	4.37	0.89	0.18

Appendix B-1 cont. Results of NDVI vs LAI regression. Minus signs indicate a SZA prior to solar noon or a VZA in the backscatter direction.

Model: $\ln(LAI/Cos(\theta_s)) = \sigma_0 + \sigma_1 * NDVI$

		From LSN data set				From AVG data set			
SZA	VZA	σ_0	σ_1	r^2	RMSE	σ_0	σ_1	r^2	RMSE
25	50	-2.45	4.04	0.77	0.23	-3.42	5.22	0.92	0.16
35	-50	-2.43	4.22	0.92	0.23	-2.38	4.05	0.94	0.19
35	-40	-2.28	4.22	0.89	0.28	-2.29	4.13	0.93	0.20
35	-30	-2.34	4.24	0.91	0.25	-2.29	4.03	0.94	0.20
35	-20	-2.43	4.19	0.92	0.24	-2.39	4.03	0.94	0.19
35	-10	-2.52	4.26	0.90	0.27	-2.53	4.17	0.95	0.17
35	0	-2.11	3.65	0.84	0.33	-2.28	3.82	0.95	0.18
35	10	-2.26	3.93	0.87	0.31	-2.31	3.91	0.95	0.17
35	20	-2.25	3.95	0.85	0.33	-2.28	3.89	0.93	0.20
35	30	-2.12	3.82	0.90	0.26	-2.09	3.65	0.94	0.18
35	40	-2.40	4.06	0.95	0.19	-2.30	3.85	0.95	0.18
35	50	-2.53	4.07	0.88	0.29	-2.48	3.96	0.91	0.23
45	-50	-2.14	4.05	0.91	0.24	-2.23	4.10	0.94	0.18
45	-40	-2.29	4.17	0.90	0.25	-2.41	4.29	0.93	0.20
45	-30	-2.13	3.98	0.89	0.26	-2.28	4.10	0.95	0.17
45	-20	-2.50	4.26	0.93	0.21	-2.53	4.23	0.94	0.19
45	-10	-2.17	3.81	0.87	0.29	-4.41	4.05	0.94	0.18
45	0	-2.12	3.78	0.84	0.31	-2.43	4.12	0.95	0.16
45	10	-2.21	3.91	0.88	0.27	-2.31	3.99	0.94	0.19
45	20	-1.95	3.65	0.86	0.30	-2.12	3.81	0.94	0.18
45	30	-2.33	4.17	0.91	0.24	-2.38	4.14	0.96	0.14
45	40	-2.55	4.27	0.93	0.21	-2.58	4.23	0.94	0.19
45	50	-2.59	4.23	0.87	0.28	-2.79	4.43	0.92	0.21
55	-50	-1.84	3.73	0.85	0.28	-1.99	3.85	0.96	0.14
55	-40	-1.94	3.81	0.91	0.21	-2.02	3.82	0.97	0.11
55	-30	-2.04	3.89	0.90	0.23	-2.19	3.99	0.97	0.12
55	-20	-2.16	3.90	0.91	0.21	-2.24	3.90	0.96	0.14

Appendix B-1 cont. Results of NDVI vs LAI regression. Minus signs indicate a SZA prior to solar noon or a VZA in the backscatter direction.

Model: $\ln(LAI/\cos(\theta_s)) = \sigma_0 + \sigma_1 * NDVI$

		From LSN data set				From AVG data set			
SZA	VZA	σ_0	σ_1	r^2	RMSE	σ_0	σ_1	r^2	RMSE
55	-10	-1.90	3.57	0.87	0.26	-2.08	3.71	0.96	0.14
55	0	-1.92	3.64	0.84	0.29	-2.10	3.78	0.95	0.16
55	10	-1.74	3.46	0.84	0.29	-1.88	3.55	0.92	0.19
55	20	-2.03	3.84	0.89	0.24	-2.12	3.86	0.96	0.14
55	30	-2.20	3.98	0.90	0.23	-2.28	3.98	0.96	0.14
55	40	-2.37	4.07	0.93	0.19	-2.30	3.88	0.94	0.17
55	50	-2.23	4.30	0.86	0.23	-2.43	4.04	0.94	0.17

Appendix B-2. Results of SRVI vs LAI regression. For SZA, minus sign indicates SZA prior to solar noon and for VZA, minus sign indicates VZA in backscatter direction.

Model: $LAI = \beta_0 + \beta_1 * SRVI$

		LSN data set				AVG data set			
SZA	VZA	β_0	β_1	r^2	RMSE	β_0	β_1	r^2	RMSE
-55	-55	-0.35	0.27	0.78	0.575	-0.35	0.27	0.91	0.329
-55	-40	-0.37	0.24	0.83	0.500	-0.28	0.23	0.90	0.342
-55	-30	-0.24	0.20	0.85	0.470	-0.25	0.21	0.94	0.262
-55	-20	-0.08	0.18	0.90	0.393	-0.06	0.19	0.99	0.128
-55	-10	0.16	0.17	0.86	0.450	0.13	0.18	0.97	0.201
-55	0	0.13	0.17	0.85	0.469	0.12	0.17	0.98	0.142
-55	10	-0.04	0.17	0.86	0.460	0.00	0.17	0.96	0.217
-55	20	-0.06	0.16	0.84	0.495	-0.01	0.16	0.95	0.255
-55	30	-0.23	0.18	0.88	0.426	-0.14	0.17	0.96	0.209
-55	40	-0.10	0.18	0.83	0.506	-0.08	0.18	0.93	0.282
-55	50	-0.35	0.19	0.82	0.516	-0.31	0.19	0.92	0.308
-45	-50	-0.29	0.28	0.86	0.520	-0.25	0.28	0.96	0.272
-45	-40	-0.38	0.29	0.92	0.449	-0.24	0.27	0.96	0.281
-45	-30	-0.23	0.23	0.89	0.486	-0.15	0.23	0.96	0.275
-45	-20	-0.14	0.21	0.93	0.395	-0.02	0.20	0.98	0.169
-45	-10	0.11	0.19	0.93	0.388	0.24	0.18	0.98	0.183
-45	0	0.21	0.18	0.90	0.473	0.32	0.17	0.97	0.224
-45	10	0.12	0.17	0.90	0.481	0.22	0.17	0.97	0.228
-45	20	0.13	0.16	0.89	0.494	0.24	0.16	0.96	0.269
-45	30	-0.05	0.17	0.91	0.453	0.11	0.16	0.95	0.305
-45	40	0.00	0.17	0.90	0.469	0.09	0.17	0.98	0.212
-45	50	-0.17	0.19	0.90	0.472	-0.10	0.18	0.97	0.241
-35	-50	-0.04	0.24	0.91	0.462	0.05	0.23	0.98	0.207
-35	-40	-0.20	0.27	0.91	0.468	-0.10	0.26	0.97	0.248
-35	-30	-0.22	0.27	0.91	0.466	-0.12	0.26	0.96	0.296
-35	-20	-0.10	0.24	0.94	0.393	0.02	0.23	0.98	0.210

Appendix B-2 cont. Results of SRVI vs LAI regression. For SZA, minus sign indicates SZA prior to solar noon and for VZA, minus sign indicates VZA in backscatter direction.

Model: $LAI = \theta_0 + \theta_1 * SRVI$

		LSN data set				AVG data set			
SZA	VZA	θ_0	θ_1	r^2	RMSE	θ_0	θ_1	r^2	RMSE
-35	-10	0.14	0.20	0.94	0.391	0.25	0.19	0.98	0.228
-35	0	0.23	0.19	0.95	0.361	0.37	0.17	0.97	0.266
-35	10	0.23	0.18	0.92	0.434	0.35	0.17	0.96	0.282
-35	20	0.14	0.17	0.92	0.439	0.25	0.16	0.97	0.259
-35	30	-0.02	0.18	0.90	0.485	0.07	0.17	0.98	0.222
-35	40	-0.10	0.18	0.92	0.443	0.03	0.17	0.99	0.174
-35	50	-0.02	0.18	0.93	0.401	0.08	0.18	0.99	0.130
-25	-50	0.01	0.22	0.94	0.384	0.10	0.20	0.99	0.170
-25	-40	-0.10	0.24	0.92	0.453	-0.01	0.22	0.97	0.239
-25	-30	-0.24	0.26	0.92	0.451	-0.13	0.26	0.97	0.258
-25	-20	-0.05	0.26	0.96	0.325	0.09	0.24	0.98	0.216
-25	-10	0.18	0.23	0.95	0.348	0.32	0.21	0.96	0.296
-25	0	0.30	0.20	0.95	0.347	0.42	0.18	0.96	0.310
-25	10	0.37	0.18	0.94	0.388	0.48	0.17	0.95	0.334
-25	20	0.34	0.18	0.93	0.425	0.44	0.17	0.95	0.320
-25	30	0.19	0.18	0.93	0.401	0.29	0.16	0.96	0.291
-25	40	-0.07	0.17	0.91	0.471	0.02	0.17	0.97	0.265
-25	50	-0.07	0.18	0.93	0.416	0.03	0.17	0.99	0.121
25	-50	0.19	0.20	0.83	0.444	0.01	0.22	0.93	0.315
25	-40	0.26	0.21	0.81	0.469	0.02	0.24	0.96	0.250
25	-30	0.39	0.22	0.90	0.335	0.22	0.24	0.98	0.169
25	-20	0.43	0.20	0.90	0.348	0.21	0.23	0.97	0.217
25	-10	0.46	0.18	0.91	0.324	0.28	0.20	0.97	0.205
25	0	0.48	0.16	0.87	0.389	0.30	0.18	0.98	0.185
25	10	0.56	0.15	0.87	0.394	0.42	0.16	0.98	0.171
25	20	0.54	0.14	0.82	0.454	0.39	0.16	0.98	0.178
25	30	0.58	0.13	0.80	0.479	0.38	0.15	0.98	0.184

Appendix B-2 cont. Results of SRVI vs LAI regression. For SZA, minus sign indicates SZA prior to solar noon and for VZA, minus sign indicates VZA in backscatter direction.

Model: $LAI = \sigma_0 + \sigma_1 * SRVI$

		LSN data set				AVG data set			
SZA	VZA	σ_0	σ_1	r^2	RMSE	σ_0	σ_1	r^2	RMSE
25	40	0.54	0.14	0.88	0.371	0.36	0.15	0.98	0.151
25	50	0.41	0.15	0.88	0.366	0.28	0.16	0.98	0.173
35	-50	-0.13	0.24	0.93	0.285	-0.25	0.25	0.94	0.244
35	-40	-0.01	0.26	0.89	0.341	-0.17	0.28	0.91	0.302
35	-30	0.07	0.23	0.92	0.298	-0.10	0.24	0.95	0.232
35	-20	0.03	0.21	0.94	0.254	-0.08	0.21	0.95	0.220
35	-10	0.06	0.20	0.89	0.342	-0.07	0.20	0.95	0.225
35	0	0.13	0.17	0.87	0.374	-0.02	0.19	0.96	0.196
35	10	0.17	0.18	0.88	0.367	0.05	0.18	0.95	0.222
35	20	0.25	0.17	0.81	0.457	0.08	0.19	0.92	0.289
35	30	0.29	0.16	0.87	0.378	0.15	0.17	0.95	0.224
35	40	0.18	0.17	0.92	0.299	0.06	0.18	0.96	0.199
35	50	0.11	0.16	0.84	0.412	-0.03	0.17	0.96	0.208
45	-50	-0.07	0.24	0.87	0.372	-0.28	0.26	0.92	0.279
45	-40	-0.11	0.23	0.92	0.291	-0.22	0.24	0.90	0.323
45	-30	0.13	0.19	0.91	0.306	-0.06	0.21	0.96	0.193
45	-20	-0.02	0.18	0.94	0.241	-0.12	0.19	0.94	0.240
45	-10	0.06	0.16	0.88	0.347	-0.12	0.18	0.96	0.210
45	0	0.17	0.15	0.84	0.402	-0.02	0.17	0.95	0.232
45	10	0.21	0.15	0.84	0.410	0.09	0.16	0.90	0.323
45	20	0.27	0.15	0.85	0.390	0.13	0.16	0.94	0.250
45	30	0.27	0.15	0.90	0.327	0.15	0.16	0.97	0.181
45	40	0.07	0.16	0.94	0.253	-0.05	0.16	0.97	0.179
45	50	0.08	0.14	0.83	0.421	-0.19	0.17	0.95	0.213
55	-50	0.26	0.16	0.68	0.389	-0.04	0.19	0.88	0.217
55	-40	0.16	0.16	0.87	0.248	0.01	0.17	0.93	0.166
55	-30	0.23	0.14	0.85	0.265	0.02	0.16	0.94	0.155

Appendix B-2 cont. Results of SRVI vs LAI regression. For SZA, minus sign indicates SZA prior to solar noon and for VZA, minus sign indicates VZA in backscatter direction.

Model: $LAI = \theta_0 + \theta_1 * SRVI$

		LSN data set				AVG data set			
SZA	VZA	θ_0	θ_1	r^2	RMSE	θ_0	θ_1	r^2	RMSE
55	-20	0.16	0.13	0.86	0.255	0.03	0.14	0.93	0.174
55	-10	0.27	0.12	0.76	0.328	0.12	0.13	0.89	0.210
55	0	0.37	0.11	0.66	0.403	0.20	0.12	0.81	0.274
55	10	0.37	0.12	0.69	0.389	0.26	0.12	0.76	0.313
55	20	0.25	0.14	0.76	0.342	0.14	0.14	0.85	0.248
55	30	0.17	0.14	0.81	0.302	0.08	0.14	0.89	0.212
55	40	0.15	0.12	0.82	0.292	0.09	0.12	0.89	0.212
55	50	0.36	0.10	0.59	0.441	0.12	0.12	0.85	0.248

Appendix C-1. Results of NDVI vs APAR regression. For SZA, minus sign indicates prior to solar noon; for VZA minus sign indicates a VZA in the backscatter direction.

		Model: APAR = β_0 + β_1 * NDVI							
		LSN data set				AVG data set			
SZA	VZA	β_0	β_1	r^2	RMSE	β_0	β_1	r^2	RMSE
-55	-50	-0.31	1.36	0.75	0.107	-0.35	1.41	0.89	0.066
-55	-40	-0.32	1.33	0.74	0.109	-0.31	1.31	0.81	0.088
-55	-30	-0.34	1.33	0.71	0.115	-0.42	1.43	0.82	0.084
-55	-20	-0.35	1.36	0.74	0.108	-0.49	1.52	0.90	0.063
-55	-10	-0.36	1.39	0.82	0.091	-0.54	1.61	0.95	0.047
-55	0	-0.39	1.42	0.91	0.064	-0.49	1.54	0.94	0.049
-55	10	-0.41	1.41	0.82	0.090	-0.39	1.38	0.84	0.081
-55	20	-0.30	1.27	0.77	0.101	-0.30	1.25	0.79	0.090
-55	30	-0.38	1.35	0.72	0.112	-0.40	1.37	0.83	0.083
-55	40	-0.27	1.23	0.60	0.135	-0.48	1.49	0.87	0.071
-55	50	-0.47	1.46	0.77	0.103	-0.46	1.44	0.82	0.085
-45	-50	-0.46	1.51	0.79	0.112	-0.52	1.59	0.93	0.061
-45	-40	-0.50	1.56	0.83	0.103	-0.50	1.57	0.92	0.065
-45	-30	-0.45	1.45	0.75	0.125	-0.56	1.59	0.88	0.080
-45	-20	-0.50	1.50	0.80	0.111	-0.91	1.65	0.94	0.058
-45	-10	-0.42	1.43	0.86	0.095	-0.56	1.60	0.97	0.043
-45	0	-0.37	1.37	0.86	0.095	-0.53	1.58	0.96	0.048
-45	10	-0.46	1.46	0.88	0.088	-0.58	1.60	0.95	0.053
-45	20	-0.41	1.38	0.83	0.103	-0.47	1.45	0.88	0.081
-45	30	-0.41	1.35	0.76	0.123	-0.48	1.44	0.84	0.094
-45	40	-0.42	1.38	0.72	0.132	-0.57	1.57	0.91	0.071
-45	50	-0.69	1.69	0.83	0.102	-0.70	1.70	0.89	0.077
-35	-50	-0.36	1.33	0.80	0.133	-0.51	1.52	0.91	0.087
-35	-40	-0.35	1.30	0.76	0.143	-0.48	1.48	0.86	0.108
-35	-30	-0.34	1.28	0.75	0.146	-0.50	1.49	0.82	0.122
-35	-20	-0.40	1.37	0.82	0.124	-0.60	1.62	0.91	0.089
-35	-10	-0.34	1.30	0.85	0.112	-0.51	1.53	0.94	0.071

Appendix C-1 cont. Results of NDVI vs APAR regression. For SZA, minus sign indicates prior to solar noon; for VZA minus sign indicates a VZA in the backscatter direction.

		Model: APAR = θ_0 + θ_1 * NDVI							
		LSN data set				AVG data set			
SZA	VZA	θ_0	θ_1	r^2	RMSE	θ_0	θ_1	r^2	RMSE
-35	10	-0.33	1.27	0.79	0.133	-0.56	1.59	0.95	0.064
-35	20	-0.35	1.25	0.75	0.145	-0.52	1.47	0.85	0.111
-35	30	-0.35	1.22	0.71	0.158	-0.52	1.43	0.78	0.135
-35	40	-0.34	1.19	0.71	0.158	-0.56	1.47	0.81	0.126
-35	50	-0.41	1.31	0.78	0.137	-0.61	1.56	0.86	0.107
-25	-50	-0.46	1.34	0.74	0.148	-0.51	1.42	0.84	0.116
-25	-40	-0.46	1.34	0.69	0.163	-0.53	1.43	0.78	0.138
-25	-30	-0.44	1.31	0.70	0.161	-0.46	1.34	0.73	0.153
-25	-20	-0.40	1.32	0.80	0.129	-0.43	1.37	0.83	0.120
-25	-10	-0.38	1.32	0.87	0.107	-0.45	1.43	0.92	0.084
-25	0	-0.37	1.31	0.89	0.095	-0.42	1.38	0.92	0.080
-25	10	-0.36	1.28	0.81	0.126	-0.46	1.43	0.94	0.072
-25	20	-0.32	1.19	0.71	0.156	-0.48	1.42	0.91	0.088
-25	30	-0.42	1.27	0.72	0.154	-0.47	1.34	0.79	0.132
-25	40	-0.52	1.33	0.68	0.164	-0.55	1.37	0.68	0.165
-25	50	-0.48	1.30	0.73	0.152	-0.52	1.35	0.72	0.155
25	-50	-0.65	1.61	0.81	0.095	-0.80	1.80	0.92	0.059
25	-40	-0.42	1.34	0.62	0.136	-0.82	1.86	0.96	0.041
25	-30	-0.37	1.34	0.71	0.118	-0.54	1.56	0.96	0.040
25	-20	-0.51	1.50	0.79	0.100	-0.66	1.69	0.99	0.026
25	-10	-0.66	1.65	0.84	0.088	-0.75	1.77	0.98	0.031
25	0	-0.78	1.78	0.92	0.093	-0.90	1.92	0.97	0.035
25	10	-0.69	1.65	0.88	0.075	-0.9	1.91	0.96	0.042
25	20	-0.57	1.49	0.81	0.096	-0.86	1.85	0.97	0.039
25	30	-0.44	1.31	0.61	0.137	-0.95	1.95	0.95	0.046
25	40	-0.67	1.61	0.76	0.107	-0.79	1.75	0.95	0.048
25	50	-0.68	1.60	0.60	0.139	-1.06	2.06	0.94	0.052

Appendix C-1 cont. Results of NDVI vs APAR regression. For SZA, minus sign indicates prior to solar noon; for VZA minus sign indicates a VZA in the backscatter direction.

		Model: APAR = β_0 + β_1 * NDVI							
		LSN data set				AVG data set			
SZA	VZA	β_0	β_1	r^2	RMSE	β_0	β_1	r^2	RMSE
35	-50	-0.44	1.39	0.91	0.082	-0.47	1.43	0.97	0.050
35	-40	-0.36	1.32	0.79	0.126	-0.44	1.47	0.97	0.046
35	-30	-0.37	1.33	0.82	0.116	-0.44	1.44	0.98	0.036
35	-20	-0.40	1.32	0.84	0.110	-0.48	1.44	0.98	0.038
35	-10	-0.47	1.41	0.90	0.089	-0.52	1.48	0.97	0.043
35	0	-0.36	1.25	0.90	0.085	-0.43	1.35	0.97	0.046
35	10	-0.41	1.34	0.92	0.076	-0.45	1.39	0.98	0.034
35	20	-0.38	1.31	0.86	0.103	-0.43	1.38	0.96	0.052
35	30	-0.33	1.24	0.87	0.099	-0.37	1.30	0.98	0.039
35	40	-0.37	1.26	0.83	0.114	-0.44	1.36	0.96	0.054
35	50	-0.46	1.33	0.86	0.104	-0.49	1.38	0.91	0.081
45	-50	-0.43	1.45	0.90	0.089	-0.53	1.60	0.97	0.051
45	-40	-0.48	1.49	0.89	0.093	-0.62	1.69	0.98	0.043
45	-30	-0.40	1.40	0.86	0.108	-0.55	1.60	0.97	0.046
45	-20	-0.52	1.49	0.88	0.100	-0.65	1.66	0.97	0.047
45	-10	-0.45	1.38	0.89	0.094	-0.59	1.56	0.94	0.070
45	0	-0.45	1.40	0.90	0.090	-0.60	1.59	0.97	0.054
45	10	-0.48	1.45	0.94	0.072	-0.57	1.56	0.97	0.047
45	20	-0.38	1.34	0.91	0.086	-0.48	1.48	0.96	0.057
45	30	-0.51	1.52	0.93	0.073	-0.58	1.60	0.98	0.043
45	40	-0.53	1.48	0.86	0.106	-0.64	1.61	0.92	0.081
45	50	-0.60	1.53	0.89	0.093	-0.73	1.70	0.92	0.081
55	-50	-0.35	1.33	0.81	0.113	-0.48	1.51	0.96	0.055
55	-40	-0.39	1.36	0.88	0.092	-0.47	1.48	0.95	0.063
55	-30	-0.39	1.35	0.82	0.117	-0.53	1.53	0.93	0.072
55	-20	-0.43	1.35	0.82	0.110	-0.56	1.52	0.94	0.068
55	-10	-0.37	1.27	0.83	0.108	-0.50	1.44	0.94	0.065

Appendix C-1 cont. Results of NDVI vs APAR regression. For SZA, minus sign indicates prior to solar noon; for VZA minus sign indicates a VZA in the backscatter direction.

		Model: APAR = β_0 + β_1 * NDVI							
		LSN data set				AVG data set			
SZA	VZA	β_0	β_1	r^2	RMSE	β_0	β_1	r^2	RMSE
55	0	-0.41	1.35	0.86	0.097	-0.52	1.50	0.97	0.047
55	10	-0.36	1.30	0.90	0.084	-0.45	1.42	0.96	0.051
55	20	-0.44	1.41	0.90	0.081	-0.52	1.51	0.95	0.061
55	30	-0.47	1.41	0.85	0.099	-0.59	1.56	0.95	0.058
55	40	-0.52	1.44	0.87	0.095	-0.58	1.51	0.92	0.074
55	50	-0.54	1.45	0.85	0.100	-0.66	1.60	0.96	0.056

Appendix C-2. Results of SRVI vs APAR regression. For SZA, minus sign indicates prior to solar noon; for VZA minus sign indicates a VZA in the backscatter direction.

		Model: $\ln(1-APAR) = \theta_0 + \theta_1 * SRVI$							
		LSN data set				AVG data set			
SZA	VZA	θ_0	θ_1	r^2	RMSE	θ_0	θ_1	r^2	RMSE
-55	-50	0.15	-0.19	0.80	0.381	0.25	-0.20	0.90	0.25
-55	-40	0.15	-0.17	0.85	0.330	0.20	-0.17	0.89	0.27
-55	-30	0.04	-0.14	0.84	0.346	0.17	-0.15	0.92	0.23
-55	-20	-0.09	-0.13	0.87	0.313	0.01	-0.14	0.95	0.18
-55	-10	-0.20	-0.12	0.90	0.272	-0.12	0.13	0.94	0.19
-55	0	-0.15	-0.12	0.93	0.223	-0.10	-0.13	0.96	0.15
-55	10	-0.03	0.12	0.93	0.230	0.01	-0.12	0.97	0.13
-55	20	0.00	-0.12	0.92	0.238	0.02	-0.12	0.96	0.15
-55	30	0.05	-0.12	0.89	0.284	0.11	-0.13	0.97	0.13
-55	40	-0.12	-0.12	0.75	0.428	0.04	-0.13	0.90	0.25
-55	50	0.18	-0.14	0.88	0.299	0.22	-0.14	0.90	0.25
-45	-50	0.24	-0.19	0.87	0.337	0.32	-0.20	0.95	0.20
-45	-40	0.28	-0.19	0.92	0.290	0.31	-0.19	0.95	0.21
-45	-30	0.18	-0.15	0.90	0.317	0.25	-0.16	0.96	0.18
-45	-20	0.11	-0.14	0.92	0.277	0.15	-0.14	0.97	0.15
-45	-10	-0.04	-0.13	0.94	0.240	-0.03	-0.13	0.98	0.14
-45	0	-0.08	-0.12	0.95	0.231	-0.08	-0.12	0.97	0.16
-45	10	-0.01	-0.12	0.96	0.200	0.00	-0.12	0.99	0.11
-45	20	-0.03	-0.11	0.93	0.254	-0.02	0.11	0.97	0.17
-45	30	0.05	-0.11	0.90	0.308	0.05	-0.11	0.93	0.24
-45	40	-0.01	-0.11	0.86	0.373	0.05	-0.12	0.94	0.23
-45	50	0.15	-0.12	0.91	0.294	0.20	-0.13	0.95	0.22
-35	-50	0.23	-0.16	0.93	0.277	0.25	-0.16	0.97	0.17
-35	-40	0.34	-0.18	0.93	0.284	0.35	-0.18	0.95	0.23
-35	-30	0.34	-0.18	0.90	0.320	0.37	-0.19	0.95	0.22
-35	-20	0.27	-0.16	0.94	0.244	0.28	-0.17	0.98	0.14
-35	-10	0.11	-0.14	0.95	0.226	0.12	-0.14	0.98	0.13

Appendix C-2 cont. Results of SRVI vs APAR regression. For SZA, minus sign indicates prior to solar noon; for VZA minus sign indicates a VZA in the backscatter direction.

Model: $\ln(1\text{-APAR}) = \theta_0 + \theta_1 * \text{SRVI}$									
		LSN data set				AVG data set			
SZA	VZA	θ_0	θ_1	r^2	RMSE	θ_0	θ_1	r^2	RMSE
-35	0	0.06	-0.13	0.96	0.194	0.04	-0.13	0.98	0.12
-35	10	0.06	-0.12	0.96	0.219	0.06	-0.12	0.99	0.12
-35	20	0.12	-0.12	0.95	0.237	0.12	-0.12	0.98	0.13
-35	30	0.22	-0.12	0.92	0.288	0.24	-0.12	0.97	0.18
-35	40	0.26	-0.12	0.91	0.306	0.25	-0.12	0.95	0.22
-35	50	0.22	-0.12	0.95	0.235	0.22	-0.12	0.98	0.15
-25	-50	0.21	-0.13	0.93	0.244	0.21	-0.12	0.97	0.14
-25	-40	0.29	-0.14	0.92	0.266	0.28	-0.14	0.96	0.17
-25	-30	0.36	-0.15	0.91	0.273	0.36	-0.15	0.96	0.17
-25	-20	0.25	-0.15	0.95	0.205	0.24	-0.15	0.99	0.08
-25	-10	0.13	-0.13	0.97	0.152	0.10	-0.13	0.99	0.10
-25	0	0.06	-0.12	0.97	0.151	0.03	-0.11	0.98	0.13
-25	10	0.02	-0.11	0.96	0.182	0.00	-0.10	0.97	0.15
-25	20	0.04	-0.10	0.94	0.225	0.02	-0.10	0.97	0.15
-25	30	0.12	-0.10	0.94	0.225	0.11	-0.10	0.98	0.13
-25	40	0.27	-0.10	0.91	0.267	0.26	-0.10	0.96	0.18
-25	50	0.26	-0.11	0.92	0.250	0.26	-0.11	0.98	0.14
25	-50	0.14	-0.12	0.86	0.243	0.08	-0.11	0.92	0.17
25	-40	0.06	-0.12	0.77	0.306	0.07	-0.12	0.94	0.15
25	-30	-0.04	-0.12	0.83	0.266	-0.04	-0.12	0.94	0.14
25	-20	-0.03	-0.12	0.87	0.236	-0.01	-0.12	0.98	0.08
25	-10	-0.05	-0.11	0.87	0.230	-0.05	-0.10	0.96	0.12
25	0	-0.02	-0.10	0.92	0.185	-0.07	-0.09	0.95	0.14
25	10	-0.07	-0.09	0.91	0.193	-0.15	-0.08	0.91	0.18
25	20	-0.07	-0.09	0.85	0.248	-0.14	-0.08	0.90	0.19
25	30	-0.11	-0.08	0.80	0.286	-0.13	-0.08	0.91	0.18
25	40	-0.11	-0.08	0.82	0.273	-0.12	-0.08	0.93	0.16

Appendix C-2 cont. Results of SRVI vs APAR regression. For SZA, minus sign indicates prior to solar noon; for VZA minus sign indicates a VZA in the backscatter direction.

		Model: $\ln(1-APAR) = \beta_0 + \beta_1 * SRVI$							
		LSN data set				AVG data set			
SZA	VZA	β_0	β_1	r^2	RMSE	β_0	β_1	r^2	RMSE
25	50	-0.06	-0.08	0.79	0.297	-0.09	-0.08	0.90	0.19
35	-50	0.22	-0.15	0.92	0.182	0.24	-0.16	0.98	0.08
35	-40	0.10	-0.16	0.79	0.301	0.20	-0.18	0.96	0.11
35	-30	0.06	-0.14	0.83	0.272	0.14	-0.15	0.98	0.08
35	-20	0.09	-0.13	0.87	0.242	0.13	-0.13	0.99	0.06
35	-10	0.11	-0.13	0.91	0.202	0.12	-0.13	0.97	0.09
35	0	0.09	-0.11	0.93	0.171	0.08	-0.12	0.98	0.09
35	10	0.06	-0.12	0.92	0.184	0.04	-0.12	0.97	0.10
35	20	0.01	-0.11	0.88	0.230	0.02	-0.12	0.94	0.14
35	30	-0.04	-0.10	0.86	0.244	-0.03	-0.11	0.95	0.13
35	40	0.00	-0.10	0.85	0.261	0.02	-0.11	0.95	0.13
35	50	0.09	-0.10	0.89	0.220	0.07	-0.11	0.93	0.15
45	-50	0.21	-0.18	0.87	0.279	0.36	-0.20	0.98	0.11
45	-40	0.24	-0.17	0.91	0.232	0.34	-0.19	0.98	0.09
45	-30	0.04	-0.13	0.85	0.291	0.16	-0.15	0.96	0.13
45	-20	0.15	-0.13	0.90	0.235	0.23	-0.14	0.98	0.09
45	-10	0.13	-0.12	0.91	0.224	0.21	-0.13	0.97	0.12
45	0	0.07	-0.12	0.90	0.246	0.14	-0.13	0.96	0.14
45	10	0.05	-0.12	0.92	0.215	0.08	-0.12	0.96	0.14
45	20	-0.01	-0.12	0.92	0.221	0.03	-0.12	0.96	0.15
45	30	-0.04	-0.12	0.90	0.240	0.00	-0.12	0.94	0.18
45	40	0.09	-0.12	0.89	0.250	0.14	-0.12	0.94	0.18
45	50	0.15	-0.11	0.91	0.231	0.26	-0.13	0.96	0.14
55	-50	0.00	-0.14	0.69	0.336	0.30	-0.19	0.93	0.16
55	-40	-0.01	-0.13	0.72	0.318	0.21	-0.16	0.90	0.18
55	-30	-0.11	-0.11	0.63	0.370	0.18	-0.15	0.87	0.21
55	-20	0.00	-0.11	0.73	0.317	0.20	-0.13	0.91	0.18

Appendix C-2 cont. Results of SRVI vs APAR regression. For SZA, minus sign indicates prior to solar noon; for VZA minus sign indicates a VZA in the backscatter direction.

Model: $\ln(1-APAR) = \beta_0 + \beta_1 * SRVI$									
		LSN data set				AVG data set			
SZA	VZA	β_0	β_1	r^2	RMSE	β_0	β_1	r^2	RMSE
55	-10	0.01	-0.11	0.81	0.267	0.13	-0.12	0.91	0.17
55	0	0.01	-0.11	0.86	0.229	0.11	-0.13	0.96	0.12
55	10	-0.01	-0.12	0.85	0.234	0.08	-0.13	0.95	0.13
55	20	0.05	-0.12	0.85	0.237	0.13	-0.14	0.91	0.18
55	30	0.08	-0.12	0.81	0.261	0.18	-0.13	0.93	0.15
55	40	0.09	-0.11	0.82	0.258	0.16	-0.11	0.90	0.18
55	50	0.05	-0.10	0.81	0.262	0.18	-0.12	0.96	0.11

Appendix C-3. Results of LAI vs APAR regression. For SZA, minus sign indicates solar zenith angle prior to solar noon.

	Model: $\ln(1\text{-APAR}) = \theta_0 + \theta_1 * LAI$							
	LSN data set				AVG data set			
SZA	θ_0	θ_1	r^2	RMSE	θ_0	θ_1	r^2	RMSE
-55	-0.22	-0.37	0.86	0.322	-0.02	-0.42	0.96	0.167
-45	-0.03	-0.45	0.92	0.272	0.14	-0.50	0.98	0.139
-35	0.16	-0.53	0.94	0.247	0.27	-0.58	0.96	0.196
-25	0.20	-0.52	0.96	0.190	0.22	-0.52	0.94	0.220
25	0.13	-0.50	0.83	0.264	0.16	-0.50	0.94	0.157
35	0.09	-0.49	0.89	0.223	0.03	-0.49	0.94	0.146
45	0.12	-0.51	0.93	0.202	0.09	-0.51	0.92	0.203
55	0.07	-0.43	0.75	0.303	0.11	-0.49	0.81	0.266